leti
cea tech

ANNUAL
RESEARCH REPORT
2015

SYSTEMS AND SOLUTIONS INTEGRATION

Leti, technology research institute

TECHNOLOGY RESEARCH INSTITUTE

LETI AT A GLANCE

Founded in **1967**

Based in **France** (Grenoble)
with offices in **USA** (Silicon Valley)
and **Japan** (Tokyo)

350
industrial partners

1,900
researchers

Committed to innovation, Leti's teams create **differentiating solutions in miniaturization and energy-efficient technologies** for its industrial partners.

Leti is a technology research institute at CEA Tech and a recognized global leader focused on miniaturization technologies enabling energy-efficient and secure IoT. Leti delivers solid expertise throughout the entire IoT chain, from sensors to data processing and computing solutions. Leti pioneered FDSOI low power platform for IoT, M&NEMS technology for low cost multisensors solutions, CoolCube™ integration for highly connected and cost effective devices.

Leti's mission is to pioneer new technologies, enabling innovative solutions to ensure Leti's industrial partners competitiveness while creating a better future. It tackles most current global issues such as the future of industry, clean and safe energies, health and wellness, sustainable transport, information and communication technologies, space exploration and safety & security.

For 50 years, the institute has built long-term relationships with its partners: global industrial companies, SMEs and startups. It tailors innovative and differentiating solutions that strengthen their competitiveness and contribute to creating new jobs. Leti and its partners work together through bilateral projects, joint laboratories and collaborative research programs. Leti actively contributes to the creation of startups through its startup program.

Leti has signed partnerships with major research technology organizations and academic institutions. It is a member of the Carnot Institutes network*.

**Carnot Institutes network: French network of 34 institutes serving innovation in industry.*

2,670
patents in portfolio

60
startups created

€315
million budget

700
publications each year

ISO 9001
certified since 2000

Systems and Solutions Integration research and innovation activities focus on the design and integration of emerging electronic technologies for the IoT and 5G, providing solutions and next-generation industrial products in the domains of factory of the future, multimedia, smart energy, smart transport, e-health, sports and leisure.

Leti's expertise covers wireless communications, innovative sensor-system design, power-management systems and security solutions for both fixed and mobile networks. It also includes connected objects with embedded power management, energy harvesting, innovative sensors, data- and information-processing capabilities, radio-communication modules and security functions.

SMEs and industrial product design are supported in businesslike environments by our state-of-the-art validation-and-testing facilities, such as an RF anechoic chamber, the Information Technology Security Evaluation Facility and the sensor system characterization laboratories.

Contents

Edito

Sébastien DAUVÉ

Head of Systems and Solutions Integration

Based on MINATEC Campus, the Systems and Solutions Integration Division (DSIS) is at the strategic core of Leti's technological solutions, adding a "system perspective" on technological trends, future trends, leading applications, state-of-the-art platform developments, and challenges for wireless communications networks, including sensor networks.

This document reports the most significant technological achievements of 2015 obtained by DSIS dedicated research activities and the division's joint collaborations with other Leti technology departments or with targeted external partners.

2015 has been characterized at DSIS by publications, patents and prototypes for applied research and validation in three major innovation and research domains of interest for the IoT and forthcoming 5G wireless networks. These are: physical and MAC-layer solutions for both short-range and mobile wireless communications (chapters 1,2,3); innovative sensor designs and MEMs-based advanced signal processing (chapter 4), and power management, including battery management-system applications and energy harvesting (chapter 5).

Indeed, the division offers innovative solution boosters based on sensors, wireless communications and power management to both leading industry and SME/industrial partners that are not familiar (yet) with electronics, but have clearly marked needs and evolution potential.

Key figures

166 permanent researchers
38 PhD students and post-docs
58 temporary employees and interns

25 M€ budget
90% external funding

48 patents granted in 2015
408 patents portfolio
26 book chapters and journal papers
110 communications in conferences and workshops

Research facilities:
3 anechoic chambers
Magnetometer test ground
Information Technology Security Evaluation Facility (ITSEF)

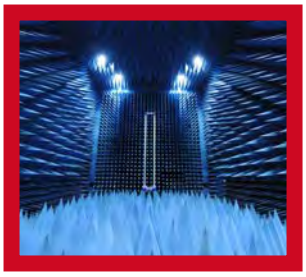

230 industrial partners

Scientific Activity

Publications

136 publications in 2015, including book chapters, and top journals or conferences. These include IEEE Transactions on Antenna and Propagation, IEEE Transactions on Electromagnetic Compatibility, IEEE Transactions on Communications, Sensors & Transducers journal, Smart Materials and Structures journal, IEEE VTC, IEEE ICC, IEEE ICUWB, International Workshop on SHM, PowerMEMS, IEEE WCNC, IEEE GlobeCom, etc.

Prize and awards

- **Mechatronics Award** for Andrès Ospina at the European Mechatronics Meeting 2015 for his work on a new tactile sensor system.
- **Best Paper Award** for Luca Di Palma at *Journées Nationales Microondes 2015* for his work on "Conception et Caractérisation Expérimentale d'une Antenne à Réseau Transmetteur à Distance Focale Réduite".
- **Best Student Poster Award** for Matthias Perez at *Electrostatics 2015* for his work on "Design and performance of a small-scale wind turbine exploiting an electret-based electrostatic conversion".

Experts

1 Research Director, 1 International Expert, 11 Senior Experts, 13 Experts.

Scientific committees

- National Research Agency "High performance infrastructures, software technology and science » committee.
- Technical Program committees of: JNM, COST 15104, EurAAP, IEEE EUROCON, IEEE GlobCom, EuCNC, IEEE VTC, IEEE PIMRC, IEEE DySPAN, Euromicro DSD.

Conferences and Workshops organizations

Workshops and special sessions organized in the following conferences: EuCAP, EuMW, EuCNC, ISWCS, IEEE ICC.

International Collaborations

University of Bologna (Italy), University of Calgary (Canada), Université Catholique de Louvain (Belgium), Czech Technical University (Czech Republic).

01

MOBILE COMMUNICATIONS

- Heterogeneous networks
- Low-power wide-area networks
- Error correcting decoders

Joint Radio Access Network and Backhaul Optimization

Research topic: mobile communications, 5G.

Authors: A. De Domenico, V. Savin and D. Kténas.

Abstract: to enable massive small-cell deployment in 5G networks, wireless backhaul gains more and more interest from operators. This architecture is flexible and cost-efficient, even though it cannot provide the same achievable rates as optical fibre. In this scenario, wireless backhaul can be seen as a limiting factor in terms of available resources and a cause of network congestion. Therefore, functions that jointly optimize the Radio Access Network and backhaul are required. In this study, we present a load-aware cell selection mechanism that jointly takes into account the radio access and backhaul characteristics to improve the overall network capacity.

Context and Challenges

Although Heterogeneous Networks (HetNets, see Figure 1) have captured the attention of the mobile industry since 3GPP LTE release 10, small cells require further enhancements to enable reliable and energy-efficient operations. In this study, we deal with the challenges of designing the connection control for future 5G HetNets. First, finding the optimal association of users and eNBs (i.e., base stations in LTE terminology) is difficult due to the large number of possible assignments in dense small-cell deployment. Second, in current technology, the association is based on the reference signal received power (RSRP) received from neighboring eNBs. Due to the power unbalance in HetNets, this solution reduces the macro cell offloading and limits the usage of the overall network resources. Third, the cell loads and their backhaul characteristics should be taken into account to optimize the cell association. These issues affect the user performance and motivate a joint RAN/BH aware connection control mechanism [1][2].

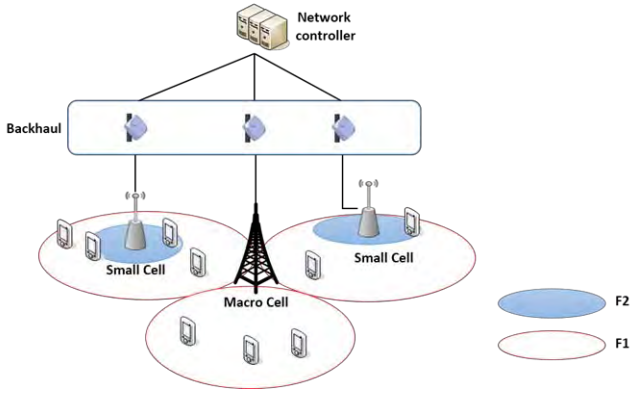

Figure 1. Heterogeneous radio access network deployment.

Main Results

Figure 2 shows the average area throughput and joint RAN/BH utilization efficiency achieved with the Centralized Connection Control and the classic RSRP-based scheme when varying the number of active users in the network. We have considered here a tri-sectorial macro cell where three hotspots, each one composed by 4 neighboring small cells, are deployed in the macro cell. Also, Cell Range Expansion (CRE) technique has been considered in the baseline solution to increase the macro cell offloading. Our results confirm that the proposed centralized connection control, which takes into account jointly the cell load and the radio link quality, can lead up to a 50% gain with respect to the classical solutions by efficiently using the overall RAN/BH available resources.

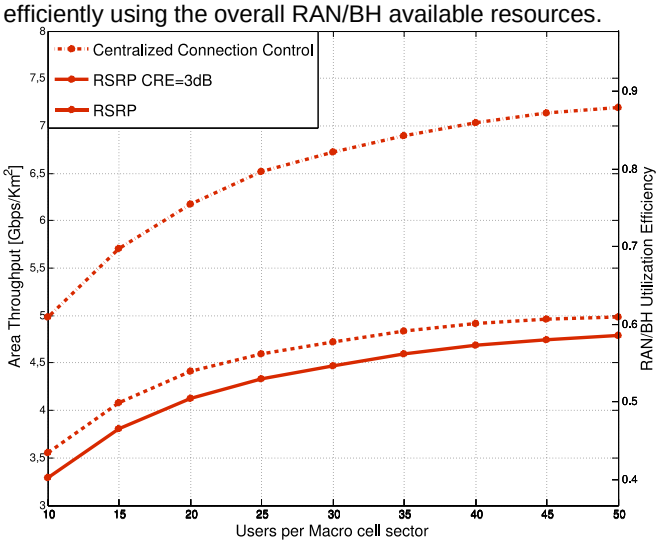

Figure 2. Area throughput and RAN/BH utilization efficiency for different number of active users.

Perspectives

Further studies will extend this investigation by focusing on the impact of the backhaul on the overall network power consumption. In addition, we aim to analyze the impact of the backhaul latency to lower layer functionalities such as scheduling and inter-cell interference coordination mechanisms.

Related Publications:
[1] A. De Domenico, V. Savin, and D. Ktenas, “Cell Selection for Joint Optimization of the Radio Access and Backhaul in Heterogeneous Cellular Networks,” to appear in Backhauling / Fronthauling for Future Wireless Systems, Wiley.
[2] E. Pateromichelakis, A. Maeder, A. De Domenico, R. Fritzsche, P. de Kerret, J. Bartelt “Joint RAN/Backhaul Optimization in centralized 5G RAN”, European Conference on Networks and Communications (EUCNC), June 29-July 2, 2015, Paris, France.
[3] A. De Domenico, V. Savin, D. Ktenas, and A. Maeder, “Backhaul-Aware Small Cell DTX based on Fuzzy Q-Learning in Heterogeneous Cellular Networks”, IEEE Int. Conf. on Communications (ICC), May 23-27, 2016, Kuala Lumpur, Malaysia.

EMF-Aware Cell Selection in Heterogeneous Cellular Networks

Research topic: mobile communications, electromagnetic field exposure

Authors: A. De Domenico, V. Savin and D. Kténas

Abstract: the growing concern on the exposure of users to the Electromagnetic Fields (EMF) has recently brought new challenges to the mobile research community. In this study, we present a novel cell association framework for heterogeneous cellular networks (HetNets), which aims to balance the load amongst heterogeneous cells so as to improve the resource usage and to increase the user satisfaction in terms of both data rate and EMF exposure. The proposed solutions lead to notable improvements with respect to legacy association schemes.

Context and Challenges

According to the latest European statistics, there is an increasing concern of the end-users about the potential health risks due to wireless communications. The reduction of the EMF exposure poses additional challenges to the mobile industry: new methodologies, metrics, and architectures are required. Recently, the European LEXNET project has proposed solutions to optimize network operations with respect to the EMF exposure,

In the current cellular technology, a User Equipment (UE) selects the enhanced NodeB (eNB) that corresponds to the strongest Reference Signal Received Power (RSRP). Due to the power unbalance between small cells and Macro cells, this solution may prevent UEs from being served by the closest eNB. Hence, this increases the uplink (UL) transmission power at the UEs, which in turns increases the user's exposure. Moreover, this approach limits the data rate, increases the UL interference, lowers the battery life, and reduces the macro cell offloading.

In this study, we analyze the cell association by jointly considering downlink (DL) and UL communications, and we study the relationship between the EMF exposure and the users' Quality of Service (QoS). In particular, we propose an algorithm named as EMF-Aware, which targets the reduction of the EMF jointly with the improvement of the user satisfaction in terms of DL rate requirements [1].

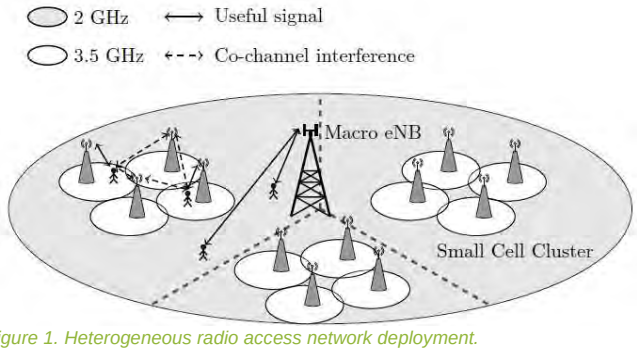

Figure 1. Heterogeneous radio access network deployment.

Main Results

In the following, we assess the effectiveness of the proposed solution. We compare its performance with respect to the approach that maximizes the fraction of UEs whose DL rate requirement is satisfied. We also consider the scheme where each UE is served by the eNB associated with the strongest RSRP and the one where each UE is associated with the closest eNB (Min Path Loss). We also consider a CRE (Cell Range Expansion) bias of 6 dB to increase the macro cell offloading. Figure 2 shows the daily Exposure due to UL with respect to the DL rate requirement for different cell association schemes. In this simulation, each UE targets 1 Mbit/s in the UL. As expected, associating UEs to nearby eNBs limits the required UL power per resource block; accordingly, CRE and Min Path Loss schemes are beneficial in terms of exposure with respect to the reference solution based on the RSRP. However, better performance can be achieved through the EMF-Aware solution, where the load balancing reduces the required number of frequency resources (e.g., by offloading to the MeNB the small cell UEs characterized by high uplink interference).

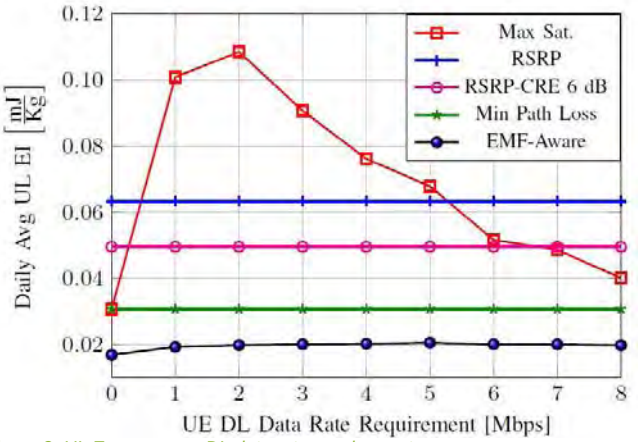

Figure 2. UL Exposure vs. DL data rate requirement.

Perspectives

Current cell selection schemes for HetNets are based only on the radio link quality, which limits the macro cell offloading and increases the EMF exposure. Our results show that satisfying the rate requirements of UEs with poor SINR comes at the cost of increasing the EMF exposure. To appropriately deal with this trade-off, in our future work we will integrate dual connectivity schemes, where DL and UL traffics are served by separate eNBs, and we will pose problem formulations to identify solutions with guaranteed performance.

Related Publications:
[1] A. De Domenico, L.-F. Diez, R. Aguero, D. Ktenas, V. Savin, "EMF-Aware Cell Selection in Heterogeneous Cellular Networks," IEEE Communications Letters, vol. 19, no. 2, Feb. 2015, pp.271-274.

Small Cell Clustering for Efficient Distributed Fog Computing: a Multi-User Case

Research topic: mobile communications, mobile edge computing

Authors: J. Oueis, E. Calvanese Strinati

Abstract: Ultra-dense deployment of radio access points is a key enabler for future 5G networks. It allows the network to cope with the ever increasing mobile data traffic. In addition, these radio access points can serve as an infrastructure for a local mobile cloud computing platform referred to as fog computing. The fog is a capillary edge cloud that enables joint optimization of communication and computational resources for maintaining an efficient and scalable network design. In this work, we address the problem of radio access points clustering for fog computing applications. We focus on the case where multiple users require fog computing services.

Context and Challenges

Mobile computation offloading allows devices to run sophisticated applications while keeping a prolonged battery lifetime of their mobile devices. Fog computing cluster, which operates by distributing computation load among neighbor radio access points endowed with computational capacities, is a cloud computing platform in proximity to mobile devices. This cluster incorporates small cells that contribute in the computation. Small cells communicate through wireless channels. Therefore, the size of the computation cluster and which are its participants depend on both computational capacities of each small cell and on the link quality between small cells. We propose a solution for setting up the computation cluster and jointly allocate computational and communication resources at small cells in order to serve a larger number of mobile users. We formulate the problem as an optimization with an objective of minimizing the cluster power consumption [1]. We optimize the computational load distribution on the participating small cells, the transmit power used by small cell clusters to exchange computational data, and the computational resources allocated at each of them. The optimization is under resources availability and power budget limitations, and latency constraints. Unfortunately, the latency constraint is non-convex which makes the optimization problem not easy to solve.

Denoting by $\boldsymbol{p} \triangleq (p_{sn}^k)\forall k,s,n, \boldsymbol{f} \triangleq (f_{kn})\forall k,n, \boldsymbol{w} \triangleq (w_{kn})\forall k,n$ respectively, the transmit powers at serving small cell s, computational rates at small cell n and computational loads associated to each mobile user k, the latency constraints Δ are as follows:

$$\Delta_{sn}^k(p_{sn}^k, w_{kn}) \triangleq \begin{cases} \frac{w_{kn}}{f_{kn}} + \frac{w_{kn}\theta}{R_{sn}^k(p_{sn}^k)} & \text{if } p_{sn}^k.f_{kn}.w_{kn} > 0, \forall n \neq s \\ 0 & \text{if } p_{sn}^k.f_{kn}.w_{kn} = 0, \forall n \neq s \\ \frac{w_{kn}}{f_{kn}} & \text{if } f_{kn} > 0, n = s \\ 0 & \text{if } w_{kn}.f_{kn} = 0, n = s \end{cases}$$

Observe that the delay constraint can be equivalently rewritten for $p_{sn}^k.f_{kn}.w_{kn} > 0, n \neq s$, and under the feasibility condition $\Delta_k f_{kn} > w_{kn}$, as:

$$g_{sn}^k(p_{sn}^k, f_{kn}, w_{kn}) \triangleq -B_{sn}\log_2(1 + a_{sn}^k p_{sn}^k) + \frac{w_{kn}f_{kn}\theta}{\Delta_k f_{kn} - w_{kn}} \leq 0$$

which is convex as can be easily verified by proving that the Hessian of $g_{sn}^k$is a semi-definite positive matrix. Additionally, the nonconvex delay constraint for $f_{kn} > 0, n = s,$ can be reduced to the linear convex constraint $w_{ks} \leq \Delta_k f_{ks}$. Thus, the initial nonconvex problem can be replaced by an equivalent convex problem by convexification of the delay constraints. The equivalent problem is a convex problem and any local optimal solution is a global optimal minimum.

Main Results

We compare the results of the joint clusters optimization to the case where all requests are handled by the serving small cell, the case where a static clustering rule of equal load distribution between active neighbor small cells is imposed, and the case where clusters are formed for each user successively.

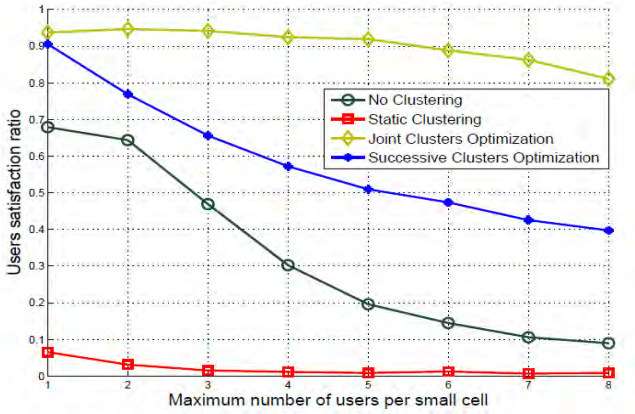

Users satisfaction ratio in dependence on number of users per small cell.

This figure shows how the joint clustering strategy for all users greatly outperforms all other strategies. The fact of taking into account all the active devices in the system allows better distribution and allocation of both computation and communication resources, and thus, higher Quality of Experience (QoE).

Perspectives

We proposed a multi-user small cell clustering optimization policy for distributed fog computing. The interest of this approach is two-fold. First, it allows adaptive sizing and resources management of computation clusters. Second, it simultaneously establishes computation clusters for all active requests for better exploitation of available resources, targeting a higher QoE. Future work includes exploiting trade-offs in cluster formation in the multi-user case for reducing the number of active small cells. In addition, we are investigating an updated implementation of this method in order to cope for its non-optimality due to the unpredictable idle time of the computing small cells.

Related Publications:
[1] J. Oueis, E. Calvanese Strinati, S. Sardellitti, S. Barbarossa, "Small Cell Clustering for Efficient Distributed Fog Computing: A Multi-User Case," 2015 IEEE 82nd Vehicular Technology Conf. (VTC-Fall), Sept. 6-9, 2015, Boston, MA, USA.

Hybrid Satellite/Terrestrial System for Multimedia Broadcast/Multicast

Research topic: mobile communications, satellite communications

Authors: N. Cassiau, D. Kténas

Abstract: satellite systems can relieve the LTE terrestrial network from a significant part of the broadcast traffic (eMBMS). A system level simulator was designed in order to simulate with a high level of accuracy point to multipoint communications, eMBMS, and satellite broadcast. A Video-on-Demand scenario was chosen to illustrate the system performance. It is shown that mobile users in a suburban environment can benefit from broadcast services directly from the satellite and that the performance of satellite broadcast is comparable to eMBMS in areas where eNBs are sparsely located. However, in such areas, simulations show that allocating resources to eMBMS dramatically decreases the unicast network performance. The study concludes that service providers could benefit from the use of satellite to release precious resources in suburban areas covered by the satellite beam.

Context and Challenges

Consumers demand for multimedia contents available anywhere, anytime and with good quality, is exploding. To meet this need, 3GPP defined an evolved Multimedia Broadcast Multicast Service (eMBMS) for Long Term Evolution (LTE) systems. This terrestrial standard allows multimedia point-to-multipoint transmissions in LTE cells with minor adaptations required in infrastructures and receivers. Even though satellite systems have inherent broadcasting capabilities, the use of too many specific standards has slowed down their integration with other telecommunication systems, in particular in the IP world. Satellite operators now aim at complementarity with terrestrial networks, in what is called hybrid terrestrial / satellite networks. In this context, this study is about defining to what extent a satellite can relieve the LTE terrestrial network from a part of the eMBMS traffic.

Main Results

The figure below shows the scenario under investigation. eMBMS schematically consists in the simultaneous transmission of the same content from several base stations to users. eMBMS introduces the concept of MBSFN area, an area which consists of a group of cells coordinated to achieve an eMBMS transmission. In the considered scenario, the terrestrial MBSFN areas are composed of large LTE cells: eNBs spacing is 1732m. These areas are here referred as sparse areas, as opposed to dense areas, composed of small LTE cells (Inter Site Distance of 500m). The satellite beam is supposed much larger than a MBSFN area.

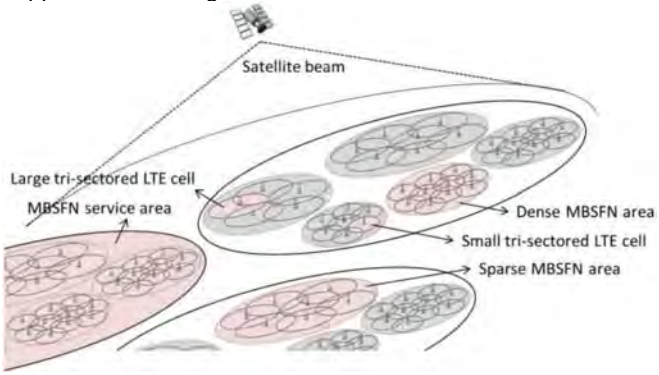

Scenario of the study and definition of terms (eMBMS = MBSFN).

An hybrid system level simulator was developed that allows to simultaneously model point to multipoint communications in LTE cellular network, eMBMS, and satellite broadcasting / multicasting. The figure below shows the measurement results obtained from this simulator. It plots the number of high rate videos that can be multiplexed by the satellite, depending on the percentage of resources allowed for that satellite. For each abscissa several sets of parameters are tested. For each set and for each resource, the coverage is indicated (in %).

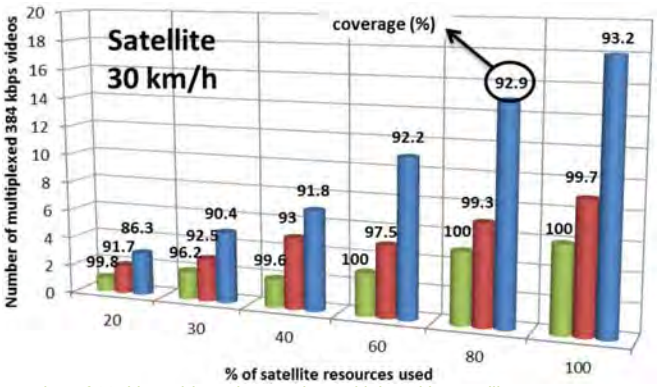

Number of 384kbps videos that can be multiplexed by satellite.

The results of this study support the conclusion that satellites have a significant role to play in future broadcast / multicast systems, especially in areas where the eNBs density is low, i.e. in rural environment. A multimedia service broadcasted by satellite can be received by users in all sparse MBSFN areas in the satellite beam with good coverage. All the cells of all these areas can therefore be released from the eMBMS resources of this service. Given the very large size of the satellite beam, the number of impacted cells can be very high. Releasing resources is all the more interesting since performance of unicast traffic in these large cells quickly decrease with the reduction of available resources.

Perspectives

This study was funded by the French space agency (CNES) that can draw on the results to argue in favor of an increased use of the satellite in the next terrestrial communication systems.

Related Publications:
[1] N. Cassiau, D. Kténas, “Satellite multicast for relieving terrestrial eMBMS: system-level study,” 2015 IEEE 82nd Vehicular Technology Conf. (VTC-Fall), Sept. 6-9, 2015, Boston, MA, USA.

Millimeter-Wave Antennas for Radio Access and Backhaul in 5G Heterogeneous Mobile Networks

Research topic: millimeter-wave antennas, 5G mobile networks

Authors: L. Dussopt, O. El Bouayadi, J.A. Zevallos Luna, C. Dehos, Y. Lamy

Abstract: Millimeter-wave communications are expected to play a key role in future 5G mobile networks to overcome the dramatic traffic growth expected over the next decade. Such systems will severely challenge antenna technologies used at mobile terminal, access point or backhaul/fronthaul levels. CEA-LETI has developed several state-of-the-art solutions of integrated antennas, phased arrays and high-directivity quasi-optical antennas enabling high data-rate 60-GHz communications.

Context and Challenges

Millimeter-wave (mmW) spectrum is seen as a key element to enable the 1000-fold higher traffic capacity per area expected in 5G mobile networks, which will be composed of sub-6 GHz macro-cells overlaid by mmW small-cells deployed in dense user areas [1]. In this scheme, mmW small-cell Access-Points (APs) will support massive data exchanges for mobile users with very high data rates, low latency, low interferences, and low power consumption per bit. A major challenge to implement this vision is the development of mmW radio and antenna systems for mobile terminals, access points and backhaul with disruptive enhancements in terms of cost, integration, power efficiency and performance as compared to current state of the art [2,3].

Main Results

Very low power consumption (300–500 mW), miniature size (100–200 mm^2) and low cost are critical requirements for radio modules in mobile terminals such as smartphones or tablets. A very compact (6.5×6.5×0.6 mm^3) 60-GHz packaged transceiver module was demonstrated. It is based on a high-resistivity silicon interposer integration technology which enables a high integration density, the feasibility of high-Q embedded passive components, good thermal properties (CTE, heat dissipation), and cost-effective high-volume production using existing collective fabrication facilities [4]. Two antennas (Tx, Rx), along with their RF feeding lines are realized on the front side. The RFIC transceiver is flip-chipped on the interposer, which is connected on the board using solder balls (Ball-Grid Array). The module is covered with a laminated low-loss polymer leading to a fully packaged module with a total thickness of only 600 µm.

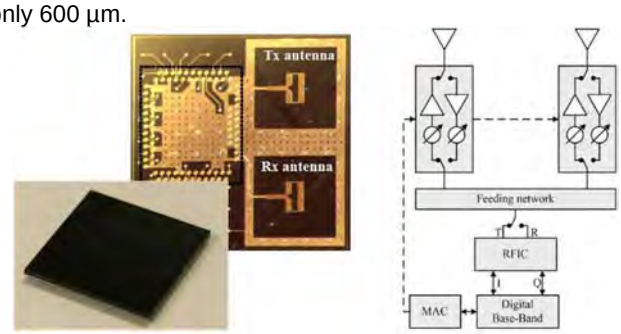

Compact transceiver module and scalable phased array architecture

Small-cell APs benefit from more relaxed specifications in terms of power consumption, size and cost, but they will have to achieve much higher mmW performances (transmit power, radiation gain, beam-steering/beam-forming capability). Large phased-array antennas are a key solution to achieve these objectives with integrated antennas in packaged modules and multi-chip (power amplifier, low noise amplifier, phase shifters, switch) RF architecture based on BiCMOS SiGe technology. A multi-module architecture is desirable to avoid the cost and reliability issues of large-size RFIC chips and packaged modules, and to provide a good scalability of the solution so that the number of modules can be chosen as a function of the targeted communication range or other specification (e.g. power consumption, size, cost).

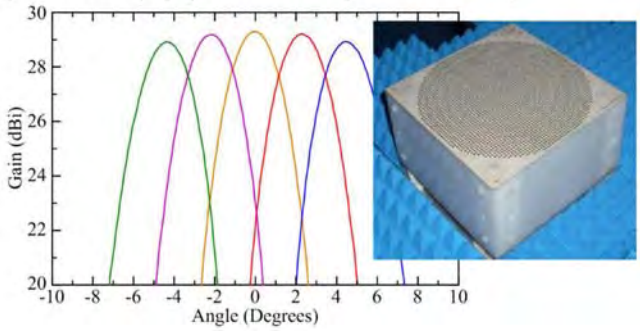

Beam-steering high-gain antenna for backhauling applications.

Finally, high-gain antennas with accurate beam-steering capability for automatic beam alignment are needed for wireless backhauling between APs and the core network. Discrete-lenses associated to switched focal antenna arrays are an attractive solutions to these needs. They have proven to be highly efficient, wideband and to provide excellent radiation properties [5].

Perspectives

Through the European project MiWaveS, lead by CEA-LETI, the integration of these technologies in a comprehensive demonstration platform is expected to provide one of the most advanced demonstration of mmW high-data rate communications feasibility in the context of 5G networks.

Related Publications:
[1] C. Dehos, J. L. González, A. De Domenico, D. Kténas, and L. Dussopt, “Millimeter-wave access and backhauling: the solution to the exponential data traffic increase in 5G mobile communications systems?,” IEEE Communications Mag., vol. 52, no. 9, Sept. 2014, pp.88–95.
[2] L. Dussopt, O. El Bouayadi, J. A. Zevallos Luna, C. Dehos, Y. Lamy, "Millimeter-Wave Antennas for Radio Access and Backhaul in 5G Heterogeneous Mobile Networks," 9th European Conference on Antennas and Propagation, Lisbon, Portugal, 12-17 April 2015.
[3] L. Dussopt, "Millimeter-Wave Technologies for 5G: Opportunities, Challenges and path toward Standards," 2015 European Conference on Networks and Communications (EuCNC 2015), Paris, France, June 29-July 2, 2015.
[4] Y. Lamy, L. Dussopt, O. El Bouayadi, C. Ferrandon, A. Siligaris, C. Dehos, P. Vincent, “A compact 3D silicon interposer package with integrated antenna for 60 GHz wireless applications,” IEEE Int. 3D Systems Integration Conference (3DIC), Oct. 2–4, 2013, San Francisco, CA, USA.
[5] J.A. Zevallos Luna, L. Dussopt, “A V-band Switched-Beam Transmit-array antenna,” Int. Journal on Microwave and Wireless Technologies, vol. 6, Issue 1, Feb. 2014, pp. 51–56.

Evaluation of LDPC Decoders in Fault Inducing Environments

Research topic: wireless communications, error correcting codes

Authors: V. Savin

Abstract: we perform a fault tolerance assessment of state-of-the-art and reliability enhanced LDPC decoders operating in fault-inducing environments. Their performance expressed in terms of error correction capability, energy consumption/bit, throughput, and area, is evaluated for 7 different LDPC decoder architectures, over different external aggression scenarios, emulated by using either voltage scaling or circuit-dependent fault injection. Based on performance and reliability profile of the comprising basic building blocks, the considered decoder architectures are compared, towards substantiating a fault-tolerant LDPC decoder architecture and its benefits in terms of throughput or power consumption.

Context and Challenges

Nowadays, the shrinking of transistor sizes has reached a level where it is extremely difficult, if not impossible, to provide reliable transistors that can properly work all the time without experiencing faults. In this condition, a desideratum of computing circuits built out of current technology nodes is fault tolerance. A circuit robust to environmental aggression (e.g., supply voltage variation, temperature, and cosmic radiation) enables an improved dependability profile and potentially extended useful lifetime expectancy. Moreover it provides a certain noise immunity, which one may trade for energy consumption by means of power supply scaling. In this work, we perform a fault tolerance assessment of state-of-the-art or reliability enhanced LDPC decoders, while emphasizing the potential benefits in terms of throughput or power consumption.

Main Results

Seven state-of-the-art and reliability-enhanced LDPC decoders have been implemented in VHDL/Verilog and mapped on a Xilinx Virtex-7 FPGA platform. All decoders have been exposed to external aggression via two approaches that emulate in different ways in-field real-life scenarios, namely voltage scaling and RTL saboteur-based simulated fault injection.

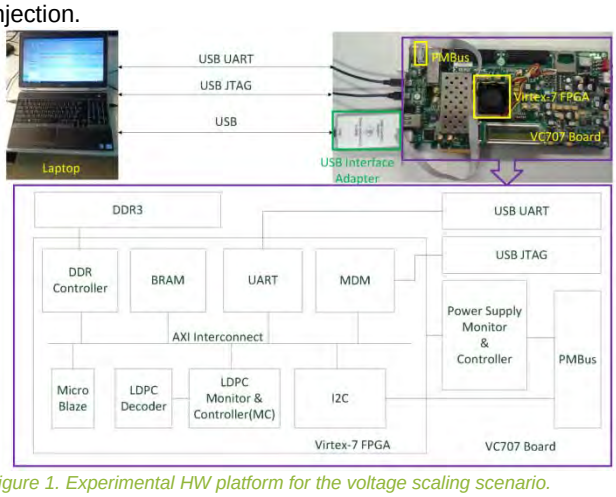

Figure 1. Experimental HW platform for the voltage scaling scenario.

We developed an experimental hardware platform that allows us to simulate the decoder exposure to environmental aggression factors, e.g., temperature, and cosmic radiation, by diminishing the power supply voltage V_{dd} under its nominal value, which may results in timing faults. In this way, we can modulate the fault presence rate by means of the V_{dd} value, but we cannot control the fault occurrence location on the decoder real estate.

We developed a hybrid fault injection HDL/C++ simulation framework that allows for decoder simulation in the presence of errors, which location and density are derived according to decoder architectural and implementation details. Related to this, we also introduced a methodology to create a fault map meant to guide the fault injection process, which is reflecting the contribution of the internal organization of each decoder basic building block to the fault error rate at its outputs.

We evaluated the implemented decoders under both scenarios, over different technology and environmental aggression profiles and quantified their figure of merit in terms of error correction performance, throughput, and energy/bit. We conducted a thorough analysis of the voltage scaling and simulated fault injection results, which confirm the fault-tolerance capabilities of LDPC decoders and serve as guideline for the selection of a decoder class that exhibits the best trade-off in terms of performance and ability to tolerate faults. In particular our experiments indicate that voltage scaling may result in energy savings between 45% and 67%, while preserving decoder's nominal throughput and error correction performance. Based on simulated fault injection results, the decoder potential to increase throughput by means of overclocking is also estimated to be between 77% and 150%, while preserving the nominal error correction performance.

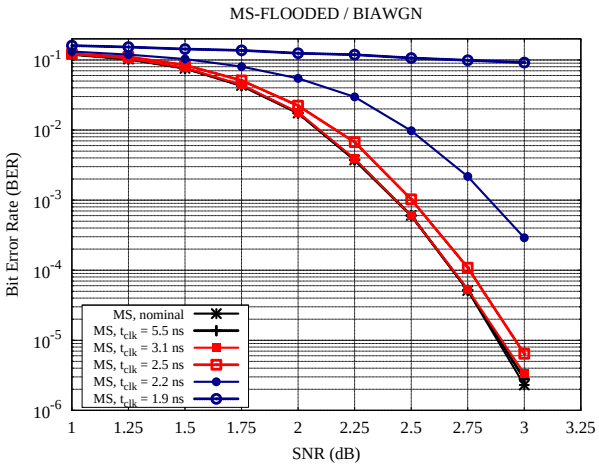

Figure 2. Bit error rate performance for the faulty Min-Sum LDPC decoder (fault injection scenario).

Related Publications:
[1] A. Amaricai, V. Savin, O. Boncalo, N. Cucu-Laurenciu, J. Chen, S. Cotofana, "Timing Error Analysis of Flooded LDPC Decoders", IEEE Int. Conf. on Microwaves, Communications, Antennas, and Electronic Systems (COMCAS), Nov. 2-4, 2015, Tel-Aviv, Israel.
[2] A. Amaricai, N. Cucu-Laurenciu, O. Boncalo, J. Chen, S. Nimara, V. Savin, S. Cotofana "Multi-Level Probabilistic Timing Error Reliability Analysis Using a Circuit Dependent Fault Map Generation", IEEE Conf. on Design of Circuits and Integrated Systems (DCIS), Nov. 25-27, 2015, Estoril, Portugal.

FPGA Design of High Throughput LDPC Decoder Based on Imprecise Offset Min-Sum Decoding

Research topic: wireless communications, error correcting codes.

Authors: T. Nguyen-Ly, V. Savin

Abstract: We propose two new LDPC decoding algorithms that may be seen as imprecise versions of the Offset Min-Sum (OMS) decoding. We show that they allow significant reduction in the memory (25%) and interconnect, and we further propose a cost-efficient check-node unit architecture, yielding a cost reduction of 56% with respect to the baseline. The proposed algorithms are then used as decoding kernels within an FPGA based layered architecture for a (3,6)-regular Quasi-Cyclic LDPC code. Synthesis post place and route results on Xilinx Virtex-6 FPGA device show a throughput increase of 48-83% with respect to the OMS decoder, while providing very close error correction performance, despite the impreciseness introduced in the processing units.

Context and Challenges

We address the design of cost-effective LDPC decoders, suitable for the new generation of communication systems, requiring increased data rates and reduced energy footprint. Our approach is to integrate imprecision mechanisms for message computing and storage in LDPC decoders, which is seen as an enabler for cost-effective, high-throughput, and/or low-power optimizations.

Main Results

Practical hardware implementations of LDPC decoders are mainly based on the Min-Sum (MS) algorithm or enhanced versions of it, such as Normalized MS (NMS) and Offset MS (OMS). In this work, we propose two new decoding algorithms that introduce two levels of impreciseness to OMS, aimed at improving cost efficiency and increasing throughput, with no or only negligible degradation of the error correction performance. The first level of impreciseness, referred to as Partially OMS (POMS), comes from replacing the offset rule by a simple erasure of the least significant bit. We also propose a simple architecture for the check-node processing unit (CNU), which avoids the use of comparator trees. Besides, the error-correction performance of the proposed POMS is very close to that of the OMS, both outperforming the conventional MS decoding. We further introduce a second level of impreciseness in the CNU, by suppressing some of the signals computed by the POMS decoder.

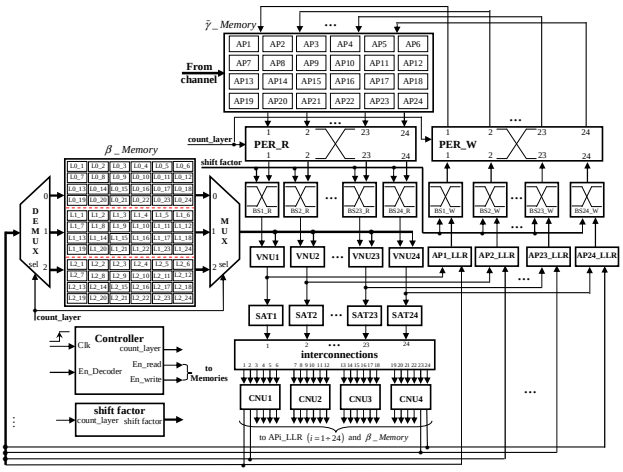

Figure 1. Block diagram for (3,6)-regular LDPC decoder.

The corresponding decoder is referred to as Imprecise-POMS (I-POMS) and we show that it allows further improvements in hardware cost and throughput. To demonstrate the benefits of the proposed POMS and I-POMS decoders in terms of hardware implementation, FPGA-based layered architectures using the proposed algorithms as decoding kernels have been implemented, for a (3, 6)-regular Quasi-Cyclic LDPC code of length 1296 bits (Figure 1). Implemented decoders have been evaluated in terms of cost, throughput (Table 1) and decoding performance (Figure 2). Implementation results on Xilinx Virtex-6 FPGA device (XC6VLX240T-1FF1156) highlight the following advantages of our proposal: (i) significant memory and interconnect savings, (ii) simple CNU architecture, requiring only a very small number of AND gates, (iii) increased throughput, up to 36% with respect to the MS and 83% with respect to the OMS, and (iv) good to very good decoding performance, despite the impreciseness introduced in the processing units.

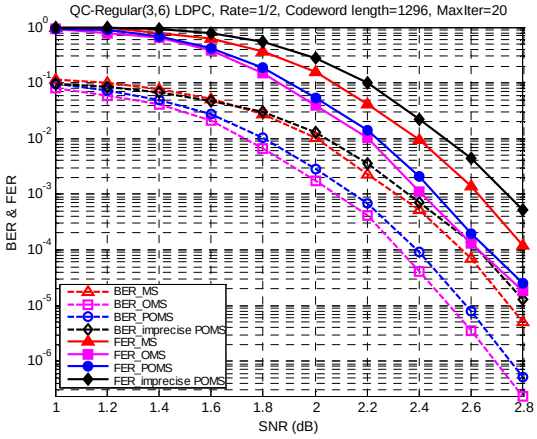

Figure 2. Decoding performance for proposed algorithms (AWGN channel).

Table 1: Implementation results (Xilinx Virtex-6 FPGA – ISE 14.6)

Decoders	No. Slice Registers	No. Slice LUTs	No. BRAMs	Maximum Frequency	Throughput @20iter	Throughput increase	SNR gain @BER=10^{-5}
MS	23352	95188	144	164MHz	1.77Gbps	0%	0dB
OMS	23352	97604	144	122MHz	1.32Gbps	-25%	+0.2dB
POMS	23352	93202	120	181MHz	1.95Gbps	+10%	+0.16dB
I-POMS	23352	90872	120	223MHz	2.41Gbps	+36%	-0.08dB

Related Publications:
[1] T. Nguyen-Ly, K. Le, F. Ghaffariy, A. Amaricai, O. Boncalo, V. Savin and D. Declercq, "FPGA Design of High Throughput LDPC Decoder based on Imprecise Offset Min-Sum Decoding", *IEEE International New Circuits And Systems Conference (NEWCAS)*, Grenoble, France, June 2015.

Random Access Protocols for Machine-to-Machine Applications in Dense Network Environment

Research topic: machine-to-machine communications, random access protocols

Authors: B. Mawlawi and J.-B. Doré

Abstract: machine-to-machine communications based on cellular networks are severely disrupted when an extremely large number of devices in the service coverage is considered. Collisions between the senders due to the large number of devices lead to communication problems. For that purpose, we proposed a new access method derived from the well-known CSMA/CA with RTS/CTS technique and proved that an important gain can be achieved in terms of system performance particularly when the network is heavily loaded. This new scheme has a particular interest for broadband machine-type communication and its future application.

Context and Challenges

Random protocols are promising candidates for future wireless systems dedicated to machine-to-machine (M2M) communication. Such protocols are usually based on a random access with simple techniques of medium sensing and deferring to reduce collisions while avoiding the use of complex schedulers. Among different protocols, Carrier-sense multiple access/collision avoidance with a Request-To-Send/Clear-To-Send (CSMA/CA-RTS/CTS) is a protocol which could be adopted for M2M scenarios. Such approach is efficient to avoid collisions between data packets but in a very dense network, the random access used to send the RTS suffers itself from a high probability of collision which degrades the performance. In order to mitigate this effect, RTS collisions should be reduced. We have studied how to adapt the classical CSMA/CA-RTS/CTS access method for dense scenario.

Main Results

CSMA/CA-RTS/CTS access method is efficient to avoid collisions between data packets but in a very dense network, the random access used to send the RTS suffers itself from a high probability of collision which degrades the performance. In order to mitigate this effect, RTS collisions should be reduced. This work proposes to address this issue by splitting the common channel in sub-channels for transmitting the RTS messages. While the common channel is used as a whole for data transmission. Multiple nodes can then contend in time and frequency for these RTS sub-channels, thereby reducing RTS collisions and increasing overall efficiency. In this work, we thus derive a complete protocol solution relying on CSMA/CA - RTS/CTS multiplexing a multi-channel configuration for RTS messages and a unique channel for data transmission [1]. An enhanced version based on users scheduling is integrated as well [2]. We also study how the access method could be optimized with a multi carrier physical layer. This strategy is shown to provide better system performance particularly for loaded networks. An accurate analytical model derived as a straightforward extension of the Bianchi model is analyzed and validated by simulations [1]. Performance in terms of saturation throughput, transmission delay and packet drop probability is discussed.

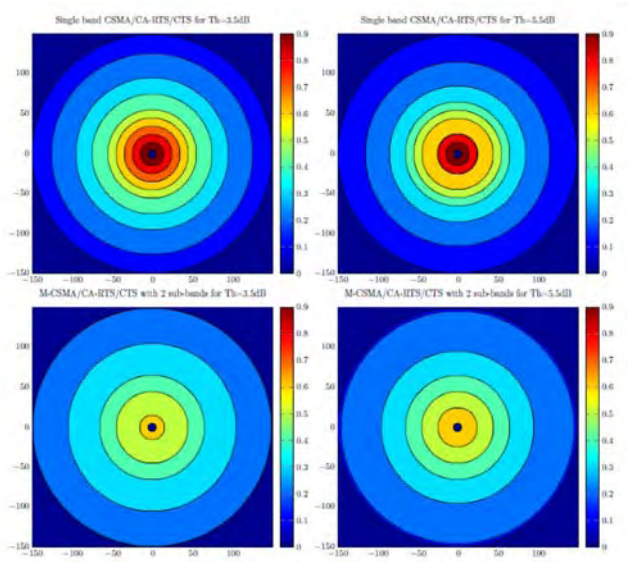

Figure 1. Successful transmission rate for Gaussian channel over a cellular network modelled by a circular map of radius = 300m, x and y axis presents the cartesian coordinates.

Moreover, we have demonstrated that the proposed scheme introduces better Quality of Service for nodes far from the access point (AP) (Figure 1); it allows far nodes to transmit even in the presence of closer nodes to the AP. The proposed scheme is more spatially fair compared to classical CSMA/CA [3].

Perspectives

The definition of a new access scheme for dense network deployment based on random access has a particular interest for the next generation of broadband machine-type communication. In particular it could give a real improvement for contexts requiring heavy wireless communications and plug and play deployments such as scenario for the industry 4.0.

Related Publications:

[1] B. Mawlawi, J.-B. Doré, N. Lebedev, J.-M. Gorce, “Modélisation Analytique du protocole Multi-Bande CSMA/CA", 25eme colloque Gretsi, 8-11 Sept. 2015, Lyon, France.

[2] B. Mawlawi, J.-B. Doré, "CSMA/CA with RTS/CTS Overhead Reduction for M2M Communication with Finite Retransmission Strategy”, IEEE Int. Wireless Communications & Mobile Computing Conf., Aug 2015, Dubrovnik, Croatia.

[3] B. Mawlawi, “Random access for dense networks: Design and Analysis of Multiband CSMA/CA”, PhD Thesis INSA Lyon, 2015. Available online.

Overview of the IEEE 1900.7-2015 Standard Based on FBMC Technology

Research topic: wireless communications, TV white spaces, FBMC

Authors: D. Noguet, J.-B. Doré, B. Miscopein

Abstract: white space communications have attracted a particular interest after some national regulators have authorized TVWS unlicensed secondary usage. The IEEE 1900.7 working group has defined a specific air interface tailored to these applications. The standard, published in 2016, is based on a Filter Bank Multi Carrier (FBMC) physical layer and a CSMA-CA MAC sublayer, both schemes proposed by Leti. To the best of our knowledge, this is the first time a radio standard is based on FBMC technology. We provide here a brief description of the technology considered by the IEEE 1900.7 working group, providing also a more global perspective related to White Space research and standardization.

Context and Challenges

In the recent years, there has been a worldwide concern related to spectrum shortage. One of the means to make new spectrum available is through sharing. The Digital Switch Over (DSO) in TV bands has resulted in making the so-called TV White Space (TVWS) UHF spectrum available. TVWS availability depends on TV broadcast frequency usage profile, thus changing across time and space. TVWS usage relies on unlicensed secondary Dynamic Spectrum Access (DSA) under the principle on a non-harmful interference with incumbent users. All broadband TVWS standards (ECMA392, IEEE802.22, IEEE802.11af) are based on Cyclic Prefix - Orthogonal Frequency Division Multiplexing (CP-OFDM) physical layer (PHY), often inherited from previous standard developments such as IEEE 802.16e or IEEE802.11a. These standards have been adapted to make them suitable for TVWS operation. However, because of the very stringent requirement on Adjacent Carrier Leakage Ratio (ACLR) to ensure interference free operation for incumbents, and the dynamic nature of DSA, it was shown in the literature that CP-OFDM was probably not the best choice for TVWS PHY, although probably the fastest in terms of market readiness and backward compatibility.

Main Results

The IEEE 1900.7-2015 standard, published in Q1 2016, results from a clean slate analysis where the working group has tried to identify the most suitable PHY/MAC technology for TVWS. In that context, Leti has proposed a Filter Bank Multi Carrier (FBMC) PHY and a contention based CSMA-CA MAC. These two technologies have been approved and are now part of the IEEE 1900.7-2015 standard. The IEEE 1900.7 PHY has been specified to be very flexible in terms of spectrum profile allocation [1]. For instance, the 2 MHz profile has been designed to cope with 6 MHz and 8 MHz TV channelization in order to fit best to regulation worldwide. This profile also enables narrower spectrum allocation. Figure 1 shows an example of 2 fragments of 2 MHz each separated by an unused 2 MHz fragment, using the IEEE 1900.7-2015 FBMC PHY [2]. Given as a reference, the LTE CP-OFDM spectrum profile is based on 1024 carriers and a guard interval (GI) of 72 samples, similar to 10 MHz LTE signal. The figure illustrates the much focalized spectrum localization of IEEE 1900.7-2015 vs CP-OFDM based systems in the edges of the spectrum and in the gap.

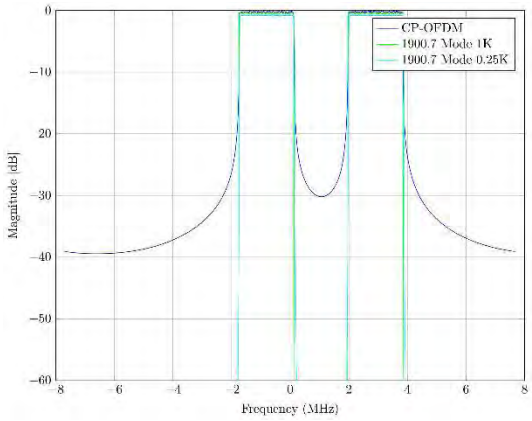

Figure 1. IEEE 1900.7 spectrum profile example.

The MAC sublayer is based on a Carrier Sense Multiple Access with Collision Avoidance (CSMA-CA) approach using “Request To Send” and “Clear To Send” (RTS/CTS) handshake mechanism [1]. A basic network operates in a master-slave mode. The network coordinator device indicates its presence in a network to other devices by transmitting beacon frames. This allows other devices to perform the network coordinator discovery and network join procedures. TVWS operation induces that before the completion of the master discovery procedure, a device does not know the operating channels. This results in a channelization combinatorial far too large to be discovered through blind scanning. In IEEE 1900.7 the data carried by a beacon frame is designed to speed up the discovery process. Additionally an optimized channel switching mechanism is implemented to maintain the connectivity when a new channel map is requested by higher layers [1].

Perspectives

IEEE 1900.7-2015 has a particular interest to give connectivity to rural area, or for outdoor wifi coverage extension. It is the first wireless standard based on FBMC modulation, which has been identified as a candidate for future 5G cellular technologies. Also, the shared spectrum concept of TVWS gives a particular interest to this standard as 5G may also resort on such a disruptive license regime. Leti has proven skills and background in efficient hardware implementation of advanced modulation modems.

Related Publications:
[1] S. Filin, D. Noguet, J.-B. Doré et al, “IEEE 1900.7 Standard for White Space Dynamic Spectrum Access Radio Systems“, IEEE Conference on Standards for Communications & Networking (CSCN’15), 2015.
[2] D. Noguet, J.-B. Doré, B. Miscopein, “Preliminary performance evaluation of the FBMC based future IEEE 1900.7 Standard”, IEEE Conference on Wireless Personal Multimedia Communications, 2015.

Blind Phase Tracking Algorithm for FBMC Receivers

Research topic: wireless communications, new waveforms

Authors: J-B. Doré, V. Berg

Abstract: Non synchronous random access is envisaged for sporadic traffic to limit the amount of signaling messages Burst data transmission is commonly used in wireless communication systems: a preamble at the start of each burst is used to synchronize the receiver. When the initial estimation of the Carrier Frequency Offset is coarse, a phase tracking algorithm is required to track any residual phase error during the payload transmission. In this work, a blind phase tracking algorithm for Filter Bank Multicarrier waveforms based on sign statistics is described. It outperforms the state of the art algorithms while reducing the requirements on complexity.

Context and Challenges

The current generation of cellular networks has been optimized to deliver high bandwidth pipes to wireless users but requires strict synchronization and orthogonality between users within a single cell. The advent of the smartphone and the expected explosion of Machine-Type-Communication (MTC) are posing new and unexpected challenges. Spectrum agility and asynchronous transmission have encouraged the study of alternative multicarrier waveforms such as Filter Bank Multicarrier (FBMC) to provide better adjacent channel leakage performance, robustness again timing misalignment without compromising spectral efficiency [1]. Channel estimation techniques have been thoroughly studied in this context [2]. However due to the noise, the estimation of the carrier frequency offset (CFO) during the preamble is not perfect and phase tracking algorithms are therefore required.

Main Results

Blind estimation of phase variations has already been explored for Orthogonal Frequency Division Multiplex (OFDM). The state-of-the-art algorithms require a significant number of active carriers. Moreover, complexity is quite significant particularly for the most promising algorithms as unconditional Maximum Likelihood (ML) estimation is required.

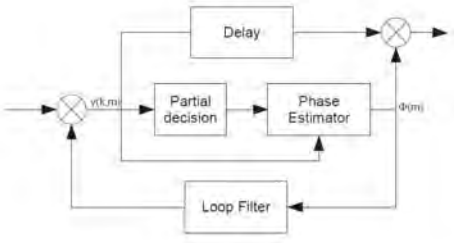

Figure 1. Proposed blind phase tracking algorithm.

In [3], two new blind algorithms designed to improve the phase tracking scheme of the receiver have been proposed. A first method is based on interference reconstruction scheme. Then, a low complexity algorithm has been evaluated based on sign statistics. Both algorithms are based on a common architecture depicted in Figure 1.

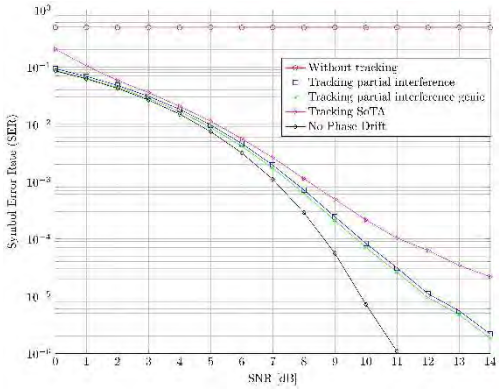

Figure 2. Performance of the proposed low complexity phase tracking algorithm based on sign approximation.

The SER (Symbol Error Rate) has been evaluated for various signal-to-noise ratio over an AWGN (Additive White Gaussian Noise) channel and the behavior of the tracking algorithms were studied (Figure 2). The proposed low complexity algorithm leads to better performance and very low error floor. A sub-optimal algorithm was designed to reduce the complexity. It consists in considering a subset of neighboring symbols to recover and mitigate the interference generated by the FBMC waveform. This algorithm outperforms the state of the art algorithm. However, the error floor introduced by the interference is still high when only neighboring carriers are used for the interference determination.
Then, a sign algorithm has been derived from it. It outperforms the other algorithms and benefits from a very low level of complexity. The proposed tradeoff between performance and complexity has a particular interest for blind phase tracking.

Perspectives

This scheme has been implemented on a FBMC proof-of-concept demonstrator and the simulation results have been confirmed by over-the-air measurements. As filtered waveforms are currently the envisaged candidates for 5G, the proposed scheme has a particular interest in wireless cellular context.

Related Publications:
[1] J.-B. Doré, V. Berg, N. Cassiau, D. Kténas, “FBMC receiver for multiuser asynchronous transmission on fragmented spectrum,” EURASIP Journal, Special Issue on Advances in Flexible Multicarrier Waveform for Future Wireless Communications, vol. 2014, 2014.
[2] J.-B. Doré, V. Berg, V., D. Kténas, "Channel estimation techniques for 5G cellular networks: FBMC and multiuser asynchronous fragmented spectrum scenario", Transactions on Emerging Telecommunications Technologies, 2015.
[3] J.-B. Doré, V. Berg, “Blind Phase Tracking Algorithm for FBMC Receivers”, Twelfth International Symposium on Wireless Communication Systems (ISWCS), 25–28 August 2015, Brussels, Belgium.

Turbo-FSK: a New Uplink Scheme for Low Power Wide Area Networks

Research topic: low power wide area networks, PHY layer, Turbo codes

Authors: Y. Roth, J-B. Doré, L. Ros (GIPSALAB), V. Berg

Abstract: The Internet of Things aims at connecting several billions of devices that are expected to be low cost, low power, and able to achieve long range wireless communication. While current Machine-to-Machine technologies tend to rely on repetition schemes to meet the required level of specifications, we proposed a new approach in a scheme called Turbo-FSK. Highly robust communication is achieved with a simple transmitter, as complexity is deported on the receiver side. Results have been compared to standard modulations using repetition schemes. A significant performance gain is achieved even with small packet sizes.

Context and Challenges

Machine-to-Machine (M2M) communication is growing exponentially such that several billions of devices are expected to be connected to the Internet-of-Things in the next decade. Low Power Wide Area (LPWA) networks are considered for long range M2M applications. The challenges for LPWA terminals include low power consumption and excellent sensitivity. A few industrial solutions exist and rely on the well-known spreading factor mechanism to lower the sensitivity level at the expense of spectral efficiency loss. Orthogonal modulations have also been used, and theory shows that the channel capacity limits can be reached with an infinite size of alphabet. As this is not a realistic option, a scheme combining orthogonal waveforms (Frequency-Shift-Keying, FSK) with repetition and a turbo decoder has been studied [1,2].

Main Results

The block diagrams of the transmitter and the receiver are given in Figure 1. The information bits are repeated λ times with different interleaving, and then modulated by a convolutional-FSK. At the receiver side, a set of λ decoders will take into account the observations of the channel and the information extracted by all the other decoders to perform an estimation of the information bits. The process is iteratively repeated.

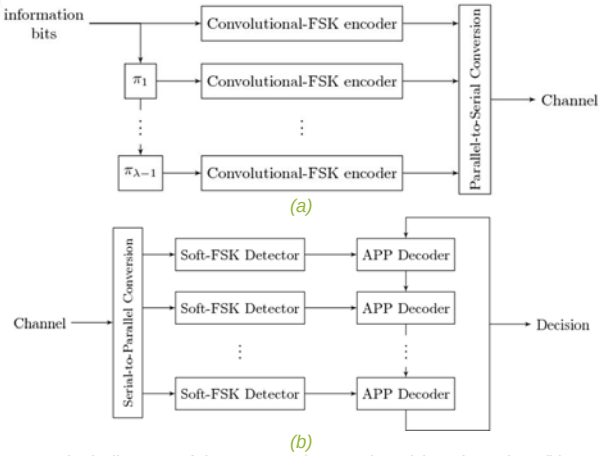

Figure 1. Block diagram of the proposed transmitter (a) and receiver (b)

The normalized spectral efficiency of the newly proposed scheme (in bits/s/Hz) can be expressed as:

$$\eta = \frac{log_2(M-1)}{\lambda M}$$

where M is the size of the FSK alphabet, N the size of the information block. Parameters M, λ and N have an impact on the performance. In the LPWA context, short values of N are envisaged.

The performance of standard M-FSK and BPSK modulations for various repetition factors λ is compared with the newly proposed scheme in Figure 2. The normalized spectral efficiency is expressed as a function of the energy efficiency, also denoted E_b/N_0, for the different schemes along with Shannon's limit.

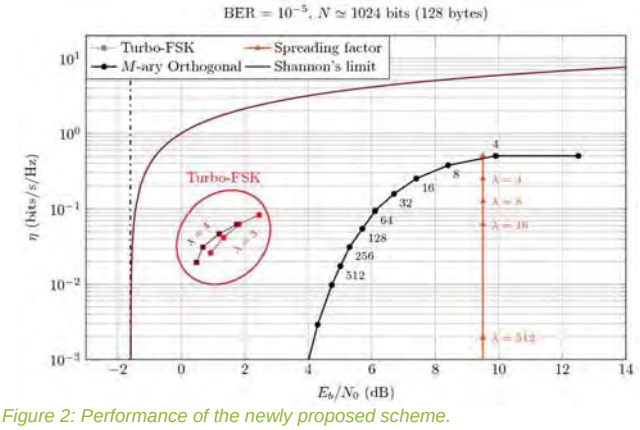

Figure 2: Performance of the newly proposed scheme.

The Turbo-FSK scheme outperforms the standard modulation currently deployed for LPWA applications. The performance is only 2.3 dB from Shannon's limit with a realistic information block size of N = 128 bytes. These results demonstrate the benefit of mixing an orthogonal waveform and repetition with turbo processing at the receiver side.

Perspectives

The proposed scheme performs very well even with small block sizes. The energy efficiency is significantly better compared to state-of-the-art schemes. However, the synchronization for the considered SNR ranges and the complexity remain open questions that are currently under investigation.

Related Publications:
[1] Y. Roth, J.-B. Dore, L. Ros, V. Berg, "Turbo-FSK: A New Uplink Scheme for Low Power Wide Area Networks", IEEE 16th Int. Workshop on Signal Processing Advances in Wireless Communications (SPAWC), June 2015, pp. 81--85.
[2] Y. Roth, J.-B. Dore, L. Ros, V. Berg, "Turbo-FSK : une nouvelle technique de communication montante pour les réseaux longue portée basse consommation", congrès GRETSI, Lyon, Septembre 2015.

02

WIRELESS SHORT-RANGE AND CONTACTLESS SYSTEMS

- Optical communications (LiFi)
- Wireless sensor networks
- Secure communications
- Secure devices

Indoor/Outdoor VLC High Data Rate Reception Using Semi-Transparent Photovoltaic Modules

Research topic: LiFi, free-space optical communication

Authors: L. Maret, D. Kténas

Abstract: light-fidelity (LiFi), also called visible light communication (VLC), rely on optical sensors to translate the received modulated optical flux into an electrical signal. The receiver is expected to operate both indoor and outdoor and photovoltaic (PV) modules appear as a candidate solution to this issue. We characterized innovative Semi-Transparent (ST) PV modules from SunPartner and we showed that these solar cells offer new performances in high ambient lighting environments, making it suitable for outdoor operation.

Context and Challenges

A new kind of optical receiver for VLC is considered in this study: innovative semi-transparent photovoltaic modules, usually built for a primary function of energy harvesting, while being invisible when integrated. Used in a mobile terminal, these modules can charge the terminal batteries, power the receiver when in operation, or at least extend its autonomy. It turns out that these modules, even if primary built for energy harvesting, are able to retrieve optical signals coming from a VLC transmitter. Firstly, we demonstrate the VLC performance of these innovative semi-transparent solar-cell modules, then we show their ability to correctly demodulate VLC signals under high ambient light environment when they are positioned near sources or outdoor.

Main Results

VLC is a communication technology using visible light spectrum by means of intensity modulation on LED, which implies that only real and unipolar signals can be transmitted through LED, in order to provide both lighting and transmission functions. Direct-Current Optical-OFDM is used here, to transmit bipolar OFDM signals with the help of the DC voltage of LED polarization. The experimental setup is shown in Figure 1.

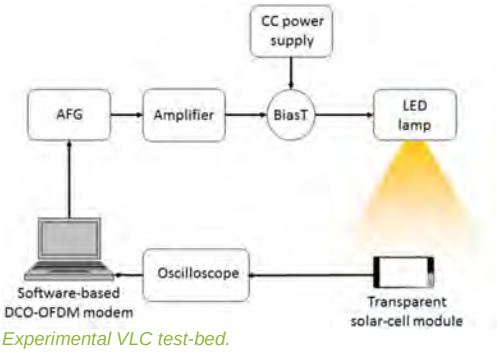

Figure 1. Experimental VLC test-bed.

In Fig. 2, the SunPartner Technologies (ST) Photovoltaic (PV) module (“Cam”) shows good bandwidth for communication, but above all, at high signal level (near sources for instance), it outperforms classical avalanche photodetector (APD, “Ham”). In Fig. 3, SNRs under high ambient light environment show that the classical APD offers a good bandwidth until 19 000 lux DC. If the ambient lighting is larger than 19 000 lux, the APD bandwidth decreases. On the contrary, the ST PV receiver is not affected by the ambient lighting until 50 000 lux.

These results prove that such innovative solar-cell modules may be able to provide a 5-MHz bandwidth for a VLC signal reception in outdoor operation with high sunny conditions.

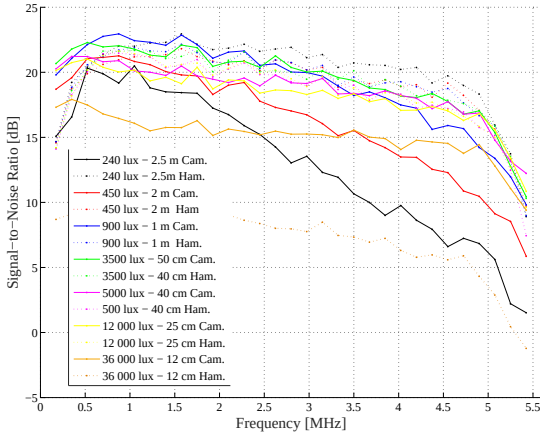

Figure 2. SNR of ST PV Module and APD function of distance.

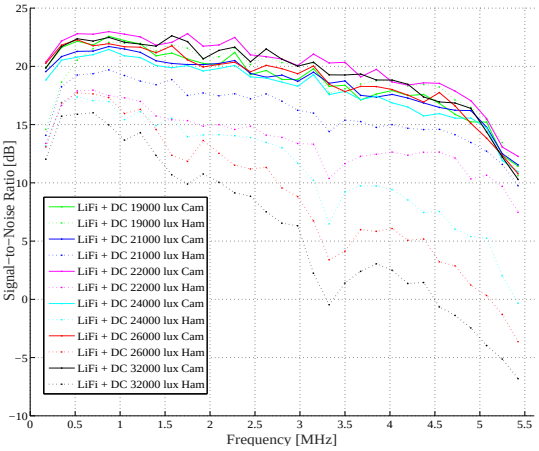

Figure 3. SNR under high ambient light environment.

Perspectives

These studies were followed by the development of one of the first LiFi demonstrator using smartphone ST PV module with 5Mbit/s downlink data rate at 1m (presented at the Mobile World Congress 2016). Perspectives include the adaptation of multicarrier waveforms for data rate increase and link throughput adaptation.

Related Publications:
[1] E. Bialic, L. Maret, D. Kténas, “Specific innovative semi-transparent solar cell for indoor and outdoor LiFi applications”, Applied Optics, Vol. 54, No 27, pp 8062-8069, September 20, 2015,

ISO/IEC 14443 VHBR: Influence of the Proximity Antennas on the PCD-to-PICC Data Link Performance

Research topics: RFID, VHBR, ISO14443

Authors: V. Berg, J-B. Doré, F. Frassatti

Abstract: The demand for faster transmission rates in radio frequency identification (RFID) has led to the adoption of phase-shift keying (PSK) modulations for the communication between proximity coupled devices (PCD) and proximity integrated circuit cards (PICC). This work derives a transmission model to analyze the inter-symbol interference generated by the PCD-to-PICC coupled antennas. An equalizer structure is then introduced and performance are compared against previous generations of very-high bit rate (VHBR) systems using amplitude shift keying, showing that PSK modulations proposed for VHBR can be robust even when the resonance of the antenna circuits is relatively high.

Context and Challenges

The RFID technology has been adopted by electronic passports to exchange biometric information with the aim of strengthening international border security. These new applications have significantly increased the requirement on the transmission rate over the contactless interface and led to the adoption of a very high bit rate (VHBR) communication amendment to the proximity standard ISO/IEC 14443. A VHBR amplitude shift keying (ASK) amendment was first adopted in 2012 to enable data rates up to 6.8Mb/s from the Proximity Coupling Device (PCD) to the Proximity Integrated Circuit Card (PICC). The standard was further amended in 2013 to enable data rates up to 27.1Mb/s with the introduction of phase shift keying (PSK). In this study, we analyze the impact of the PCD-to-PICC transmission channel on the performance of the VHBR data link using a linear system and we derive an equalizer-based receiver structure adapted to the nature of the received signal at the PICC.

Main Results

The frame structure introduced by PSK amendments (ISO/IEC 14443-amd5) can be used as the training sequence of an equalizer structure. Previous work proposed an alternative receiver based on a Viterbi algorithm to improve the performance of the PSK receiver [1]. In [2], we proposed to evaluate how the inter-symbol interference (ISI) generated between the PCD and the PICC may be mitigated using an interference canceller based on a decision feedback equalization structure.

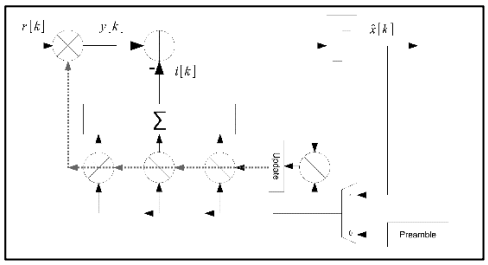

Proposed equalizer structure for VHBR PSK receivers.

A linear transmission model of the proximity antennas from the PCD to the PICC for VHBR RFID communications has been proposed and derived. Then, this transmission model has been analyzed using a realistic set of parameters in order to estimate ISI as a function of the overall quality factor (Q-factor) of the system. The impact of ISI on the performance of VHBR-PSK has been measured eventually and it was concluded that with a simple interference canceller structure, PSK VHBR communication could be more robust than ASK VHBR communication.

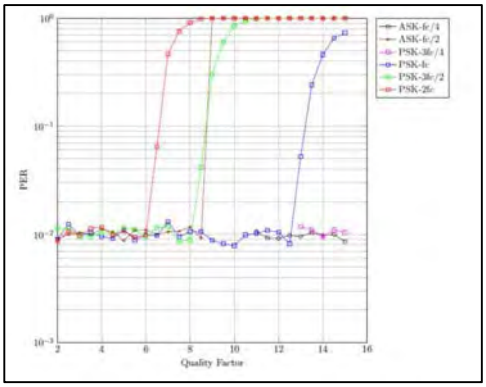

Packet Error rate (PER) performance and comparison with VHBR ASK.

A proof-of-concept based on discrete components has been developed. These results are validated in the laboratory by field experiments.

Perspectives

These results are even more noticeable as ASK VHBR provides lower data rates than PSK VHBR. The model was further refined to understand the impact of the regulation circuit of the PICC on the transmission channel. Although the linearity of the PICC circuit is far from perfect in a PICC circuit because of the constraints on the technology, this model gives a fair understanding of the potential robustness of VHBR PSK under realistic conditions. An ASIC has been designed and taped-out. It integrates a new RF front end architecture associated with dedicated baseband processing based on the principles described in this work.

Related Publications:
[1] J.-B. Dore, N. Touati, and F. Pebay-Peyroula. “MLSE detector for beyond VHBR contactless air interface,” 2012 IEEE Int. Conf. on RFID-Technologies and Applications (RFID-TA), pp. 222–227, Nov 2012.
[2] V. Berg, J.-B., Dore, F. Frassati, “ISO/IEC 14443 VHBR: influence of the proximity antennas on the PCD-to-PICC data link performance,” 2015 Int. EURASIP Workshop on RFID Technology (EURFID), pp.81-86, 22-23 Oct. 2015.

Context Aware Decision Module for Mobility Management in Wireless Sensor Networks

Research topic: protocols, wireless sensor networks

Authors: L. H. Suraty Filho, B. Denis, M. Maman

Abstract: context-aware systems are able to react specifically to the actual environment conditions and rapidly adapt its behavior according to the changing context without explicit user intervention. A group-weighted fuzzy-based (GWFQDA) decision module has been proposed allowing the definition of profiles with respect to the application needs. This module has been applied for mobility management of WSNs with low-duty cycle and battery/computational constraints. Results show that our approach achieves a higher packet delivery ratio while maintaining a reasonable end-to-end delay. It can also reduce the number of disconnections and thus improves the overall network performance.

Context and Challenges

How to continuously inter-operate a large number of mobile nodes in an efficient way is highly challenging in large scale Wireless Sensor Networks (WSN). Mobility traditionally leads to a degradation of the link quality, to frequent route changes and connectivity loss. In order to address the different challenges encountered in a scenario with strong mobility, we need a context-aware decision module adapting automatically and dynamically to its environment thanks to the combination of a multitude of metrics and considering the battery/computational constraints and low-duty cycle of WSNs.

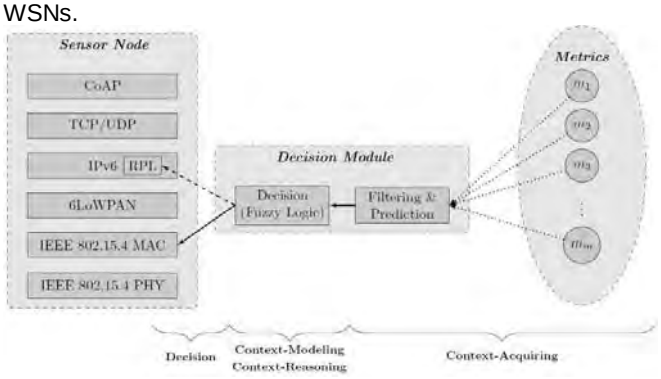

Figure 1. Context-aware decision module on IoT reference model.

The decision module is composed of a context-acquiring part gathering raw information regarding the environment, a context-modeling part assembling parameters (battery size, signal strength, etc.) into groups (energy, link quality, network distribution, etc.) according to their closeness and a context-reasoning part elaborating relevant higher-level information.

In this study, this context-aware decision module has been applied for mobility management i.e. it will decide whether a mobile sensor node will remain attached to the same Access Point (AP) or will handover to a new one.

In the literature, several approaches propose a threshold and hysteresis margin method using signal strength but they can lead to incorrect or undesirable handoff decisions. Heuristic and adaptive techniques (e.g., neural networks, fuzzy logic, etc.) have thus been proposed to consider various input criterion but they can lead to an increased complexity of the system. For this reason, we have proposed a group-weighted fuzzy-based (GWFQDA) decision module integrated within IEEE 802.15.4 standard easing the integration and the differentiation of metrics. This module uses both fuzzy-logic and grouping metrics allowing the definition of profiles with respect to the application needs. The Quantitative Decision Value (QDV) of each candidate AP a, group of metrics g and metric m_g belonging to group g is then defined as follows:

$$QDV_a = \sum_g \beta_g \sum_{m_g} \alpha_{m_g} w_{m_g} QEV_{a,m_g}$$

where α_{m_g} represents the weight assigned to the metric *m* of group *g* and β_g represents the weight assigned to the group *g*. The AP with the highest QDV is then selected.

Main Results

This mobility and multi-context management module adapts in real-time the intra-cluster communications depending on the detected local and temporal context patterns (i.e. in terms of nodes activity, mobility, energy autonomy, traffic, etc.) and triggers a handover mechanism ensuring the stability of the whole network.

We used WSNet, an event-driven packet-oriented network simulator, to validate and compare the performance of the proposed solution with those of conventional approaches (e.g. Standard without handover, Hysteresis, FQDA with or without threshold). Results show the importance of managing mobility on WSN and indicate that our approach achieves a higher packet delivery ratio while maintaining a reasonable end-to-end delay. It can also reduce the number of disconnections and thus improves the overall network performance.

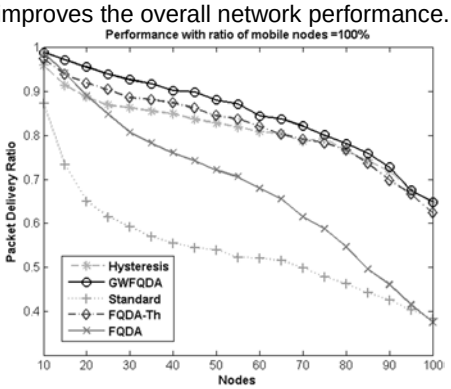

Figure 2. Average Packet Delivery Ratio for all the mobile nodes.

Perspectives

The proposed GWFQDA can be extended to an extensive number of metrics and does not require computational and storage capabilities, thus enabling fine adaptability to the WSN problem. More research regarding the integration of new metrics, the inter-cluster handover and the optimal selection of weights are expected in future works.

Related Publications:
[1] L. H. Suraty Filho, B. Denis, M. Maman, "Design and Analysis of Distributed Mobility Management Schemes for Wireless Sensor Networks", European Wireless 2015.

Link Selection Schemes for High Precision Localization in Cooperative Vehicular Networks

Research topic: intelligent transportation systems, localization

Authors: G. M. Hoang, B. Denis

Abstract: Dedicated Short Range Communications (DSRC) support high-precision cooperative localization in GPS-enabled vehicular networks, by enabling decentralized data fusion and vehicle-to-vehicle radio measurements. However, considering all the radio links with respect to neighboring vehicles (i.e., regardless of their actual contribution into the fusion problem) generates high computational complexity and heavy communication loads, which adversely congest the DSRC channel for other services. In this study, we thus propose theoretical selection criteria to identify the best subset of neighbors under various practical GPS conditions. We show that significant traffic could hence be saved, disclosing interesting perspectives in terms of transmit rate/power control or fusion rate control.

Context and Challenges

High-precision localization is flagged today as a critical requirement and major enabler of emerging Cooperative Intelligent Transport System (C-ITS) applications. For instance, Road Hazard Warning (RHW), safety of vulnerable road users and autonomous driving or platooning would require a precision of a few 10s of cm, which is not yet available by any mass market low-cost GNSS technology. Accordingly, Dedicated Short Range Communication (DSRC) (a.k.a. IEEE 802.11p or ITS-G5), which has been originally intended for wireless communications between vehicles (V2V), is now envisaged to support new cooperative positioning (CP) functionalities. The latter aim at fusing on-board GPS estimates with V2V range measurements relying either on the Received Signal Strength Indicator (RSSI) of broadcasted Cooperative Awareness Messages (CAMs) or even more accurate ranging technologies (e.g. Ultra Wideband) (Fig. 1). However, most recent state-of-the-art contributions assume exhaustive cooperation causing channel congestion, as well as homogeneous and too optimistic input measurements (i.e., in terms of GPS quality and V2V radio channel).

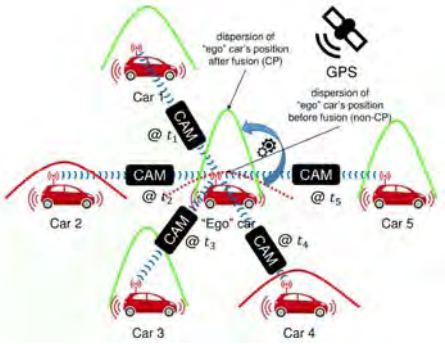

Figure 1. Typical cooperative localization scenario in a GPS-enabled vehicular network, where Context Awareness Messages (CAMs) convey information about local estimates and related uncertainty (red or green schematic densities).

Main Results

In this context, one stake is to define rigorous and robust criteria to select only the best subset of available links with respect to neighboring cars, while coping with varying GPS operating conditions (including possibly large-scale error correlation) and intrinsic capabilities (i.e., low-cost, RTK, …). Then, new computationally efficient link selection algorithms have been proposed, relying on several variants of the Cramer-Rao Lower Bound (CRLB) [1], including a Bayesian formulation that better accounts for neighbors' location uncertainties [2]. The latter bounds characterize the expected position accuracy conditionally to selective V2V connectivity and link quality. The previous selection process is made compatible with a core fusion engine based on particle filtering, which also compensates for CAMs asynchronism through specific prediction models [1].

Simulation results show that selective fusion significantly reduces both computational complexity and required network traffic at limited precision degradation in comparison with exhaustive fusion when applying the nominal CRLB-based selection criterion in most cases (incl. long-term GPS-denied conditions), whereas its Bayesian variant (B-CRLB) is preferable in case of higher dispersion of local GPS quality/conditions among neighboring vehicles (results not shown herein) [2].

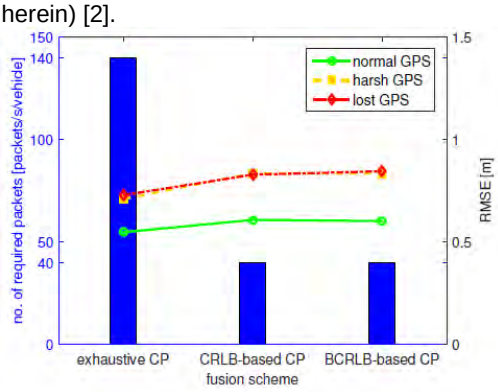

Figure 2. Trade-off between the number of required packets in CP (blue/left) and localization RMSE depending on GPS conditions (lost-yellow-green/right).

Perspectives

Future works concern CAMs overhead reduction, transmission rate/power control, as well as space-time correlation of GPS errors and V2V measurements [3].

Related Publications:

[1] G.M. Hoang, B. Denis, J. Härri, D. Slock, "Distributed Links Selection and Data Fusion for Cooperative Positioning in GPS-aided IEEE 802.11p VANETs", Workshop on Positioning, Navigation and Communication 2015 (WPNC'15), March 2015, Dresden, Germany.

[2] G.M. Hoang, B. Denis, J. Härri, D. Slock, "Select Thy Neighbors: Low Complexity Link Selection for High Precision Cooperative Vehicular", IEEE Vehicular Networking Conference 2015 (IEEE VNC'15), Dec. 2015, Kyoto, Japan.

[3] G.M. Hoang, B. Denis, J. Härri, D. Slock, "Breaking the Gridlock of Spatial Correlation in GPS-aided IEEE 802.11p-based Cooperative Positioning", IEEE Trans. on Vehicular Technology, Connected Vehicles Series, June 2016.

Channel-Based Cooperative Group Key Generation for Decentralized Wireless Networks

Research topic: physical layer security, secret key generation, ad hoc wireless networks

Authors: I. Tunaru, B. Denis

Abstract: in small-scale decentralized wireless networks, nodes can benefit from sharing the wireless medium to generate common secret keys and improve communications security through symmetric cryptography. We propose a new method to jointly generate and distribute group keys within cooperative scenarios involving more than two nodes, while exploiting all the available radio links in a full mesh topology and reducing over-the-air traffic. We show that an approach based on advanced deconvolution methods can save protocol resources and achieve longer keys in comparison with conventional key distribution methods, with acceptable degradations in terms of key bit matching agreement ratio.

Context and Challenges

Large amounts of personal and critical data are locally produced, exchanged, and collected in emerging device-centric applications (e.g., context-aware services, crowd sourcing in the Internet of Things, nomadic social networking...). Wireless communication means must thus securely carry information from remote sensors or users to centralized core networks, or even directly between mobile devices. Contemporary security architectures still mainly rely on high layer symmetric cryptography (based on common secret keys) for data encryption/decryption and Public Key Cryptography (PKC) for authentication and symmetric key distribution. However, in wireless decentralized or ad hoc networks, symmetric key distribution through PKC remains very challenging since it requires the presence of a central certified entity. Alternative approaches such as the Diffie-Hellman protocol or a pre-distribution of keying material, are respectively computationally demanding, neither flexible nor scalable enough. On the contrary, physical layer key generation, which relies on channel reciprocity (enabling agreement between legitimate users) and channel spatial decorrelation (ensuring secrecy with respect to distant attackers) can be extended to cooperative and/or mesh contexts in order to generate group keys for secure local broadcast communications or longer pairwise keys.

Main Results

Building on top of previous studies regarding quantization and reconciliation for single-link symmetric key generation [1]-[3], a novel original method has been proposed to exploit multipath channels in full mesh network topologies. This solution enables to jointly generate and distribute secret group keys from the physical layer. The main idea consists in adjusting transmitted probing signals through advanced deconvolution methods (incl. Least Squares with or without regularization, Maximum A Posteriori, Expectation-Maximization, Cross-validation…) so that receiving nodes can observe replica of their non-adjacent channels and hence, can directly apply quantization accordingly. Realistic simulation-based evaluations have been conducted with Impulse Radio - Ultra Wideband (IR-UWB) signals, which enjoy rich mutual multipath information but inherently lead to challenging deconvolution tasks in the temporal domain. In comparison with more conventional key distribution methods, significant protocol traffic (i.e., the overall number of required packets transiting over-the-air) could be saved before issuing a group key (e.g., 30% decrease in a simple 3-node scenario) or equivalently, longer keys can be generated at lower latency in one shot (i.e., within one protocol cycle) (Fig. 1).

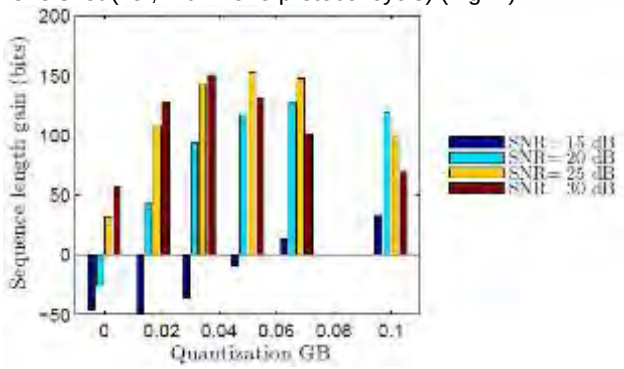

Figure 1. Average key length gain (in bits) vs. conventional group key distribution.

On the other hand, the suffered degradation in terms of bit agreement ratio (i.e., among the different keys generated in the group) remains acceptable and fairly high over large ranges of SNRs and for practical settings (Fig. 2).

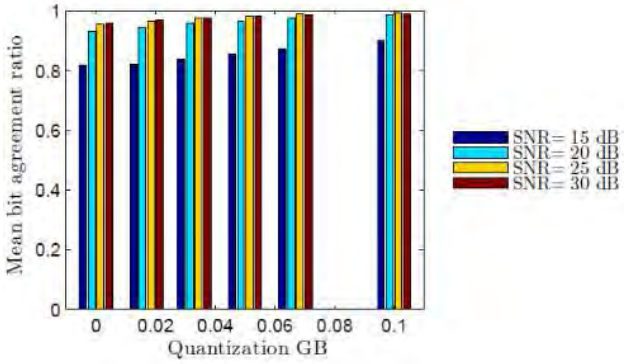

Figure 2. Average bit agreement with the new group key generation/distribution method (3 nodes).

Perspectives

Future works should concern the applicability of previous concepts to other radio technologies (incl. narrow-band, OFDM…), as well as complexity and feasibility within integrated IR-UWB devices with programmable transmitters.

Related Publications:
[1] I. Tunaru, B. Denis, B. Uguen, "Random Patterns of Secret Keys from Sampled IR-UWB Channel Responses", IEEE Int. Conf. on Ultra Wideband 2014 (IEEE ICUWB'14), Sept. 2014, Paris, France.
[2] I. Tunaru, B. Denis, B. Uguen, "Public Discussion Strategies for Secret Key Generation from Sampled IR-UWB Channel Responses", IEEE Conf. on Communications 2014 (IEEE COMM'14), May 2014, Bucharest, Romania.
[3] I. Tunaru, B. Denis, B. Uguen, "Reciprocity-Diversity Trade-off in Quantization for Secret Key Generation", IEEE Int. Symp. on Personal Indoor, and Mobile Radio Communications 2014 (IEEE PIMRC'14), Sept. 2014, Washington DC.
[4] I. Tunaru, B. Denis, B. Uguen, R. Perrier, "Cooperative Group Key Generation Using IR-UWB Multipath Channels", IEEE Int. Conf. on Ubiquitous Wireless Broadband 2015 (IEEE ICUWB'15), Oct. 2015, Montréal, Canada.

Preserving Privacy in Secured ZigBee Wireless Sensor Networks

Research topic: security, wireless sensors networks

Authors: J. Dos Santos, C. Hennebert, C. Lauradoux

Abstract: we expose concretely the information leakage occurring in an IEEE 802.15.4-based ZigBee meshed network. We deployed an IoT platform and used a killerbee sniffer to eavesdrop the communication between the motes. Metadata and control traffic are exploited in depth to recover protocol instances, routes, identity, capability and activity of the devices. We experiment different levels of security for the communications from none to the best available. Even when security is enforced, information leakages are not avoided. We propose simple countermeasures to prevent an outsider from monitoring a ZigBee network.

Context and Challenges

The ZigBee standard enables objects to be organized into meshed Wireless Sensor Networks (WSN) and to distribute their resources on the Internet via a gateway. The densification and the coexistence within a single area of several private and independent WSNs increase the security and privacy risks. It becomes therefore necessary to protect the network from outsiders and to prevent any device from connecting without authorization. Two complementary mechanisms could contribute to the security and the privacy protection. Prevention techniques are based on the use of cryptography and protocols. Intrusion Detection Systems (IDS) may be implemented to alert in case of attacks.

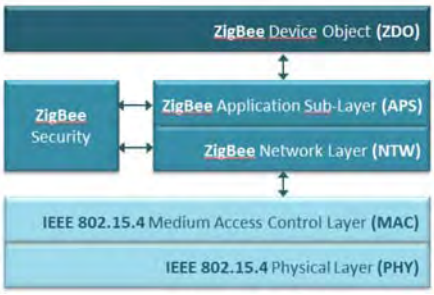

Figure 1. ZigBee communication stack.

The ZigBee standard allows the use of two security preventions at the network layer and at the application layer. This work investigated the privacy leaks occurring even when these two mechanisms are enabled.

Main Results

We conducted three experimental campaigns. Because the frames exchanged during the bootstrap phase are MAC frames, the ZigBee security is useless to protect privacy. First leak concerns the possibility to join a bad WSN. When a node holds no PAN ID, due to the metrics used to choose the WSN, a node can be associated to the bad WSN. We showed also the importance of the metadata, regardless the phase eavesdropped. They indicate the capabilities (battery, sleeping) and the role of a node (coordinator, end device or router) and enable an attacker to launch more powerful targeted attacks. We show that the full topology of a secured ZigBee WSN can be reconstructed by traffic analysis even when a node is out of the range of the sniffer.

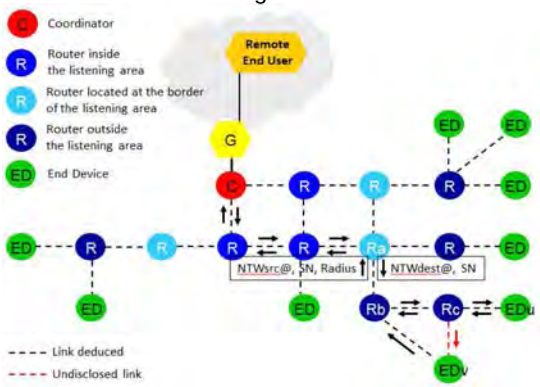

Figure 2. Reconstructed topology of a secured ZigBee WSN.

The three experiments highlight that enabling the security both at NTW and APS layers does not preserve the privacy in ZigBee WSN because many privacy leaks come from the NTW header content. The devices and their activity remain traceable. We propose simple solutions to prevent privacy. The first is to use MAC security. By this way, the MAC frames exchanged during the bootstrap could be ciphered and authenticated allowing only legitimate devices to join the WSN. The traceability, the monitoring of their activity and the reconstruction of the topology of the WSN based on the use of NTW metadata would be avoided. But, the ZigBee PRO XBee front-end used in this experiment does not provide the capability to enable IEEE 802.15.4 MAC security. So, it implies to develop a new chip radio enabling IEEE 802.15.4 security functions [1] and compatible with the ZigBee standard. Nevertheless, the MAC header content remains in clear and includes private information notably the MAC addresses of the neighbor motes. To preserve privacy at this layer, one solution consists in the use of pseudonyms for the MAC addresses.

Perspectives

The future work will be dedicated to assign dynamic pseudonyms for motes including IEEE 802.15.4 MAC security functions [2].

Related Publications:
[1] C. Hennebert, J. Dos Santos, “Security Protocols and Privacy Issues into 6LoWPAN stack: A synthesis”, IEEE Internet of Things Journal, vol. 1, no. 5, Oct. 2014, pp. 384-398.
[2] J. Dos Santos, C. Hennebert, C. Lauradoux, “Privacy Issues in 6LoWPAN wireless sensor network”, Connected security World, eSmart 2015, Marseille, France, Sept. 2015.

From Code Review to Fault Injection Attacks: Filling the Gap using Fault Model Inference

Research topic: smart cards, information security.

Authors: L. Dureuil, M.-L. Potet, P. de Choudens, C. Dumas, J. Clédière

Abstract: we propose an end-to-end approach to evaluate the robustness of smartcard embedded applications against perturbation attacks. Key to this approach is the fault model inference phase, a method to determine a precise fault model according to the attacked hardware and to the attacker's equipment, taking into account the probability of occurrence of the faults. Together with a fault injection simulator, it allows to compute a predictive metrics, the vulnerability rate, which gives a first estimation of the robustness of the application. Our approach is backed by experiments and tools that validate its potential for prediction.

Context and Challenges

Security devices such as smartcards are subject to drastic security requirements and certification processes. To evaluate their robustness against fault injection, automated tools [1,2] that simulate fault injection have been developed.

However, these tools rely on “imprecise” fault models, and yield many results that must then be verified by hand. Furthermore, the “traditional” metrics used to qualify the result of an analysis does not take into account the probability of occurrence of a fault.

Main Results

Our approach starts at the device level with fault model inference (FMI), a three steps process that aims at finding a probabilistic fault model (PFM) precisely tied to the device under attack and the equipment of attack. The first step is the parameter discovery step, where a classic cartography of the interesting attack parameters is performed; the second step is then the raw model construction that performs many attacks on the interesting attack parameters. The third step is the model generalization, where interesting properties of the raw model are highlighted to build the PFM. The three steps are carried on using a program specifically designed to output the injected fault.

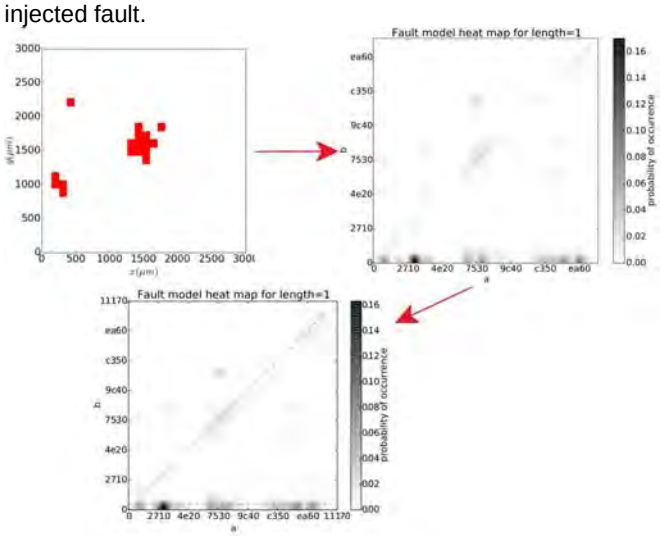

Figure 1. The three steps of fault model inference.

We then combine this PFM at the application level by using it as input of our fault injection simulator (CELTIC), to know which faults should be injected. We also use the PFM as output to compute a new metrics, the vulnerability rate:

$$\mathcal{V} = \sum_{p \in \mathcal{P}} \underbrace{\sum_{f \in \mathcal{F}_S} Pr(F = f \mid p)}_{\text{Fault Model \& CELTIC}} \cdot \underbrace{Pr(p)}_{\text{Attacker choice}}$$

Card	Command	$\mathcal{V}$	$\mathcal{T}$	φ
A	VerifyPIN	2.35×10^{-5}	3.2×10^{-2}	3.40×10^{-5}
A	SecureVerifyPIN	2.08×10^{-6}	8.5×10^{-5}	0
A	GetChallenge	2.01×10^{-5}	1.75×10^{-3}	2.94×10^{-5}
A	SecureGetChallenge	7.1×10^{-7}	2.74×10^{-6}	0
B	GetChallenge	1.1×10^{-3}	1.2×10^{-3}	1.4×10^{-3}
B	SecureGetChallenge	0	2.14×10^{-4}	0

Figure 2. Comparisons of metrics and predicted elapsed time.

We performed the FMI on two smartcards to infer FMI and we compared on several applications the vulnerability rate ($\mathcal{V}$) given by CELTIC with a “traditional” vulnerability rate ($\mathcal{T}$) in use in the literature, and a physical vulnerability rate (φ) for reference. We demonstrated on these examples that $\mathcal{V}$ is consistently on the same order of magnitude than φ, which is not the case for $\mathcal{T}$. We further demonstrated that $\mathcal{V}$can be used to predict the elapsed time before an attack is successful, which alleviates the need for physical tests.

Perspectives

It would be interesting to compare our results with other fault observation means, such as fault model extraction. Moreover, further tests are required to conclude on the impact of fault model reuse in multiple fault scenarios.

Lastly, CELTIC is not able to cope with the combinatory explosion associated with handling multiple fault attacks. Simulating multiple fault attacks without losing the ability to compute a vulnerability rate is currently still an open problem.

Related Publications:
[1] L. Dureuil, M.-L. Potet, Ph. de Choudens, C. Dumas, J. Clédière, "From Code Review to Fault Injection Attacks: Filling the Gap using Fault Model Inference", Smart Card Research and Advanced Application Conference (CARDIS), 2015.
[2] M-L. Potet, L. Mounier, M. Puys, and L. Dureuil, “Lazart: A symbolic approach for evaluation of the robustness of secured codes against control flow injections”, 7th IEEE Int. Conf. on Software Testing, Verifcation and Validation (ICST 2014), pp. 213-222, 2014.

Enhancing Dimensionality Reduction Methods for Side-Channel Attacks

Research topic: information security, side-channel attacks.

Authors: E. Cagli, C. Dumas, E. Prouff

Abstract: advanced Side-Channel Analyses make use of dimensionality reduction techniques to reduce both the memory and timing complexity of the attacks. The most popular methods to perform such a reduction are the Principal Component Analysis (PCA) and the Linear Discriminant Analysis (LDA). Indeed, they lead to remarkable efficiency gains but their use in side-channel context also raised some issues. We present an in-depth study of these two methods, we propose some extensions and provide a comprehensive comparison of the existing and new methods in real cases.

Context and Challenges

The side-channel traces are usually acquired by oscilloscopes with a very high sampling rate, which permits a powerful inspection of the component behavior but produces high-dimensional data. Reducing the dimensionality of the data is an important issue for Side-Channel Attacks (SCA). The present work focuses on the so-called projecting extractors whose image components are linear combinations of the original data.

The PCA has been applied both in an unsupervised way, i.e. on the whole data, and in a supervised way, i.e. on traces grouped in classes and averaged. The main competitor of PCA in the supervised context is the LDA, that thanks to its class-distinguishability asset, is known to be more meaningful and informative than the PCA method for side channels. Nevertheless, the LDA is often set aside because of its practical constraints; it is subject to the so-called Small Sample Size problem (SSS), i.e. it requires a number of observations (traces) which must be higher than the dimension (size) of them. One of the open issues in PCA concerns the choice of the components that must be kept after the dimension reduction.

Main Results

Our main contribution consists in proposing a new selection methodology, called cumulative ELV selection:

$$ELV(\alpha_i, j) = \frac{\lambda_i \cdot \alpha_i[j]^2}{\sum_{k=1}^{r} \lambda_k}$$

where r is the rank of the covariance matrix, and λ_i is the eigenvalue associated to the i-th component α_i.

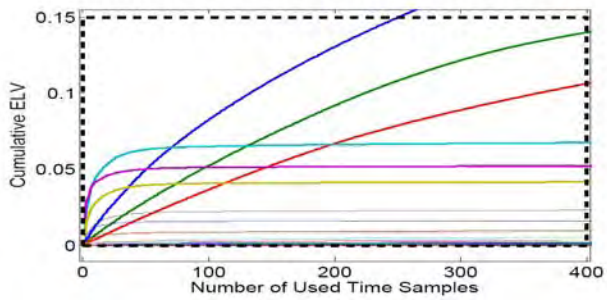

Figure 1. Cumulative ELV trend of principal components.

The reasoning behind the ELV selection methodology is essentially based on the observation that, for secure implementations, the leaking information, if existing, is spread over a few time samples of each trace.

		Parameter to minimize			
Method	Selection	N	N' (SSS)	N' (¬SSS)	C
PCA standard	EGV	-		-	-
PCA standard	ELV	-		-	-
PCA standard	IPR	-		-	+
PCA class	EGV	-	-	-	-
PCA class	ELV	+	★	★	+
PCA class	IPR	+	★	+	-
LDA	EGV	★		+	★
LDA	ELV	+		+	★
LDA	IPR	+		+	★
S_W Null Space	EGV		★		
S_W Null Space	IPR		+		
Direct LDA	EGV		★		
Direct LDA	IPR		+		
Fisherface			-		
S_T Spanned Space			-		

Figure 2. Overview of the performances of different extractors in tested situations (star denotes the best one, + the second choice and – the lower performance).

We discussed the generality and the soundness of this methodology and showed that it can raise the PCA performances, making them close to those of the LDA, even in the supervised context. This makes PCA an interesting alternative to LDA in those cases where the LDA is inapplicable. For the sake of comparison, we also analyzed many propositions to circumvent the SSS problem that have been made in literature, especially by Pattern Recognition and Face Recognition communities. The gain given by these techniques does not outperform the PCA method equipped with our ELV selection.

Perspectives

Being our core consideration very general in side-channel context, we believe that our results in the supervised context are not case-specific and theses methods are promising. Moreover, further studies are envisaged to improve the attacks in the unsupervised case.

Related Publications:
[1] E. Cagli, C. Dumas, E. Prouff, “Enhancing Dimensionality Reduction Methods for Side-Channel Attacks”, CARDIS 2015

03

ANTENNAS AND PROPAGATION

- Miniature antennas
- Antenna arrays
- Millimeter-waves
- Propagation

Impact of Small Antenna on Linear Power Amplifier Performance in a Co-design Approach

Research topic: compact antennas, antenna-front-end co-design

Authors: E. Ben Abdallah, A. Giry, S. Bories, D. Nicolas, C. Delaveaud

Abstract: this study investigates the co-design of a small antenna and a power amplifier (PA) for LTE applications. Special attention is paid to the load–pull optimization to derive suitable values of the antenna input impedance at the operating frequency and the first higher-order harmonics. The impact of the antenna impedance variations in the operating band on the PA performance is also addressed. It is found that the PA linearity is improved when operating is below the antenna resonance frequency. A microstrip patch antenna with an optimal impedance is developed to demonstrate the benefits of the co-design approach.

Context and Challenges

Power Amplifiers (PA) and antennas are usually designed separately and optimized for common real impedance at the interface, typically 50 Ω in microwave technologies. The co-design approach consists in designing jointly these elements in order to relax some constraints (reference impedance) and to optimize the system performance (efficiency, linearity). This approach allows the direct connection between the amplifier and the antenna [1]. The challenge of co-design consists in finding the tradeoff between the maximum performance of the PA and the feasibility of an antenna with the convenient impedance. The purpose of this work is to achieve the optimized antenna impedance co-designed with the PA for the LTE standard and to determinate the benefit of the co-design.

Main Results

A load-pull approach enables the optimization of the load impedances at the operating frequency and the first higher-order harmonics for given PA specifications. These impedances represent the ideal antenna input impedance. Under 2-tone excitation, the results show that the antenna should be tuned to a low impedance (2.9+0.5*j* Ω) at the operating frequency (f_0) and about a short circuit at $2f_0$. Once the PA sees suitable impedances at both f_0 and $2f_0$, it remains quite insensitive to the 3rd harmonic impedance.

The antenna impedance is modeled through its resonating equivalent circuit, a parallel *RLC* lumped-element circuit, in order to study the PA sensitivity to this antenna impedance response in the operational band. It was demonstrated that the resonane frequency of the small antenna should be higher than the PA operating frequency.

A microstrip patch antenna is designed on a Roger Duroid 5880 substrate of thickness λ/100 (narrow-band operation). The antenna resonance is at 913 MHz, 13 MHz above the PA operating frequency. A feeding probe located along the median plan is used to excite the antenna and a capacitive coupling with a disc placed at the top of the probe is used to tune the antenna impedance to f_0 at 2.9+0.5*j* Ω. Two spur lines are etched on the two non-radiating edges of the patch in order to allow the impedance control at $2f_0$ without perturbing the impedance setting at f_0, and keep a symmetrical radiation pattern.

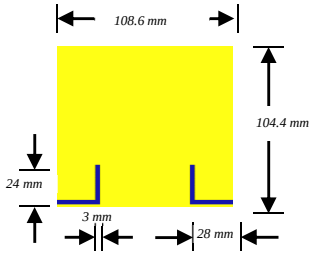

Patch antenna layout (ground plane not shown).

To estimate the benefit obtained by the co-design approach with this antenna, the output power (P_{out}), power added efficiency (PAE) and third order intermodulation (IMD3) are estimated for different input power levels (P_{in}). The following figure compares the simulated results between a classical antenna [2] (the antenna resonance is below the PA operating frequency and it provides the optimal impedances) and the proposed one using a two-tone stimulus with Δf = 5 MHz.

The linearity of the PA is improved and the PAE increases by about 12% for an IMD3 of -30 dBc (3GPP threshold). These results demonstrate the benefit of the co-design approach when the antenna resonance is above the PA operating frequency.

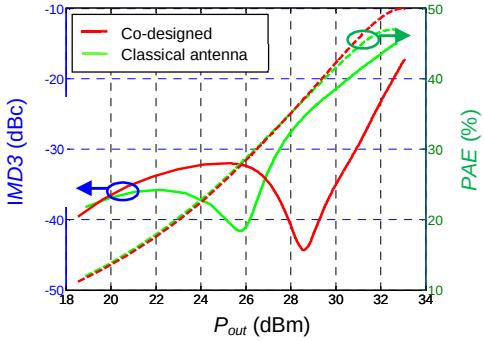

Simulated PA performance (PAE, Pout, and IMD3).

Perspectives

Future works will focus on the design of antennas with a higher miniaturization level co-designed with the power amplifier.

Related Publications:

[1] S. Bories, M. Pelissier, C. Delaveaud, and R. Bourtoutian, "Performances analysis of LNA-antenna co-design for UWB system," European Conf. on Antennas and Propagation (EuCAP 2007), Nov. 11-16, 2007, Edinburgh, UK.

[2] E. Ben Abdallah, A. Giry, S. Bories, D. Nicolas, C. Delaveaud, "Impact of small antenna on linear power amplifier performance in a co-design approach," IEEE 13th Int. New Circuits and Systems Conf. (NEWCAS), 7-10 June 2015, Grenoble, France.

LTE Small-Cell Dual-Band Frequency Agile Antenna Design Optimized for Carrier Aggregation

Research topic: compact antennas

Authors: C. Jouanlanne, C. Delaveaud

Abstract: a compact frequency-agile antenna is designed and optimized for a specific LTE small-cell base station using Carrier Aggregation (CA) technic for network capacity improvement. Available CA modes have driven the design of the antenna towards the frequency-agile volume-optimized antenna solution, which only covers the required instantaneous bandwidth (LTE band 20) while standard static antennas would require a wider bandwidth and therefore more volume to be compatible with all the CA modes.

Context and Challenges

Nowadays, LTE Small cells are heavily deployed in urban and even indoor environments and can require to be integrated for instance in urban furniture and therefore miniaturized. Regular base station antennas are usually bulky and cannot be hidden, which can be an issue in the case of small-cell base stations. Also, improving the base station capacity is a hot topic that can be achieved thanks to Carrier Aggregation (CA) which consists in spreading the data into several carriers (within the same band or not) simultaneously. 3GPP has proposed this technique supporting up to 100 MHz system bandwidth for LTE-Advanced (LTE-A). To handle bandwidths up to 100 MHz in different frequency bands, innovative solutions are required for antenna and RF front-end. Concerning the antenna solution, the focus is on the operating bandwidth optimization enabling antenna miniaturization at low operating frequencies. This paper addresses the issue of innovative multi-band frequency agile antenna which is able to adjust its bandwidth according to the active CA configuration.

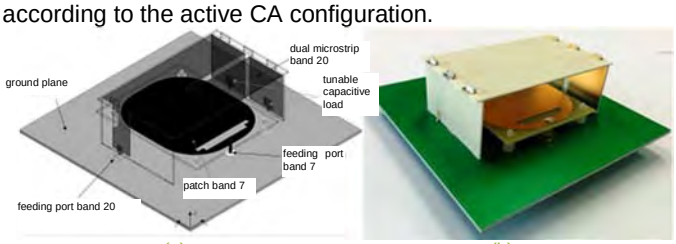

(a) (b)

Figure 1. (a) Simulation model of the antenna system and fabricated LTE small-cell dual-band frequency-agile antenna system (b).

Main Results

The proposed studied scenario is a small-cell base station supporting intra-band CA in LTE band 7 (2620-2690 MHz) and inter-band CA in LTE band 20 (791-821 MHz) & LTE band 7 (2620-2690 MHz) [1]. Due to its low operating frequency bandwidth, only band 20 antenna requires a miniaturization work. Based on the fact that the size of an antenna is proportional to its bandwidth, the main idea with this antenna design is to achieve the miniaturization by limiting the frequency bandwidth to a single band 20 sub-channel instead of the whole band 20, reducing the instantaneous bandwidth from 70 MHz to twice 10 MHz. This aspect also brings filtering capability to the antenna which will eventually help relax filter requirements of the RF front end. Consequently, the band 20 antenna consists of a thin microstrip antenna (figure 1a) miniaturized thanks to classical loading and folding techniques. Thus, this antenna has been made dual resonant with two very narrow closely spaced resonances and the frequency agility technique has been used to tune both antenna resonances at the right frequency according to the active CA configuration (see figure 2 to observe the agile behavior). Two digitally tunable capacitors (DTCs) are used as frequency agility active components in this design. LTE band 7 antenna is a classical microstrip patch antenna with wide band properties. Both antennas are co-located on a square 100x100 mm² ground plane and the antenna system only occupies a small volume of 66x54.5x23mm^3 (λ_0/5.7xλ_0/7x λ_0/16.5 with λ_0 = 379 mm @791 MHz).

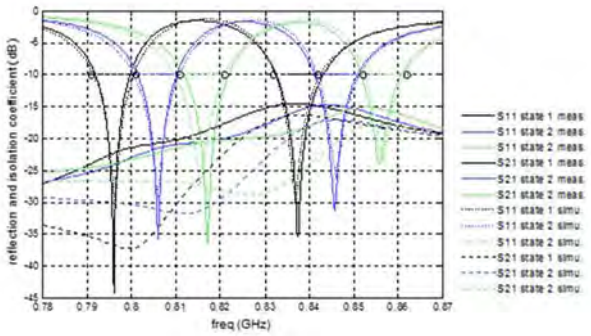

Figure 2. Measured and simulated reflection coefficient at band 20 RF port and isolation between both RF ports of the proposed antenna system.

This geometrical arrangement with the band-20 antenna right above the band-7 antenna is possible due to their orthogonal polarizations as well as the fact that their respective strong near field spots are distinct and do not interfere significantly.

Perspectives

A dual band (LTE band 7 & band 20) dual-port frequency agile antenna system capable to adapt its frequency bandwidth to the active CA configuration has been developed. Frequency agility is used to reduce the antenna instantaneous bandwidth at low frequencies which enables miniaturization without performance reduction. The future work considers extending the agility properties to support more CA scenarios. Equally, this antenna will be associated with reconfigurable RF front-end capable to work at different operating points to improve the energy efficiency depending on CA configuration.

Related Publications:
[1] C. Jouanlanne, C. Delaveaud, “LTE small cell dual-band frequency agile antenna design optimized for carrier aggregation”, European Conf. on Networks and Communications (EuCNC), 2015, Paris, Frande.
[2] C. Jouanlanne, C. Delaveaud, “Compact Dual-band Frequency Agile Antenna Designed for Carrier Aggregation LTE Small Cell”, 20th Int. Symp. on Wireless Communication Systems, 2015, Brussels, Belgium.

About Radiation Efficiency Optimization of a Miniaturized Antenna

Research topic: compact antennas

Authors: Y. Dia, L. Huitema, C. Delaveaud, S. Bila and M. Thevenot.

Abstract: This work investigates the miniaturization of a compact omnidirectional antenna while keeping a high radiation efficiency. More specifically, it is demonstrated that for constant antenna dimensions, a lower operating frequency (1.8 GHz versus 2.5 GHz) can be obtained with very similar radiation efficiency. This means that the antenna presents the same radiation efficiency while having reduced electrical dimensions (compared to operating wavelength). Measurements obtained with a set of prototypes confirm the original simulated results.

Context and Challenges

The generalization of radiofrequency links to equip connected objects contributes to the emergence of new needs for miniature antennas. Some systems, such as sensor networks, transmit small amounts of information at low data rate over narrow frequency bands. Low UHF frequencies, having favorable propagation properties, are generally preferred for these systems reinforcing the need for the miniaturization of antenna in order to allow an easier integration inside electronic devices. However, fundamental physical limits constrain the antenna miniaturization with the well-known trade-off between electrical size (geometric size compared to the wavelength), radiation efficiency and operating bandwidth. If the bandwidth limitation is widely studied in the literature, the development of electrically-small antennas with high radiation efficiency becomes one of the most important challenges for compact antenna designers. Efficiency for this kind of communication devices is essential due to the low power resources. In this context, studies on the optimization of the radiation efficiency of miniature antennas have been initiated.

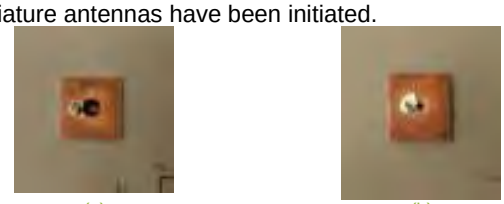

(a) (b)

Figure 1. Compact antenna prototypes (a), reference antenna (2.5GHz) (b) specific optimized design (1.8GHz).

Main Results

The studied antenna structure is based on a monopolar wire-patch antenna which provides dipole-like radiation characteristics [1]. Using a classical design approach, geometrical parameters have been optimized to design a first antenna structure (reference antenna) matched on a 50Ω impedance at 2.5 GHz. It exhibits small dimensions of 24mm x 24mm x 4mm ($\lambda_0/5$ x $\lambda_0/5$ x $\lambda_0/30$) with a high radiation efficiency of about -0.2 dB. Then, using electromagnetic simulation tools, the evolution of the antenna radiation efficiency has been carefully studied according to the intrinsic tuning geometrical parameters. Some original behaviors have been identified. Especially, for fixed top-hat dimensions and substrate permittivity, the antenna radiation is mainly driven by three parameters: the substrate thickness (antenna height), the ground wire diameter and the distance between the ground wire and the feeding probe. At a constant antenna height, we sought to optimize the two other parameters for maximizing the radiation efficiency. The radiation efficiency has consequently been improved at lower frequencies while the ground wire is thinner and the distance between the two wires is larger. A consequence of the efficiency antenna optimization is a poor impedance matching due to the significant increase of the antenna quality factor. To validate these important results, two antenna prototypes have been designed, manufactured and measured. They present the same dimensions, use the same material (dielectric and metal) but different wire diameter and positions. Measured and simulated radiation efficiencies are compared in figure 2: the optimized antenna operates at 1.9 GHz (1.8 in simulation) with a radiation efficiency similar to the reference at 2.5 GHz. These results show that the radiation efficiency can be maintained while miniaturizing the antenna ($\lambda_0/7$ x $\lambda_0/7$ x $\lambda_0/30$). The ripple on the measured radiation efficiency is related to the compensation process of the impedance mismatch which is more pronounced with the optimized antenna.

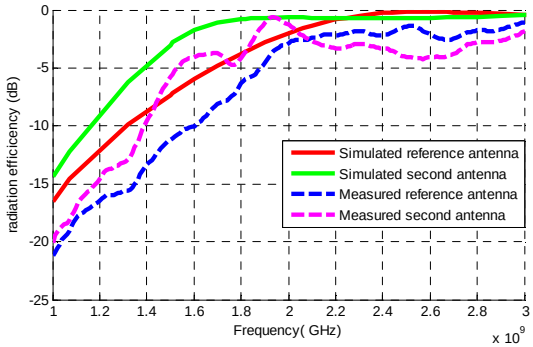

Figure 2. Comparison of measured and simulated radiation efficiencies of antenna prototypes (second = optimized antenna).

Perspectives

Radiation optimization of monopolar wire patch antenna has been studied as a function of the geometrical parameters. An original behavior has been used to demonstrate that a similar high level radiation efficiency can be reached at low frequencies while keeping the same antenna dimensions, involving the reduction of its electrical size. This property is obtained at the cost of significant quality factor increase leading to 50-Ω mismatching impedance conditions. Other miniature antennas structures will be studied to try to identify similar behaviors. The issue of high quality factor complex impedance can be solved in a future global RF front-end/antenna co-design approach.

Related Publications:
[1] S. Sufyar, C. Delaveaud, "A miniaturization technique of a compact omnidirectional antenna ", Radioengineering, vol. 18, no. 4, Dec. 2009.
[2] Y. Dia, L. Huitema, C. Delaveaud, S. Bila, M. Thevenot, "About radiation efficiency optimizing of a miniaturized antenna," 9th European Conf. on Antennas and Propagation (EuCAP), April 13-17, 2015, Lisbon, Portugal.

Design of High Directivity Compact Parasitic Array for Beam-Steering Applications

Research topic: compact antennas, antenna arrays

Authors: A. S. Kaddour, A. Clemente, S. Bories, C. Delaveaud

Abstract: two synthesis methods of directive and compact parasitic antenna arrays with beam-steering capabilities are compared to calculate the complex excitation coefficients of each array element needed to synthetize the antenna radiation pattern in a given direction. The theoretical analysis has been experimentally validated at 1.75 GHz. The realized antenna is composed of eight parasitic monopoles (length 0.21λ) surrounding a single driven element and arranged on a finite circular ground plane with a radius of 0.6λ and forming a circular array with radius 0.1λ.

Context and Challenges

Dense deployment of small cells is one of the main topics of investigation in 3GPP LTE release 12, which aims to meet the ever-increasing data-rate requirements of future generations of wireless communications. In this heterogeneous network architecture, classical macro base stations are complemented with low-power low-cost small cell to extend the cellular network coverage (both in indoor and outdoor environment) and improve performance experienced at end users by shortening the distance between user equipment's and access nodes. Nevertheless, the density of deployed small cells and their proximity to users reinforce the public concern about electromagnetic field exposure. In this context, compact and directive antennas could be a solution to both interference and electromagnetic field exposure reduction. Parasitic antenna arrays are promising solutions in order to realize high directivity compact antennas with a beam-steering capability.
The main objective of this work is to compare two optimization methods [1] (phase shifting and optimization based on spherical wave expansion) and present the operational principle of a compact array for beam-steering applications.

Main Results

The designed parasitic antenna array operates at 1.75 GHz and is composed of nine monopoles with a length of 0.21*λ*. The antenna consists of one driven element (central monopole) surrounded by eight parasitic monopoles. The parasitic elements are arranged on a finite circular ground plane with a radius of 0.6*λ* and forming a circular antenna array of radius 0.1*λ*. The ground plane has been used in view of the final integration of the antenna on a small-cell equipment.

(a) (b)

Figure 1. a) Fabricated circular parasitic antenna array, (b) Schematic view of the proposed prototype.

Each parasitic element is connected to a resistive and/or reactive load calculated starting from the optimal complex excitation. These coefficients are extracted using the two optimization methods by imposing a maximum of directivity in a desired direction. A theoretical maximum directivity of 7.2 dBi and 10.5 dBi has been obtained using the phase shifting method [1] and the synthesis method based on spherical wave expansion [2], respectively. The theoretical maximum directivity of 10.5 dBi has been obtained when negative resistances are used (spherical wave expansion method).
Due to the symmetry of the antenna structure, the main beam can be steered on the horizontal plane with a step of 45° by rotation of the complex excitation coefficients calculated for the main beam direction (θ_0, φ_0) = (90°,0°). In order to validate the operational principle and to reduce the complexity of the beam-steering network, a simplified passive prototype has been realized (Fig. 1 (a)). In the proposed simplified array, six monopoles are connected to a 50 Ω load and two monopoles are connected to the optimized impedance loads Z_1 and Z_2 (Fig. 1(b)) using spherical wave expansion synthesis method.

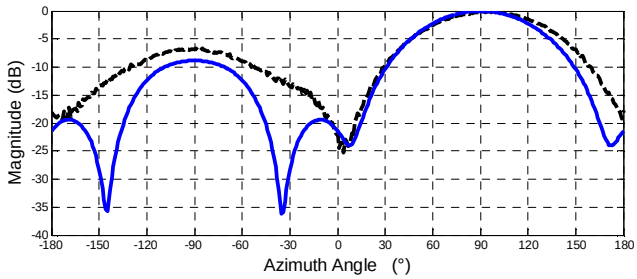

Figure 2. Simulated and measured radiation patterns of the circular array computed in the H-plane.

The measured and simulated radiation pattern computed in the H plane is presented in the figure 2. A good agreement is obtained considering the electromagnetic simulation radiation pattern computed at 1.75 GHz. A maximum directivity of 7.9 dBi has been measured in very good agreement with the simulation results.

Perspectives

Further works deal with spatial selectivity improvement and the implementation of the antenna beam-steering feature using RF switches.

Related Publications:
[1] A.S. Kaddour, A. Clemente, S. Bories, C. Delaveaud, "Design of high directivity compact parasitic array for beam-steering applications," 9th European Conf. on Antennas and Propagation (EuCAP), April 13-17, 2015, Lisbon, Portugal.
[2] A. Clemente, M. Pigeon, L. Rudant, and C. Delaveaud, "Design of a super directive four-element compact antenna array using spherical wave expansion," IEEE Trans. on Antennas and Propagat,, vol. 63, no. 11, Nov. 2015, pp. 4715-4722.

Design of a Super Directive Four-Element Compact Antenna Array Using Spherical Wave Expansion

Research topic: compact antennas, antenna arrays

Authors: A. Clemente, M. Pigeon, L. Rudant, C. Delaveaud

Abstract: a super-directive four-element compact parasitic antenna array has been designed and optimized using an ad-hoc procedure based on the Harrington maximum directivity definition and spherical wave expansion. The proposed array has been designed at 868 MHz; its electrical size is 0.45λ$_0$ × 0.36λ$_0$ (diameter of minimum sphere circumscribing the antenna equal to 0.57λ$_0$). A maximum directivity of 11.7 dBi has been measured at 871 MHz in satisfactory agreement with theoretical results and electromagnetic simulations.

Context and Challenges

Directive compact antennas offer new opportunities for wireless applications in terms of spectral efficiency, reduced environmental impact and use modes. However, the conventional techniques for enhancing the directivity often lead to a significant increase of the antenna size. Consequently, the integration of directional antennas in small wireless devices is relatively limited. This difficulty is particularly critical for the frequency bands below 1 GHz if object dimensions are limited to a few centimeters. With the explosion of the number of wireless communication systems (WiFi wireless networks, RFID tags, wireless sensor networks, object remote control, connected objects, etc.), the problem of electromagnetic pollution has also emerged. Super-directive compact antennas are an innovative and attractive solution to both integration and interference mitigation needs.

In this work, a procedure for the design of super-directive antenna arrays is demonstrated [1],[2]. The proposed method has been applied for the optimization of a super-directive four-element parasitic antenna array working at 868 MHz. Our objective is to get the highest directivity with a compact antenna to obtain an efficient spatial filtering function independently from the power efficiency. The block diagram of the procedure is presented in Figure 1; its full description is presented in [1].

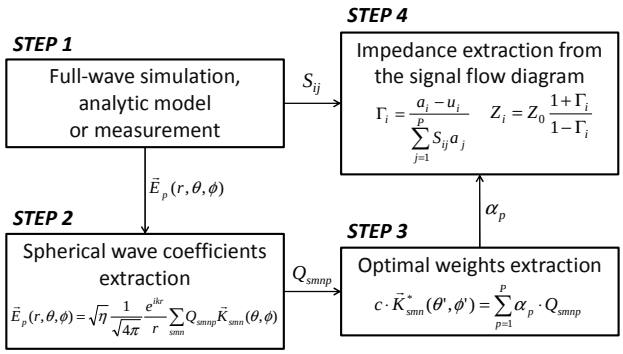

Figure 1. Schematic diagram of the proposed parasitic array optimization procedure.

Main Results

The realized super-directive compact array operates at 868 MHz and consists of four 0.4λ$_0$ (139.1 mm) electrical dipoles (thickness 2.2 mm) printed on a 124.6×156 mm² Rogers RO4003 substrate (thickness equal to 0.813 mm). The inter-element spacing is 0.1λ$_0$ (34.6 mm). Only one element is fed and the others are connected to impedance loads extracted using the proposed optimization procedure. A maximum directivity of 11.7 dBi has been measured at 871 MHz. To our best knowledge, this is the first practical demonstration of a super-directive four-element compact array in the open literature. The theoretical performances of a four-dipole array and the simulated and measured directivity of the realized prototype are presented in Figure 2.

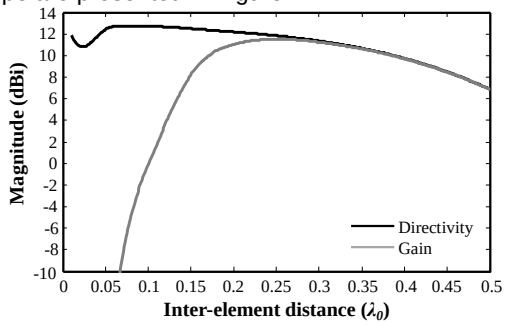

(a)

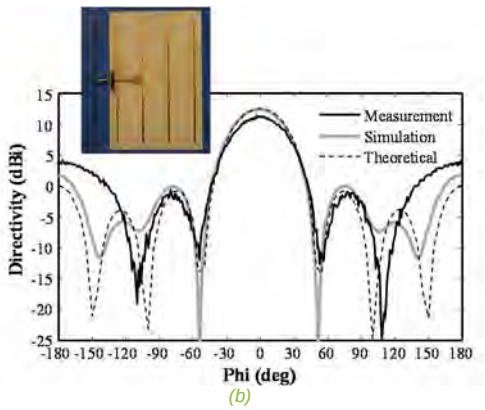

(b)

Figure 2. (a) Maximum directivity and gain of a four-dipole array as a function of the inter-element distance. (b) Theoretical, simulated and measured radiation patterns of the realized antenna.

Perspectives

A procedure to optimize super-directive compact parasitic arrays has been developed and demonstrated. A maximum directivity of 11.7 dBi has been experimentally demonstrated (-3 dB beamwidth of 40°-50°). Losses phenomena (leading to limited gain) are under investigations. The possibility to significantly increase the gain and the directivity with an antenna of identical dimensions will be analyzed in the future.

Related Publications:
[1] A. Clemente, M. Pigeon, L. Rudant, C. Delaveaud, "Design of a super directive four-element compact antenna array using spherical wave expansion," IEEE Trans. on Antennas and Propagat,, vol. 63, no. 11, Nov. 2015, pp. 4715-4722.
[2] A. Clemente, M. Pigeon, L. Rudant, and C. Delaveaud, "Super directive compact antenna design using spherical wave expansion," IEEE AP-S Int. Symp. (APS-URSI), 2014.

High-Directivity Compact Antenna with Non-Foster Elements

Research topic: compact antennas, superdirectivity

Authors: L. Batel, L. Rudant, J-F. Pintos, K. Mahdjoubi, A. Clemente, C. Delaveaud.

Abstract: this contribution introduces a new method using Non-Foster elements to achieve a broadband high-directivity compact antenna. The analysis is computed considering a three-element compact parasitic antenna array. The impedance loads associated to each parasitic element have been calculated using an optimization procedure based on spherical wave expansion. This method shows the possibility to obtain a high directivity of 10.4 dBi over a wide bandwidth around 868 MHz.

Context and Challenges

Performance characteristics of passive electrically small antennas (ESA) are limited by fundamental physics. This contribution focuses on the directivity performance and offers perspectives for wireless communications in terms of spatial selectivity and electromagnetic environmental impact. Non-Foster elements are classically used in matching networks for ESA in order to increase their impedance matching bandwidth. Thanks to their reactance properties, Non-Foster elements are proposed here as an innovative method to improve the directivity bandwidth of a compact antenna array. An optimization procedure to implement super directive compact arrays has been presented in [1]. The optimization computed as a function of the frequency shows that the optimal reactance associated to the parasitic elements of two- and three-dipole arrays [2] behaves as a Non-Foster element. Those elements exhibit a negative slope of their reactance and are typically associated to negative capacitance or inductance. A few practical implementations of Non-Foster elements are represented in the state of the art because they suffer from instability issues. One implementation using active radio-frequency circuits is proposed in [3].

Main Results

The antenna considered for this study is a three-dipole parasitic array. The structure of this array and its dimensions are provided in Fig. 1a. Only the first dipole is fed with a 50 Ω transceiver. The others are parasitic radiating elements and they are loaded with complex impedance Z1 and Z2 made of lumped elements.

In the first step of the study, the antenna array has been optimized at the single frequency of 868 MHz. The blue curve in Fig. 1b shows the antenna maximum directivity as a function of frequency. This behavior is achieved considering the optimal impedance loads calculated at 868 MHz. Typically, Z1 is an inductance of 0.9 nH and Z2 an inductance of 3.3 nH.

Considering Fig. 1b, the proposed three-dipole parasitic antenna array achieves a high directivity of 10.4 dBi at 868 MHz. From Fig. 1b, the high directivity property is achieved within a limited frequency band with classical inductance loads. The directivity level decreases quickly when shifting from the optimal frequency. A directivity higher than 10 dBi is achieved in the frequency band 866-869 MHz (less than 1% at 868 MHz). The bandwidth limitation is a direct consequence of the superdirectivity. A small variation of the optimal loads can produce significant directivity degradation.

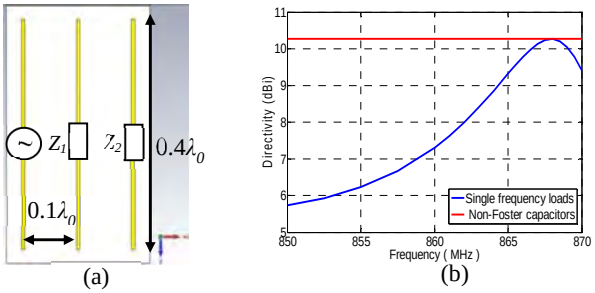

Figure 1. Antenna structure (a) and optimal directivity as function of frequency (b).

In order to avoid this directivity decrease with frequency, the optimization procedure has been used to optimize the antenna directivity as a function of the frequency in the band 850-870 MHz. This broadband directivity result is depicted by the red curve in Fig. 1b. The reactance of the optimal impedances (Z1 and Z2) to achieve this broadband directivity is presented in Fig. 2. It exhibits a negative slope for the two loads. This behavior is similar to the Non-Foster capacitance ((-j)/(2π.f.C)) with $C < 0$. It appears that integrating a Non-Foster capacitance on the parasitic antennas improves significantly the bandwidth of the directivity compared to the classical Foster impedance loads.

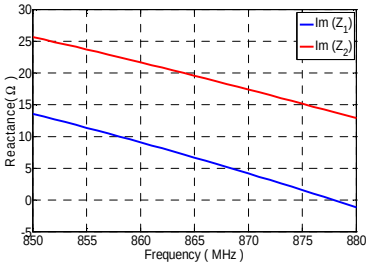

Figure 2. Reactance of the optimal loads associated to the parasitic dipoles calculated as a function of the frequency.

Perspectives

An innovative use of Non-Foster elements has been proposed. Two Non-Foster capacitances are used to improve the directivity bandwidth of a three-dipole compact parasitic antenna array. This preliminary investigations offer good perspectives for the association of Non-Foster elements and small antennas for high directivity and superdirectivity applications.

Related Publications:

[1] A. Clemente, M. Pigeon, L. Rudant, C. Delaveaud, "Design of a super directive four-element compact antenna array using spherical wave expansion," IEEE Trans. on Antennas and Propag,, vol. 63, no. 11, pp. 4715-4722, Nov. 2015.

[2] L. Batel, L. Rudant, J.F. Pintos, A. Clemente, C. Delaveaud, K. Mahdjoubi, "High directive compact antenna with Non-Foster elements" Int. Workshop on Antenna Technology (iWAT), Seoul, Republic of Korea, 4-6 March 2015.

[3 L. Batel, L. Rudant, J.F. Pintos, K. Mahdjoubi, "Sensitivity of negative impedance converter circuit with respect to PCB design effects" Int. Workshop on Antenna Technology (iWAT), Seoul, Republic of Korea, 4-6 March 2015.

In-Situ Monitoring Method for Direction Finding Antennas

Research topic: antenna calibration, optically modulated scattering

Authors: L. Ghattas, S. Bories

Abstract: an innovative design and implementation of a non-disturbing solution for quasi-real time radiation antenna monitoring is presented. The proposed system is based on the optically-modulated scattering (OMS) technique. Its capability to detect the presence of obstacles perturbing the nominal antenna radiation pattern is evaluated on a direction finding system. In such applications, the system-level accuracy is directly determined by the accurate knowledge of the complex antenna responses.

Context and Challenges

Antenna arrays for Direction finding (DF) are usually designed and tested in controlled environments such as anechoic chambers. However, the radiation pattern of antennas may change significantly when they are placed in their operational environment. In such perturbed close-distance environment, the antennas calibration validity becomes a major issue which can lead to DF performance degradation and costly recalibration process. The proposed patented solution consists in an innovative design and implementation of a non-disturbing solution for quasi-real time antenna monitoring.

The system is based on the optically-modulated scattering (OMS) technique. To detect the variable obstacles that disrupt the nominal DF Antenna (DFA) calibration, we compared the received current response to an incident electromagnetic (EM) wave for the two following cases: nominal near-field (NF) response [I0] and in-situ NF response [I], for which scatterers and obstacles reflections are taken into account. The incident EM wave is sequentially generated from one of the OMS probes which includes a miniature dipole and an unbiased photodiode whom impedance is modulated by the amplitude of the optical signal coming through the fiber.

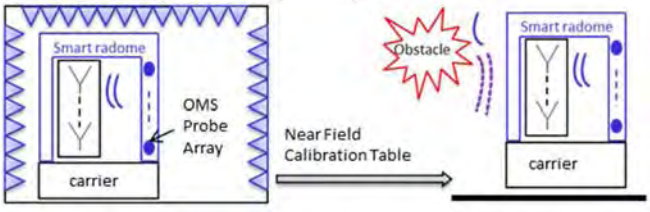

Proposed system for DF antenna monitoring: (a) NF calibration in a controlled environment, (b) NF DF antenna response measured in a perturbed environment.

Main Results

First, the impact of a perturbing obstacle in close DFA environment is demonstrated with a model combining EM simulations and antenna processing [1]. For a given 2° accuracy, the DF sensitivity is degraded up to 20 dB due to errors in the DFA calibration table. The effect of this biased calibration is analyzed quantitatively in the following cases: a high integration on the carrier and time variable obstacles.

Two major requirements have to be considered in order to provide accurate in-situ monitoring measurements: minimum disturbance of the field under test and operation over a wide band of frequencies (typically two decades in DF applications).

The second part of the study concerned the OMS technique implementation. A model that predicts the OMS scattered power is developed to set the configuration (optimal probe length …) [1]. The presence of a nearby (up to 90 cm distance) metallic rod perturbing the nominal configuration is detected by measuring the variation of the OMS scattered field by the probe with a received power variation larger than 5%. Finally, an overall design of the system shows that it is possible to measure a variation in the order of 1% of the coupling between an auxiliary antenna and the DFA with a SNR of 50 dB for a transmitted power of 0.1 W and measuring time of 0.01 s per sample point leading to a global measurement time less than 22 seconds. At last, the correlation between the monitored DFA NF responses and DF accuracy has been established and compared to other existing methods [2].

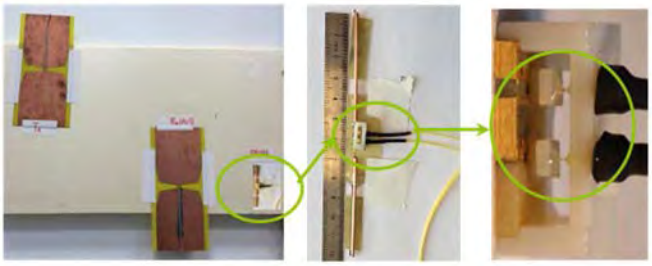

Validation and characterization of the OMS technique on the whole UHF frequency band. Zoom on the photodiodes.

Perspectives

The next step will consider a full demonstrator where OMS probes are embedded into the DFA radome. In the mid-term, our objective is not only to detect a perturbation but also to compensate it by updating the far-field DFA calibration tables. This will aim to reach a TRL 6. This study has focused on DF application but the proposed in-situ monitoring system could also find large interest in other applications where antenna radiation characteristics are critical for the application (radar, radio navigation…).

Related Publications:

[1] L. Ghattas, “Autodiagnostique des perturbations des réseaux d’antennes", PhD Thesis, Centrale-Supélec, Jan. 2015.

[2] L. Ghattas, S. Bories, M. Hirvonen, D. Picard, “Optically modulated scatterer probe for in-situ antenna monitoring,” 8th European Conf. on Antennas and Propagation (EuCAP), 6-11 April 2014.

1-bit Reconfigurable Unit-Cell for Ka-Band Transmitarray Antennas

Research topic: millimeter-wave antennas

Authors: L. Dussopt, L. Di Palma, A. Clemente, R. Sauleau P. Potier, P. Pouliguen

Abstract: Millimeter-wave wireless systems are emerging as a key enabling technology for high data rate communications (indoor local/personal area networks, mobile communications (5G), satellite communications (SATCOM)) and radars (automotive, industry, autonomous vehicles/drones, security). Electronically-reconfigurable antennas with beam-steering/beam-forming capabilities are required in such applications. A unit-cell for reconfigurable transmitarray antennas has been developed in Ka-band (27-30.5 GHz) and demonstrated outstanding performances in terms of efficiency, paving the way towards fully-reconfigurable large-size antennas for next-generation millimeter-wave systems.

Context and Challenges

Transmitarray antennas are gaining more and more interest for millimeter-wave wireless and radar applications where a high radiation gain is needed. They are based on a thin multi-layer array of transmitting unit-cells focusing/collimating the radiation to/from one or several focal sources by locally tuning the phase of the transmitted signals. Antenna reconfigurability is a key requirement in many applications in order to steer or shape the radiated beam and enable such functions as beam auto-alignment, tracking mobile target, mitigate interferences, etc… In the context of transmitarray antennas, phase reconfiguration at the level of each unit-cell with minimum RF loss is a major challenge to enable these functions.

Main Results

An electronically-reconfigurable unit-cell with 1-bit of phase quantization was proposed for the first time in the 27.5-30 GHz frequency band, which is used for the uplink in Ka-band SATCOM applications. The present design, based on the structure originally proposed in our previous work in X-band, integrates two p-i-n diodes and includes a new bias network design [1-2].

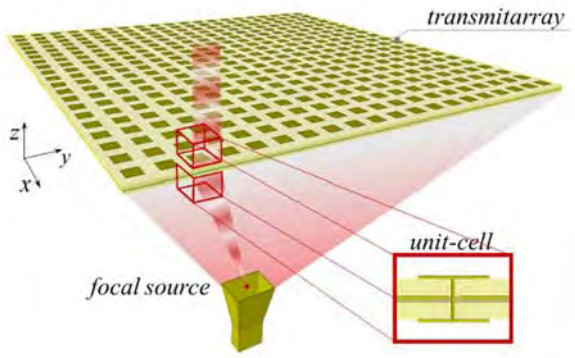

Schematic view of a reconfigurable transmitarray antenna

The proposed unit-cell, whose dimensions are 5.1×5.1 mm^2 (i.e. half-wavelength in free-space at 29.4 GHz), consists of four metal layers and two identical substrates with a total thickness of 1.2 mm only. It includes patch antennas on each external layer of the assembly connected together with a metallic via hole. The two inner layers are used for the ground plane and the biasing network. Two PIN diodes are included in one of the patch antennas to select the currents directions and implement a 180° differential phase shift. The two PIN diodes are controlled in opposite states through a single bias line with a biasing current of ±5-10 mA. In contrast to previous realizations at lower frequencies, the design of the biasing network has been a specific challenge here to minimize the coupling between bias lines and the antennas while talking into account the PCB design rules and the numbers of bias lines to be routed in the full transmitarray. Hence, while a single line is needed per unit-cell, the unit-cells located on the edges of a 20×20 transmitarray will have to allow the routing of up to 10 bias lines in the vicinity of the patch antennas. A detailed sensitivity analysis has been performed to verify the robustness of the design to PCB fabrication tolerances.

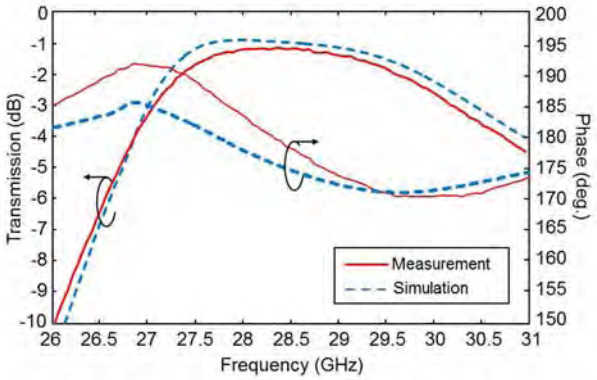

Transmission magnitude in 0° phase state and differential phase shift of the unit-cell.

The unit-cell has been fabricated and characterized in a dedicated waveguide test set-up. It demonstrated a minimum insertion loss of 1.1 dB only, a 3-dB transmission bandwidth of 3.5 GHz (27-30.5 GHz, 12.2%) and a reflection coefficient lower than -10 dB. The performances are nearly identical in the two phase states.

Perspectives

The low insertion losses and low complexity of this unit-cell makes it a promising building block for large Ka-band reconfigurable transmitarrays with good efficiency and reduced cost. Such a reconfigurable transmitarray with 20×20 elements has been fabricated and demonstrated recently outstanding beam-steering performances and efficiency; these results will be published soon.
These reconfigurable antennas are envisioned to address the needs for portable SATCOM terminals, future 5G millimeter-wave base stations, and various radar applications.

Related Publications:
[1] L. Di Palma, A. Clemente, L. Dussopt, R. Sauleau, P. Potier, P. Pouliguen, "1-bit reconfigurable unit-cell for Ka-band transmitarrays," *IEEE Antennas and Wireless Propagation Letters*, 2015.
[2] L. Di Palma, A. Clemente, L. Dussopt, R. Sauleau, P. Potier, P. Pouliguen, "1-Bit Unit-Cell for Transmitarray Applications in Ka-Band," *9th European Conference on Antennas and Propagation*, Lisbon, Portugal, 12-17 April 2015..

Radiation Pattern Synthesis for Monopulse Radar Applications using a Reconfigurable Transmitarray in X-Band

Research topic: millimeter-wave antennas

Authors: L. Dussopt, L. Di Palma, A. Clemente, R. Sauleau, P. Potier, P. Pouliguen

Abstract: Millimeter-wave radars have a high potential for industrial, surveillance and security applications. Reconfigurable transmitarray antennas have proven very high performances in millimeter-wave frequency bands in terms of efficiency, bandwidth, beam-steering and beam-forming. We investigated the synthesis of Σ- and Δ-radiation patterns with a reconfigurable transmitarray antenna for monopulse radar applications in X band and showed very promising performances in terms of gain, side-lobe level and null depth.

Context and Challenges

Monopulse radars systems are the dominant tracking technology for military and space applications. With the emergence of cost-efficient millimeter-wave technologies, they are also considered in many industrial and security applications for surveillance and automated tracking and guidance of autonomous mobile systems. Electronic beam-steering and beam-forming is a major challenge to enhance the reliability, accuracy and tracking speed of current mechanically-steered radars.

Main Results

An X-band (10 GHz) electronically-reconfigurable antenna developed in our previous work [1] was used to demonstrate the synthesis and reconfiguration of monopulse radiation patterns. This antenna is based on a transmitarray of 400 phase-shifting radiating elements using PIN diodes and a focal feed which can be composed of a single or multiple horn antennas.

This transmitarray has been used with two feed configurations in which the sum (Σ) and difference (Δ) patterns required in monopulse radar applications can be generated sequentially in a switched mode or simultaneously [2].

The Σ pattern is generated as a classical pencil beam with a constant or linear phase distribution across the transmitarray aperture. In the case of a single focal source, the Δ pattern is synthesized by splitting the aperture in two halves with 180° difference between them in order to generate an anti-symmetric phase distribution. The orientation of the frontier between the two halves determine the axis of the two beams composing the Δ pattern. In this configuration, the two patterns can be obtained sequentially with a very fast switching rate.

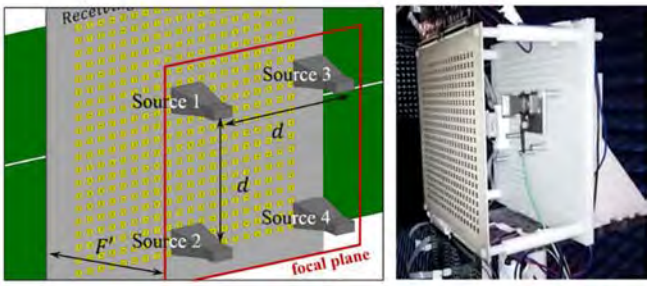

Reconfigurable transmitarray with a four-element focal array.

In the case of a focal array of several focal sources, the two patterns can be generated with the same phase-shifting distribution across the transmitarray aperture by a simple combination (analog or digital) of the focal sources. This means the Σ and Δ patterns can be obtained simultaneously, which is a significant advantage for an accurate tracking of fast mobile targets.

Radiation performances have been measured in anechoic chamber for the two feed configurations (single and multiple focal sources) and a very good agreement between simulated and experimental data was obtained in terms of radiation gain, beamwidth, null depth, and side-lobe level (SLL). In broadside direction, the Σ pattern exhibits a gain of 22.9 dBi and SLL of -19.7 dBi. For the Δ pattern, the gain, SLL and null depths are 20 dBi, -11.4 dB, and 22 dB, respectively.

The capabilities to steer the beams in the horizontal and vertical planes were demonstrated as well for steering angles up to ±40°. The gain levels decrease by about 3.5 dB at 40° steering angle while the SLL and null-depth are degraded but maintained at a good level. Radiation performances could probably be improved through a lower phase quantification at the expense of additional complexity and lower efficiency. To our best knowledge, this is the first demonstration of monopulse radiation pattern synthesis using the transmitarray antenna technology.

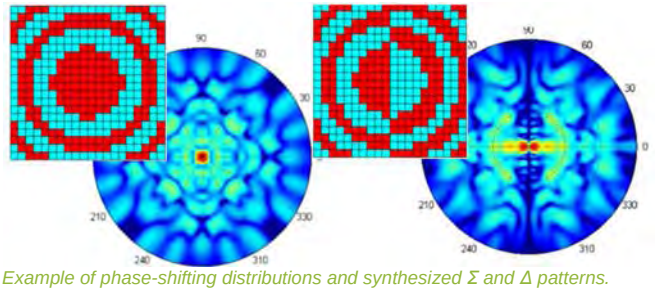

Example of phase-shifting distributions and synthesized Σ and Δ patterns.

Perspectives

After this proof of concept demonstration in laboratory environment, the perspectives are the development of advanced prototypes for operation in real conditions. In order to enhance the compactness and tracking accuracy, developments at higher frequencies such as 30-GHz and 60-GHz are considered as well.

Related Publications:
[1] A. Clemente, L. Dussopt, R. Sauleau, P. Potier, P. Pouliguen, "Wideband 400-element Electronically Reconfigurable Transmitarray in X Band ," IEEE Transactions on Antennas and Propagation, vol. 61, no. 10, October 2013, pp. 5017-2027.
[2] L. Di Palma, A. Clemente, L. Dussopt, R. Sauleau, P. Potier, P. Pouliguen, "Radiation Pattern Synthesis for Monopulse Radar Applications using a Reconfigurable Transmitarray in X-band," 9th European Conference on Antennas and Propagation, Lisbon, Portugal, 12-17 April 2015.

Millimeter-wave Backscattering Measurements with Transmitarrays for Personal Radar Applications

Research topic: millimeter-wave propagation, radar applications.

Authors: F. Guidi, A. Guerra, A. Clemente, R. D'Errico, L. Dussopt, D. Dardari

Abstract: the concept of personal radar has recently emerged as an interesting solution for next 5G applications. In fact, the high portability of massive antenna arrays at mm-waves enables the integration of a radar system in pocket-size devices (i.e. tablets or smartphones) and enhances the possibility to map the surrounding environment by guaranteeing accurate localization together with high-speed communication capabilities. The aim of our research is to investigate the capability of such personal radar solution using real measured data collected at mm-waves as input for the mapping algorithm.

Context and Challenges

Currently, next 5G mobile technology is still at its infancy, as its practical adoption is expected in the next decade, with a consequent explosion of research studies and projects for its assessment. To put forth on the need to achieve high data rates and D2D communication, massive arrays and millimeter-wave (mmW) technology have become a matter of investigation. It is expected that their joint adoption will play a key role in future 5G communications scenarios. Indeed, the reduced wavelength at mmW paves the way for packing a large number of antenna elements into a small area and for adopting massive arrays systems at base station (BS) or access points (APs) as well as at mobile end. In this context, transmitarrays (TAs) are a recent cutting edge antenna array technology. The concept of a smart personal radar, recently proposed in [1], is based on the idea of a massive array operating at mmW frequencies able to electronically scan the surrounding environment and to reconstruct a map of it.

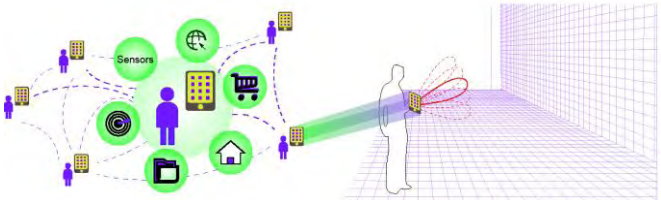

Figure 1. Personal radar concept.

Main Results

We characterized real mapping performance by exploiting measurements collected in the 58.5-61.5 GHz band in a typical office environment (a corridor) with two 400-elements TAs. For each measurement position, the radar rotates its position in order to emulate a real radar which scans the environment. Then, such data is exploited in the mapping algorithm, which is based on the adoption of an Extended Kalman Filter (EKF). Contrarily to conventional radar approaches where environment mapping is preceded by a detection phase, here all the available energy measurements are included in the observation model [1]. The case study here described refers to a corridor environment whose layout is juxtaposed to the estimated RCS maps in the results. We adopt a grid-based approach where the environment is discretized in cells having area (0.1 m × 0.1 m) each according to the TA radiation patterns.

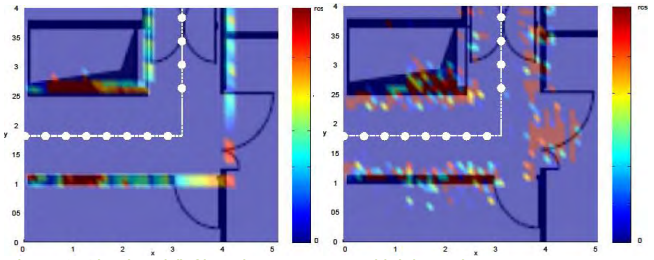

Figure 2. Simulated (left) and measurement (right) results.

In the two maps reported in figure 2, simulation results (left), are compared to measurement results (right). As shown in the figure, there is a nice match between the real maps and those estimated, especially for what simulated data are concerned. Discrepancies between results are due to different phenomena. First of all in the simulations a simple scattering model has been assumed. As a consequence, when considering collected measurements as an input for the mapping simulator a mismatch between the model and the real scattering behavior can cause performance degradation. Secondly, in simulations we have assumed a free space propagation condition for each interrogated cell supposing that the multipath effects is implicitly taken into account when including all the array pattern information in the grid-based approach. Finally, in the simulation results the far-field assumption has been made. Thanks to this hypothesis, it is possible to exploit the far-field TA radiation pattern both in the prediction and the measurement phases when evaluating the mapping performance.

Perspectives

The feasibility of the personal radar concept has herein been demonstrated through measured data, where two (20x20) linearly-polarized TAs have been used in a bistatic radar configuration to scan a real office environment. The data collected have been exploited for map reconstruction using a grid-based Bayesian state space approach. Results have demonstrated the feasibility of the mmW personal radar, previously proved only through simulations, and that a good quality of map reconstruction can be achieved even when a limited set of phase values in the TA are available. New refined mapping models will be required in order to improve the match between the map reconstruction and the real map.

This research was supported in part by the IF-EF Marie- Curie project MAPS (Grant 659067).

Related Publications:

[1] F. Guidi, A. Guerra, D. Dardari, "Personal Mobile Radars with Millimeter-Wave Massive Arrays for Indoor Mapping", IEEE Trans. on Mobile Computing, vol. 15, no. 6, 2015, pp. 1471-1484.

[2] A. Guerra, F. Guidi, A. Clemente, R. D'Errico, and D. Dardari, "Millimeter-wave Backscattering Measurements with Transmitarrays for Personal Radar Applications", Proc. IEEE Globecom, LION Workshop, Dec. 8, 2015, San Diego, CA, USA.

[3] A. Guerra, F. Guidi, A. Clemente, R. D'Errico, L. Dussopt, and D. Dardari, "Application of Transmitarray Antennas for Indoor Mapping at Millimeter-Waves", European Conf. on Networks and Communications (EuCNC), June 29-July 2, 2015, Paris, France.

Radio Channel Characterization at 2.4 GHz in Nuclear Plant Environment

Research topic: radio channel, propagation.

Authors: H. Farhat, L. Minghini, J. Keignart, R. D'Errico

Abstract: this work presents a radio channel measurement campaign at 2.4 GHz conducted in a nuclear power plant. The aim of this study is to investigate radio propagation characteristics in this particular industrial environment. Given the presence of thick concrete walls and large metallic structures, the propagation conditions are expected to be very harsh. Path loss models and fading statistics have been extracted for different Line of Sight and Non Line-of-Sight scenarios.

Context and Challenges

Wireless sensor networks (WSNs) have gained world-wide attention in recent years and their use is expanding in industrial applications where machinery automation and sensor systems are traditionally realized through wired communications, which could be replaced by low-cost wireless solutions. Nevertheless an optimized deployment of the WSN, demands an exact knowledge of the channel characteristic in the investigated environments.

In a nuclear power plant, given the presence of thick concrete walls and large metallic structures, the propagation conditions are expected to be very harsh. In the framework of the CONNEXION project, a channel measurement campaign at 2.4 GHz was carried out by CEA LETI. Here we report the first results of the channel modeling in this frequency band.

Main Results

A frequency domain channel sounder based on Vector Network Analyzer was employed on one side, an automatized positioner was used to scan a 2-D spatial grid, which together with a high-resolution SAGE algorithm, permitted us to extract multipath parameters including the propagation direction in azimuth at Tx or receiver Rx in order to investigate small scale fading distribution. The spatial grid dimensions was 7x7 with a step of $\lambda/2$ referred to the 2.4 GHz frequency. The measurement bandwidth was between 2 and 2.8 GHz with 500 kHz steps.

Different propagation scenarios were considered in this channel measurement campaign. The first one (CM1) aims to investigate the propagation in a machine room in LOS (Line-of-Sight) and Non-LOS (NLOS) conditions. The positioner was placed in equidistant locations with a 1 meter step, for a total number of 4 positions in LOS and 5 positions in NLOS condition.

In order to characterize strong NLOS communication conditions that may occur in nuclear power plants, another scenario (CM4) has been studied. In its first topology (NLOS^2), the Tx and Rx were separated by a huge concrete wall of around 60 cm thickness, while in the second one (NLOS3), the Tx position was chosen so that an additional metallic door separated Tx from Rx. In both configurations the positioner was placed in regular positions with a 50 cm step for a total number of 8 positions in NLOS^2 and 6 positions in NLOS^3 condition.

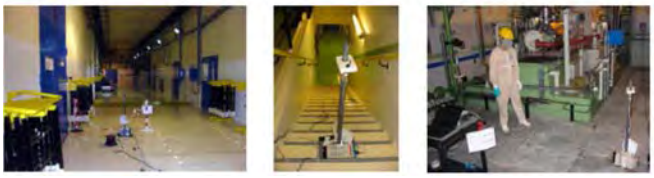

Figure 1. Measurement scenarios in nuclear plants.

In LOS condition, the path loss exponent presents a lower value than in free space. This result is a common value in indoor LOS and it is due to the energy contribution of the secondary multipath components. The average fading depth in this case is equal to -7.5 dB which is even smaller than the NLOS scenarios. This is due to the high reverberating measured environment that presents a large number of metallic scatterers. The NLOS and NLOS^2 configurations present a similar path loss exponent n and the same fading dips. The main difference is on a 14 dB additional loss that can be explained by the higher wall thickness that generates the NLOS condition in the case. The harshest scenario is the NLOS3 configuration which presents a very important path loss component (n=5.7).

The fading envelope has been extracted for all scenarios and different distributions have been tested; Rician and Gamma distribution were found to be well suited for the scenarios

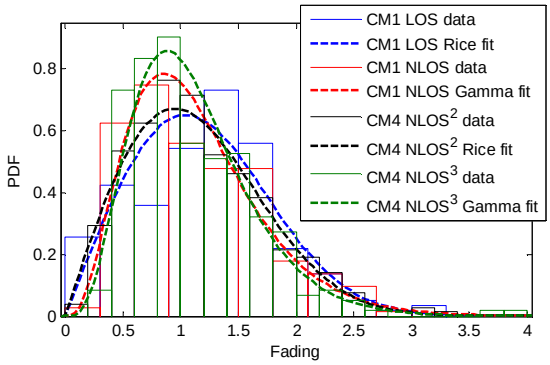

Figure 2. Fading distribution fitting in LOS, NLOS and strong NLOS scenarios.

Perspectives

A full channel model is being derived from this work and implemented in a channel emulator. This model is available to benchmark different wireless solution in harsh environments.

Related Publications:

[1] H. Farhat, L. Minghini, J. Keignart, R. D'Errico, "Radio channel characterization at 2.4 GHz in nuclear plant environment," 9th European Conf. on Antennas and Propagation (EuCAP), April 13-17, 2015, Lisbon, Portugal.

04

SENSORS AND SYSTEMS

- Sensors
- Signal processing

MagnetoCardioGraphy (MCG) and MagnetoEncephaloGraphy (MEG) Recordings with an Optically-Pumped ^{4}He Magnetometer at Room Temperature

Research topic: optically-pumped sensors, magnetometry.

Authors: S. Morales, M.C. Corsi, W. Fourcault, C. Gobbo, F. Lenouvel, G. Cauffet, M. Le Prado, F. Berger, G. Vanzetto, E. Labyt.

Abstract: MCG and MEG are two functional non-invasive imaging techniques recording the magnetic fields arising from the electrical activity of the heart and the brain, respectively. Preliminary proofs of concept confirm the possibility to record MCG/MEG signals from healthy volunteers by using an optically-pumped magnetometer (OPM) based on the parametric resonance of ^{4}He atoms in a near-zero magnetic field at room temperature. The achieved sensitivity of the first OPMs dedicated to biomagnetic field measurements is around 210 fT/√Hz in the 2-300 Hz band.

Context and Challenges

MCG/MEG are functional imaging technologies characterized by their non-invasiveness, high temporal resolution, high spatial resolution (compared to ECG ElectroCardioGraphy or EEG ElectroEncephaloGraphy), and high sensitivity. They yield information not accessible through their electrical counterpart ECG and EEG. The amplitude of biomagnetic fields is more than 10^6 smaller than the Earth's magnetic field. Hence, MCG/MEG measurements require ultrasensitive sensors such as superconducting quantum interference devices (SQUIDs). Wide dissemination of MCG/MEG is hindered by some limitations of commercial SQUIDs: high cost (2 M€), operational constraints (sensors cooled with helium) or infrastructure needs (examinations carried out in a bulky and heavy magnetically shielded room). Moreover the thermal insulation required for the cooling significantly increases the distance "source-sensor" and decreases the signal strength. Thus for ten years, high sensitivity optically pumped magnetometers based on heated alkali vapor have emerged as an interesting alternative for MCG/MEG measurements (most of the developments are still at the research stage).

Main Results

Optically pumped magnetometers developed at CEA-LETI are based on the parametric resonance of ^{4}He. At low magnetic field, resonant variations of the absorbed light are observed when a static magnetic field is swept around the zero-field value (Hanle effect). Resonance also appears in an amplitude modulated magnetic field obtained by adding a RF field in the direction of the field to be measured. A vector measurement of the three components of a low magnetic field can be derived by using two RF magnetic fields (orthogonal to each other and to the direction of polarization of the pump light). In this detection scheme implemented in our OPM, to first order, resonance signals detected on the transmitted light at Ω, *w* and Ω ∓ w are proportional to the three components of the magnetic field to be measured (Ω, *w* are the pulsations of the two RF fields). In addition to providing tri-axis vector measurements, one specificity of our OPM is that the ^{4}He vapor is neither cooled nor heated. The sensor is operated at room temperature without thermal insulation. The distance "sensor-subject" is thus reduced and the signal strength is increased. This maintenance-free sensor is a promising cheaper alternative to SQUIDs. Our first prototypes achieve a sensitivity around 200 fT/√Hz in the 2-300 Hz band.

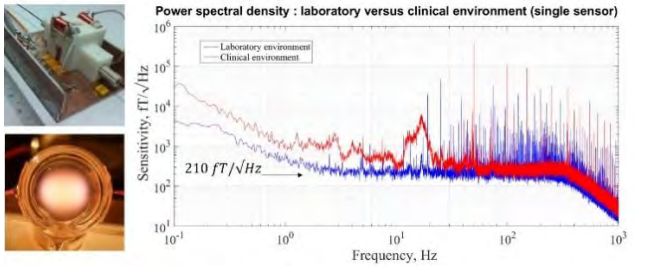

Figure 1. Sensitivity of the CEA-LETI's OPM dedicated to biomagnetic field measurements.

Operability of our device has been demonstrated by phantom measurements cross-validated with real measurements carried out on healthy subjects. Typical features of the cardiac cycle (QRS complex, P and T waves) are clearly resolved on MCG recordings (Figure 2a,b). Concerning MEG signals, similar latencies (difference of less than 4%) and morphologies have been obtained with OPMs and SQUIDs in the case of auditory evoked fields (Figure 2c) and alpha rhythm modulation related to eyes closing/opening.

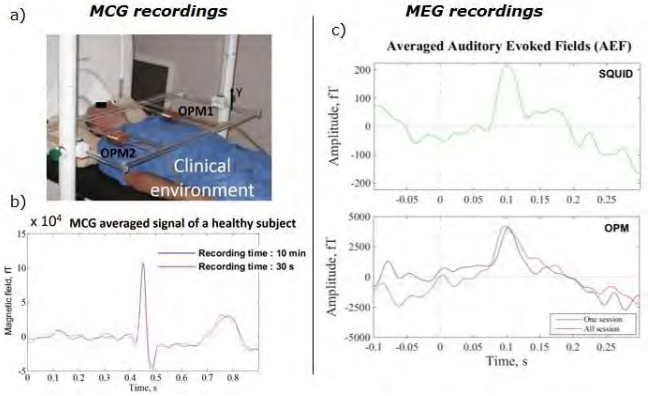

Figure 2. a) Experimental setup for MCG recordings; b) Averaged MCG signals (ICA signal processing); c) averaged MEG signals obtained with a SQUID or an OPM placed in the right temporal area. The increase in the signal amplitude for the OPM measurement is owed to the smaller distance sensor/source.

Perspectives

Further work will concentrate on improving the sensitivity of the OPM and designing an OPM array dedicated to multichannels MCG/MEG recordings enabling mapping approaches.

Related Publications:
[1] S. Morales, MC. Corsi, E. Labyt et al., "Room temperature optically-pumped 4He magnetometer for biomedical measurements: MCG – MEG", 3rd Workshop on Optically Pumped Magnetometry, October 9th, 2015, Helsinki, Finland.
[2] S. Morales, MC Corsi, W. Fourcault, C. Gobbo, F. Bertrand, F. Alcouffe, F. Lenouvel, G. Cauffet, M. Le Prado, F. Berger, G. Vanzetto, E. Labyt, "MagnetoCardioGraphy (MCG) and MagnetoEncephaloGraphy (MEG) recordings with an optically pumped 4He magnetometer at room temperature", 3rd Advanced Technology Workshop on Microelectronics, Systems and Packaging for Medical Applications (IMAPS), Nov. 25th-26th, 2015, Lyon, France.

Low Noise Electrometer for Marine Applications

Research topic: optically-pumped sensors, electrometry, magnetometry.

Authors: M. Le Prado, M. Baicry, C. Lefrou, L-L. Rouve

Abstract: the measurement of weak electric fields in seawater concerns numerous applications. Low noise at low frequency is often required and difficult to achieve. Current-based electrometers using magnetometers are demonstrated to be good candidate for this purpose. The global transfer function is theoretically and experimentally studied. It allows the design of a sensor whose expected noise level is of 0.15 nV.m^{-1}.Hz$^{-1/2}$ at 1 mHz, which is very promising.

Context and Challenges

The measurement of electric fields in seawater concerns many applications (geophysics, oil prospection, vessels detection, etc.). Commercial marine electrometers measure the electrical potential difference between two separated electrodes. Their noise at frequencies down to 1 mHz is degraded compared to the noise at 1 Hz. To reduce the noise, the distance between both electrodes is increased and can reach few hundreds of meters. This strategy is however limited by the sensitivity of the potential of electrodes to parameters such as temperature, oxygen concentration, which variations from one electrode to the other also give low frequency noise. These long electrometers are obviously not used vertically.

Another type of electrometer based on low impedance current measurement was studied. The measurement is done via the magnetic field *B(I)* generated by the current between the two electrodes. Leti develops magnetometers with very low noise level at low frequencies between 1 Hz and 1 mHz, which can greatly benefit to this application. However, this technology of electrometers has only been studied assuming an impedance equivalent to that of the seawater. We therefore have to consider other cases.

Main Results

We designed a current based electrometer, firstly solving the problems of former devices, and secondly able to simultaneously measure the magnetic and electric fields using a switch that allow sequential measurement of the Earth magnetic field B_0 and $B_0 + B(I)$. From which we compute $B(I)$.

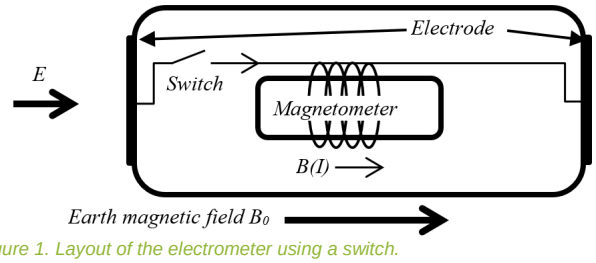

Figure 1. Layout of the electrometer using a switch.

We modeled the transfer function of the current electrometer taking into account impedances of all components: electrodes, coils, switch, the conductivity of the seawater and the kind of magnetometer. The whole model was developed and validated step by step thanks to electrical or electrochemical characterizations. Figure 2 matches the current obtained in the coil at 0.02 Hz with the model or experimentally, for various electrode diameters (2.5 - 5 cm) and separating distances (2.5 - 20 cm). The electrodes used, for their low impedance properties, are in Ag/AgCl.

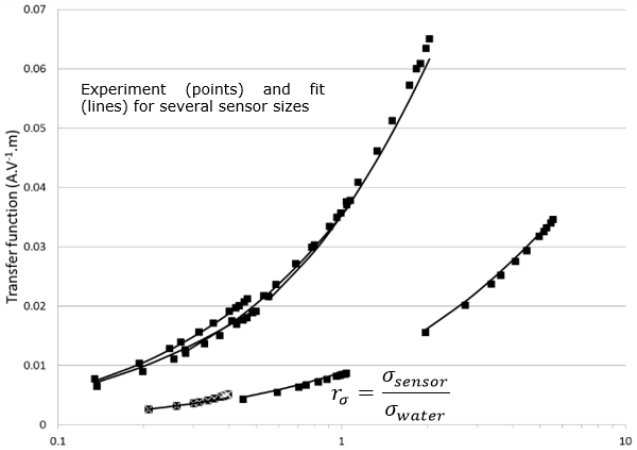

Figure 2. Variations of the current into the coil for different sensor sizes.

The agreement between the model and the experimentation is better than 12%. The model led us to a good understanding of the current electrometer properties and we identified a way to calibrate it, varying for example the size of electrodes [1], to make it usable whatever the conductivity of the seawater. We also designed, thanks to a multi-parametric optimization approach, an electrometer optimized in terms of low frequency noise for an arbitrary size of 1.5 *m* long, 0.4 *m* radius, using an optically pumped helium magnetometer having a magnetic noise of 1 $pT.Hz^{-1/2}$ [2]. The noise of such a current electrometer would be 0.15 $nV.m^{-1}.Hz^{-1/2}$.

Perspectives

Next step of the development of our current electrometer is to realize a full prototype and to test it in seawater. We will also duplicate the system presented here to achieve three axes measurements.

Related Publications:
[1] M. Baicry, C. Lefrou, L-L. Rouve, M. Le Prado, E. Chainet, "Performance improvement of a current based marine electrometer", Marelec 2015, Philadelphia.
[2] J-M. Léger, F. Bertrand, T. Jager, M. Le Prado, I. Fratter, J-C. Lalaurie, "SWARM absolute scalar and vector magnetometer based on helium 4 optical pumping", Eurosensors XXIII, 6 - 9 sept. 2009, Lausanne, Switzerland.

Carbon for High-Resolution Acoustic MEMS

Research topic: micro-electromechanical sensors

Authors: S. Thibert, N. Sridi, J.C. Gabriel, M. Delaunay, A. Ghis

Abstract: new material opportunities for integrating microelectromechanical systems are explored. Nanometer-thin carbon membranes show extraordinary mechanical properties combining flexibility and tenacity, while being compatible with classical microfabrication processes. This work addresses the feasibility and use opportunities of Capacitive Micromachined Ultrasonic Transducers (CMUT) having a vibrating surface in the micrometric range. Reducing the vibrating area induces an increase in the spatial resolution. To get significant displacements of the membrane, its thickness is reduced down to the nanometer range.

Context and Challenges

Diamond-like carbon (DLC) has drawn attention in the past for its wear and electrochemical properties. For MEMS applications, DLC has been mainly identified as a good candidate for coating layers due to its low roughness that reduces friction between mobile parts. Furthermore, the Young's modulus of some carbon materials has been reported to range from a few tens MPa to more than 1TPa, depending on the thickness and atoms arrangement. This triggered our interest in carbon materials, and beyond graphene, in DLC, as a core material for MEMS and not just for simple coatings.

The present study is a device-oriented approach that considers the feasibility and advantages of using freestanding nanometer-thick DLC as a vibrating membrane in acoustic MEMS.

Main Results

Micrometer-sized CMUTs have been fabricated using base devices providing sets of 150-nm deep trenches open into silicon dioxide covered with a gold patterned layer. The trenches range from 0.5 µm to 2 µm in width and from 1 µm to 100 µm in length. A buried electrode is lying below the floor of each trench. Contact pads for the gold wedges and for the buried electrodes are made coplanar. The mobile part of the MEMS is an ultrathin membrane reported over this pattern.

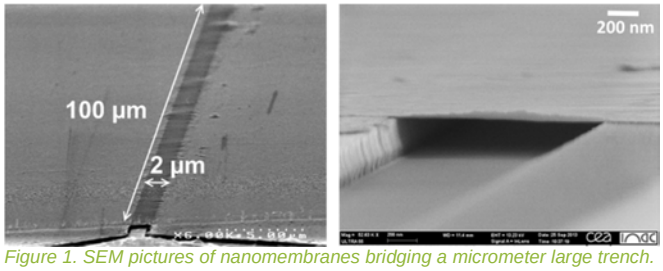

Figure 1. SEM pictures of nanomembranes bridging a micrometer large trench.

These membranes are elaborated using the ECR technique, onto a secondary substrate previously coated with PMMA. A first 2-10 nm thick layer of carbon is deposited, and then covered by a 2-nm thick layer of Nickel. Nickel is used to enhance the electrical conductivity of the membrane. The substrate is then flipped onto the trenched device, and the PMMA sacrificial layer is removed. The Ni-C membrane bridges over the trenches, and is electrically connected to the gold pattern.

The mechanical properties of such membrane have been measured through two experiments. The first experiment consists in applying a punctual force via an AFM tip while measuring the induced deflection. This allows for figuring the stiffness of the membrane for both linear and nonlinear behavior. The second experiment consists in electromechanically deflecting the membrane by applying a voltage potential between the membrane and the floor of the trench, via the buried electrode. Resulting deflections depending on the applied voltage are measured using the AFM in tapping mode. Both experiments provide similar estimation of the bending rigidity of the NiC bilayer membrane. Very large deflections up to 70 nm have been obtained for 2-µm large suspended area, this reveals the outstanding flexibility and tenacity of these membranes.

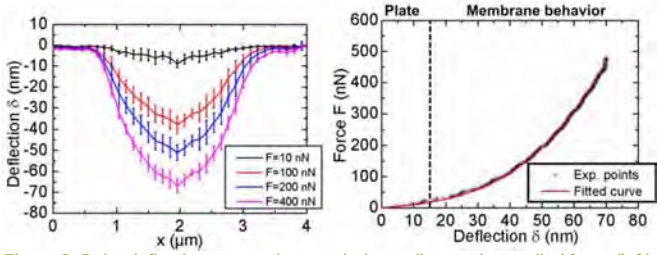

Figure 2. Point deflection across the trench depending on the applied force (left). Deflection at the center of the trench (right).

Perspectives

Mechanical deformation under RF excitation is currently analyzed to qualify the resonance figure. This study opens the way to unprecedented reduction of the active area of vibrating systems, and hence to an increase in acoustic imaging resolution.

Related Publications:
[1] A. Ghis, N. Sridi, M.Delaunay, J.C. P. Gabriel, "Implementation and mechanical characterization of 2 nm thin diamond like carbon suspended membranes", Diamond and Related Materials, Volume 57, August 2015, pp. 53-57.
[2] S. Thibert, A. Ghis, M.Delaunay "Mechanical Characterization of Ultrathin DLC Suspended Membranes for CMUT Applications", Physics Procedia, Volume 70, 2015, pp. 974-977.

GaN-Wire Based Self-Powered Flexible Force Sensor: Finite Element Modeling of Sensor Unit Cell

Research topic: flexible system integration, GaN piezoelectric wires, adaptable sensors

Authors: E. Pauliac-Vaujour, A. El Kacimi, J. Eymery

Abstract: teams of CEA Leti and CEA INAC have developed a new technology of adaptable self-powered flexible force sensor for surface-distributed measurement and highly integrated applications. This thin sensitive film relies on the properties of CEA's nanocomposite whose active elements are intrinsically-piezoelectric, specifically-grown GaN wires. Simulation tools for the optimized and application-driven design of such sensors have been developed. Finite element models are used to explain the influence of the wires' characteristics and geometric arrangement on the response of the device by calculating the potentials imposed by deformation, symmetry and crystallinity.

Context and Challenges

System integration is the new paradigm for consumer electronics and information technologies. With the ever increasing demand for connected objects and embedded intelligence, it has become necessary to focus on new forms of systems that are capable of adapting to the ever more numerous constraints related to industrial integration, such as increased sensitivities, increased conformability, low cost, low energy consumption, wireless communication, etc. One of the routes to innovative integrated solutions is the large-scale implementation of smart materials and nanotechnologies. Here we report on an example of a system which involves a conformable, self-powered sensor for 3D force and displacement measurement, and which aims to tackle the issue of low power and high integration, in particular.

Main Results

The sensor exhibits a capacitive structure composed of a thin nanocomposite layer stacked between two thin-film electrodes. Electrode evaporation was carried out in CEA's clean-rooms, while a specific process was implemented to assemble a nanocomposite with controlled structural and geometrical characteristics, based on predictions extrapolated from the results of finite element (FEM) simulations. Simulations were carried out using COMSOL Multiphysics®. Measurements of the sensitivities of our devices were already reported (Fig. 1) [1].

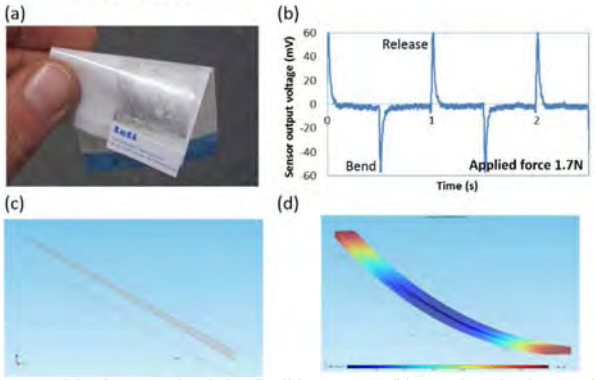

Figure 1. (a) Photograph of the flexible sensor; (b) Bend and release signal generated upon a 1.7 N force [1]; (c) Structure in the FEM model of a single conical wire of hexagonal cross-section with a spontaneous polarization along the c- (piezoelectric) / x- (crystallographic) axis. Wire length 120 µm, top radius 0.7 µm, conical angle 1°; (d) Simulation of the displacement undergone by the nanocomposite (case of a single wire). Color bar ranges from 0 to 1.2 µm.

Our newly improved model outdoes existing literature in a sense that it accounts for the crystallography of GaN by referencing the c and b-axes of the GaN hexagonal wurtzite structure with regards to the x and y-axes of COMSOL. This offers a better understanding of the potential generation phenomenon for such types and arrangements of wires within the nanocomposite and depending on the way the sensor is solicited in the application.

Additionally, parametric studies were carried out at constant surface and constant volume to account for the intrinsic correlation existing between the different geometrical parameters of wires (Fig. 2). We were able to determine that there exists an optimum of wire length for potential generation (the 50 µm – 120 µm range in the studied case) and that short wires are more sensitive to conical angle variations than long wires. However, although conicity is mandatory for potential generation, a small value of conicity (few 0.1°) is sufficient for charge separation and potential generation, since saturation occurs from a certain angle (from 0.1° for longer wires to several degrees for shorter ones).

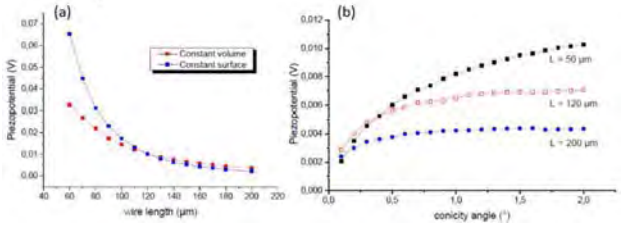

Figure 2. Simulated evolution of the generated piezopotential as a function of the (a) wire length at 1° conicity angle in both constant volume and constant surface models and (b) conicity angle for different wire lengths. Top radius 0.7 µm. The potential is taken in the middle of the m-facet of the wire.

Perspectives

These calculations are of particular relevance in the technological choices to be made regarding wire growth, nanocomposite assembly and device design with a view to optimizing the global sensor performances in the context of the targeted applications [2,3]. Perspectives include the investigation of different types of deformations and crystallographic orientations of the nanocomposite, along with the corresponding experimental sensor assembly and characterization (real case testing).

Related Publications:
[1] S. Salomon, J. Eymery, E. Pauliac-Vaujour, "GaN wire-based Langmuir-Blodgett films for self-powered flexible strain sensors", Nanotechnology 25 (2014) 375502.
[2] A. El Kacimi, E. Pauliac-Vaujour, J. Eymery, "Ultra-long GaN wires for piezoelectric applications", ICNS conference, Beijing (2015).
[3] A. El Kacimi, E. Pauliac-Vaujour, J. Eymery, "Wire-based flexible piezoelectric sensor for SHM applications", COMSOL conference, Grenoble (2015).

Emotion Estimation using Wearable Physiological Sensors: Feature Relevance Analysis

Research topic: wearable sensors, signal processing

Authors: C. Godin, F. Prost-Boucle, A. Campagne, S. Charbonnier, S. Bonnet, A.Vidal

Abstract: emotion estimation using wearable sensors is a technological development that can be useful for several applications from telemedicine to entertainment. In order to better understand the contribution of each signal, and thus sensor, several feature selection algorithms were implemented on two databases freely available to the research community. Both databases manipulate emotions by showing participants short videos (video clips or part of movies). Features extracted from Galvanic Skin response were found to be relevant for arousal in both databases and other relevant features were only available for one.

Context and Challenges

Sensors measuring the physiological activity can be used in order to estimate emotions. In literature, several studies to estimate emotions are reported. These studies differ in many ways: emotion elicitation and evaluation, classification methods and sensor systems used. All these differences make difficult to compare the results of those studies.

The goal is to evaluate the relevance of particular features to emotion classification. Furthermore, we will aim at identifying features that appear to be relevant whatever the database used (meaning those features could be used to classify emotions whatever the way emotions are induced). To achieve this goal, we explore and compare peripheral signals from the two databases "DEAP" and "MAHNOB-HCI" freely available for the research community.

Main Results

The first result is that the classification task using valence and arousal labels was not easy, for both databases. A second result is that better results were obtained with the MAHNOB database than with the DEAP database. It was also interesting to identify the relevant features for each label, their variation, and whether they correspond to well-known physiological reactions.

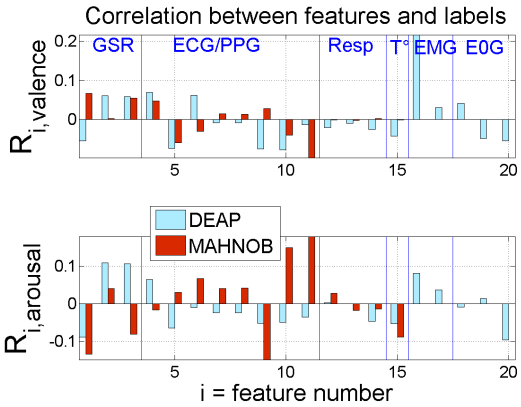

Figure 1. Correlation values between features and valence (top) and arousal (bottom).

The most important feature seems to be the HRV power in three frequency bands. Those features are commonly used in emotion estimation. These features were only relevant for MAHNOB perhaps because it was not correctly estimated using PPG in DEAP. For DEAP, eye blinking rate for arousal and variance of zygomatic EMG for valence, were both well-known relevant features for respectively vigilance and attention. Features extracted from GSR show a significant correlation with arousal for both DEAP and MANHOB databases. This result is not surprising given the close relationship found in the literature between the skin activity level and individual's emotional state. Using a forward search algorithm associated with a Bayesian classifier, optimal accuracy was achieved only with a few set of features (from 1 to 5) and this accuracy is equivalent to previous study.

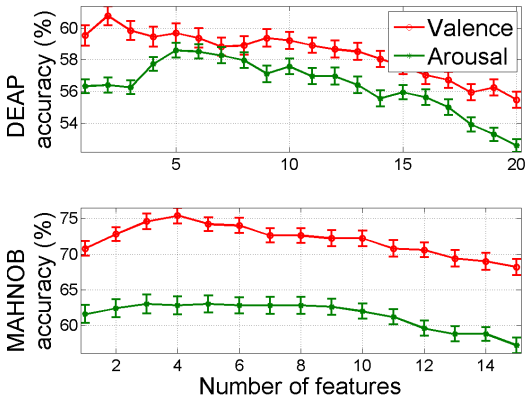

Figure 2. Classification accuracy with 95% lower and upper bound for each database and each label (2 classes) with respect to the number of features (forward selection).

DEAP valence	16 2
MAHNOB valence	10 11 1 14
DEAP arousal	2 15 17 20 16
MAHNOB arousal	10 11 6

Features in selected order by forward search

Perspectives

Those results should be confirmed by new experiments, which should use the most complete set of sensors possible, including all the signals recorded in DEAP and MANHOB databases, in order to obtain results comparable with those databases. It would also be interesting to measure both PPG and ECG in order to confirm our hypothesis that PPG is not precise enough for HRV spectral analysis.

Related Publications:
[1] C. Godin, F. Prost-Boucle, A. Campagne, S. Charbonnier, S. Bonnet, A. Vidal, "Selection of the Most Relevant Physiological Features for Classifying Emotion," 2nd Int. Conf. on Physiological Computing Systems, 2015, pp. 17–25.

Transportation Mode Recognition using Smartphone Embedded Sensors

Research topic: signal processing, classification, transportation mode recognition.

Authors: O. Lorintiu, F. Masculo, A. Vassilev, M. Desvignes, O. Michel

Abstract: Thanks to the increase in processing power and in the number of sensors present in today's mobile devices, context-aware applications have gained a renewed interest. This study focuses on a particular type of context, the transportation mode used by a person, and it summarizes a method for automatically classifying different transportation modes with a smartphone. It takes into account battery life constraints by using low-power sensors and by the implementation of a low-complexity algorithm. The method was evaluated with real data presenting promising results: an accuracy of around 95% was obtained when classifying 8 different classes with a random forest.

Context and Challenges

Detecting transportation modes has gained an increasing attention in recent years thanks to the widespread of smartphones and wearable devices with new sensors and increasing computing power. Thus the correct recognition of this particular dimension of a person's context has applications in various fields such as the automation of mobility surveys, the estimation of transportation's environmental impact and health/fitness applications. In this research, we aim at constructing a system that fusions a higher number of low-power sensors than in most studies that focus mostly on GPS and accelerometer and that consumes little resources.

Main Results

Independently of the chosen approach or sensors the transportation mode recognition follows a general scheme. The first step is the acquisition of sensor data which is followed by a preprocessing step that typically involves segmenting the sensor stream in windows of analysis as well as the conditioning of the signals. Next, discriminant features are extracted from the data windows, thus greatly reducing the dimension of the data. The extracted features are then fed into a previously trained classification algorithm that outputs a first estimate of the user's context. This estimate can be improved by a post-processing step that filters erroneous classifications, delivering the final estimate of the user's context..

Figure 1. Android application.

The method proposed in [1] acquires the raw data from the accelerometer and the magnetometer. These sensors were chosen as a starting point for the development of the algorithm because they are available in most current smartphones, they have very low power consumption and, most importantly, they are available in all files of our database. After preprocessing the features are extracted from the accelerometer and magnetometer signals. We propose a low-dimensional and physically interpretable features space in order to limit the over-fitting training risks.

The classification was performed using random forests and it was validated using 10-fold cross-validation and out-of-bag (OOB) error in order to estimate the classifier's accuracy on unseen data. The proposed approach was tested on data acquired with an Android app shown in Figure 1. The app records data from the sensors as well as the transportation modes annotated by the user. The features were calculated for the files in our database that had the following modes: still, walk, run, bike, car, bus, tram, train.

The random forest obtained a total accuracy of 95.4%with 10-fold cross-validation and the OOB error was of 5.65 %..

Perspectives

Future endeavors will focus on:

- Collecting more data for training a better classifying model, particularly for the classes that are underrepresented. It is also important to verify that the data acquired represents a large number of scenarios.
- As shown in Figure 1, we have access at a large number of sensors that can provide novel and more adapted features for classification.
- Another key point in transportation mode recognition that has yet to be investigated is how to merge information from multiple time scales.

Another very important characteristic that has often been neglected is the fact that a person's transportation mode does not change erratically over time, thus we can model the evolution of transitions with Hidden Markov Models (HMMs).

Related Publications:
[1] F. Masculo, A. Vassilev,, M. Desvignes, O.Michel, "Reconnaissance de modes de transport avec capteurs embarqués.", GRETSI 2015, Lyon, France.

A Novel Method of Point Identification based on UWB Finger Printing in an Industrial Environment

Research topic: wireless communications, signal processing

Authors: M. El Majihi, S. De Rivaz

Abstract: this paper proposes a new approach based on UWB fingerprinting algorithm to identify tool positions in an industrial environment characterized by heavy multipath wave propagation. Its main advantage is the accuracy and reliability of identification compared to RSS (Received Signal Strength) fingerprinting or trilateration algorithms. An accuracy of a few centimeters with an error probability inferior to 10^{-4} has been demonstrated.

Context and Challenges

In order to improve the quality control and reduce process times in the industry, there is a need to identify special points in the assembly line by localizing the tool used, for instance identifying which screw is being processed. This can be achieved by localizing the screw gun when operated. Specifications associated to this need require an indoor localization accuracy of a few centimeters in a real-time mode (low computational complexity). The more points close to each other, the bigger the probability of false alarm associated to points identification is, because of measurements noise and bias caused by the multipath channel, or moreover by the non-line-of-sight (NLOS channel) in an industrial environment. The proposed system uses Ultra Wide Band transceivers [1], one is fixed on the tool (mobile node) and the others (at least one) are placed at different locations (reference nodes). The mobile node establishes an UWB link with all the nodes each time its position changes and stores the channel impulse response (CIR). The algorithm developed uses the whole channel impulse response as a fingerprint [2] for a specific position. It takes advantage of channel impulse response reproducibility for the same mobile position and non-reproducibility for different positions to differentiate the mobile positions. The UWB transceiver used provides a sample every 1 ns (a sampling frequency of 1 GHz) [3]. The channel impulse response contains 64 samples. At this level of timing and because of jitter, there will be a synchronization problem between the stored CIRs.

Main Results

The algorithm first step is the synchronization of CIRs. A cross-correlation is applied between each CIR and reference CIR (the first stored CIR), these CIRs have been stored during a communication between the mobile node and the same reference node.

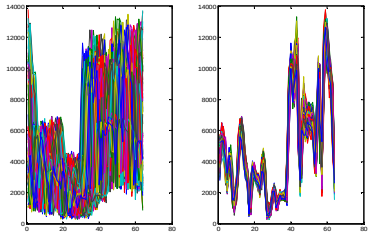

Figure 1. An example of 1000 CIRs stored at the same position before and after synchronization.

Figure 1 shows the similarity of CIRs stored at the same position before and after synchronization even if the environment is really harsh (presence of metallic objects everywhere). The optimal fingerprinting CIR is the arithmetic mean of several CIRs, it is an optimal filter of the Gaussian noise related to measures. A point (i) will be characterized by its matrix fingerprint:

$$A_i = \begin{pmatrix} r_{00} & r_{01} & \cdots & r_{0n} \\ r_{10} & r_{11} & \cdots & r_{1n} \\ \vdots & \vdots & \vdots & \vdots \\ r_{m0} & r_{m1} & \cdots & r_{mn} \end{pmatrix}$$

where r_{jk} is the sample (k) of the CIR related to the reference node (j), and (n+1) is the CIR size.

In order to identify a position, the likelihood ratio used is the standardized scalar product. It is measured between a current CIR and different fingerprinting CIRs. Figure 2 shows the result of a statistical study done in an industrial environment. The screw 4 is surrounded by 3 others screws (distance = 6 cm). The distributions of likelihood ratio between the 4 screws fingerprinting CIRs of and stored CIRs at the position 4 illustrate that the choice of the value 0.95 as a decidability threshold distinguishes the screw 4 from 1, 2 and 3. Gaussian extrapolation of measures calculates an error probability inferior to 10^{-4} for screw 4 identification.

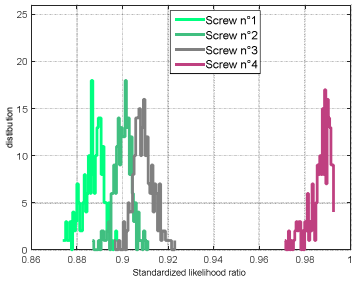

Figure 2: Likelihood ratio distributions for Screw 4 with its own fingerprinting CIR and with 3 others fingerprinting CIRs.

Perspectives

Thanks to the CIR fingerprinting method, centimetric point identification was reached in an industrial environment. Asymptotic precision of 1 cm without error is possible, but it requires to improve the UWB measure frequency (limited to 4 Hz due to hardware constraints) and to filter the CIRs used in the algorithm (to reject some CIRs that contain aberrant values).

Related Publications:
[1] I.Oppermann, M. Hamalainen, J. Linatti, “UWB Theory and Applications”, John Wiley & Sons Ltd, 2004.
[2] W. Ni, W. Xiao, Y. Toh et C. Tham, “Fingerprint-MDS based Algorithm for Indoor Wireless Localization” IEEE 21st International Symposium on, p1972-1977, Sept. 2010.
[3] M. Pezzin and D. Lachartre, “A fully integrated LDR IR-UWB CMOS transceiver based on 1.5-bit direct sampling,” in Proc. IEEE Int. Conf. Ultra-Wideband, Sep. 2007, pp. 642–647.

05

ENERGY

- Energy harvesting
- Battery monitoring systems

Batteryless Power Management Circuits for Electrostatic and Piezoelectric Energy Harvesters

Research topic: energy harvesting

Authors: S. Boisseau, P. Gasnier, J. Willemin, M. Perez, M. Geisler, G. Despesse

Abstract: we report on two batteryless power management circuits implementing non-linear energy extraction methods (Synchronous Electric Charge Extraction – SECE) to increase the energy harvesters' usable output powers. The first one is dedicated to electret-based flutter energy harvesters and the second one to piezoelectric energy harvesters in parallel. Both circuits are able to self-start and to supply wireless sensor nodes from scratch by using a two-energy-path scheme (non-optimized passive path / optimized active path). A power gain up to 150 compared to passive circuits has been reached on electrostatic devices and of up to 4 on piezoelectric ones.

Context and Challenges

Power management circuits are essential to turn the raw output energy provided by energy harvesters into a 3-V DC supply source for electronic circuits, sensors, µcontrollers…
Passive power management circuits (diode-bridge-capacitor) have low efficiencies but do not require any power source. Active power management circuits have high conversion efficiencies; yet, they have to be powered to operate. Then, problems arise when using batteryless systems, starting from scratch, as the circuits and the transistors of the power converter cannot be powered. A first solution based on a two-energy-path scheme had already been proposed in [1] (figure 1), implementing the Synchronous Electric Charge Extraction technique (SECE). SECE consists in entirely extracting the energy stored in the scavenger and to transfer it to a buffer capacitor through a flyback converter as soon as the scavenger reaches its maximum output voltage. Variants and improvements of this circuit have been proposed this year.

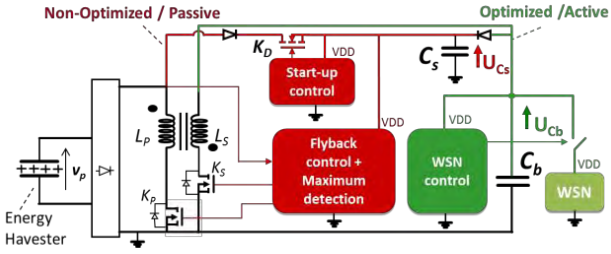

Figure 1. Two-energy-path scheme proposed in [1].

Main Results

The two-energy-path scheme has firstly been adapted to electret-based flutter energy harvesters to supply a Bluetooth Wireless Sensor Node from airflows [2]. The power conversion efficiency reaches 60% and a current of 1.2 µA only is required to supply it. Moreover, it can deal with input voltages higher than 300 V. A 200-µF capacitor (C_b) is used to store the harvested energy and to power the Bluetooth sensor node as soon as the voltage reaches 3.2 V.
The active power management circuit enabled the increase of the energy harvester's usable output power by up to 150 as compared to a passive diode-bridge capacitor circuit, proving its high benefit for electret-based airflow energy harvesters.

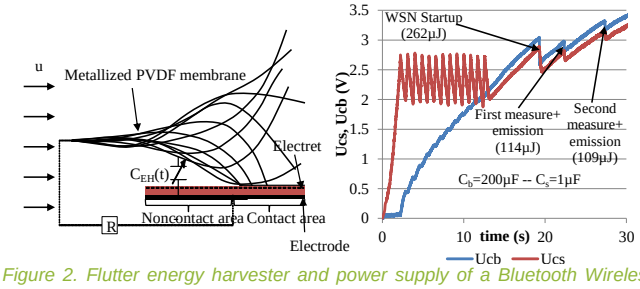

Figure 2. Flutter energy harvester and power supply of a Bluetooth Wireless Sensor Node from airflows [2].

The concept has also been adapted to implement the Synchronous Electric Charge Extraction technique to multiple piezoelectric vibration energy harvesters. The novelty of our circuit lies in its ability to handle multiple energy harvesters operating at different frequencies and different output voltages with a single and standard flyback coupled inductor. The power harvested by the multiple scavengers is stored in a single and common storage capacitor. By construction, the power management circuit is capable of dealing with high input voltages (> 100 V). Its power consumption is about 1.15 µA/3 V per energy harvester and its conversion efficiency reached 83%; its good performance has been validated by simulations and experiments on two vibration energy harvesters. Eventually, the circuit enabled an increase of the usable output power by a factor of 4 as compared to a passive circuit.

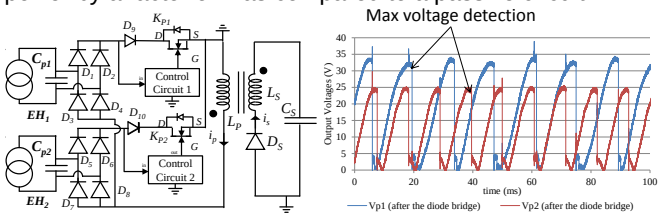

Figure 3. Power management circuit for multiple piezoelectric energy harvesters proposed in [3].

Perspectives

Research is now focused on the integration of the circuits in ASICs, on the increase of the number of energy harvesters and on the adaptation of non-linear techniques to electromagnetic devices.

Related Publications:
[1] S. Boisseau, P. Gasnier, M. Gallardo and G. Despesse, "Self-starting power management circuits for piezoelectric and electret-based electrostatic mechanical energy harvesters," 13th Int. Conf. on Micro and Nanotechnology for Power Generation and Energy Conversion Applications (PowerMEMS), Dec. 3-6, 2013, London, UK.
[2] M. Perez, S. Boisseau, P. Gasnier, J. Willemin, N. Pourchier, M. Geisler, J.L. Reboud, "Electret-based aeroelastic harvester and its self-starting battery-free power management circuit," 13th IEEE Int. NEW Circuits and Systems (NEWCAS) Conf., June 7-10, 2015, Grenoble, France.
[3] S. Boisseau, P. Gasnier, M. Perez, C. Bouvard, M. Geisler, A.B. Duret, G. Despesse, J. Willemin, "Synchronous electric charge extraction for multiple piezoelectric energy harvesters," 13th IEEE Int. NEW Circuits and Systems (NEWCAS) Conf., June 7-10, 2015, Grenoble, France.

Electret-Based Electrostatic Converters for Airflow Energy Harvesting

Research topic: energy harvesting

Authors: M. Perez, S. Boisseau, J.-L. Reboud (G2ELAB)

Abstract: two different techniques to convert the kinetic energy of airflows into electrical energy to supply wireless sensor nodes have been investigated. The first option is classical and consists in designing a small windmill which rotates thanks to aerodynamic lift of rigid blades. The second option is less known and operates thanks to an aeroelastic instability called "fluttering". The conversion of mechanical energy into electrical energy is performed thanks to an electret-based electrostatic transducer using the capacitance variations of a capacitive structure.

Context and Challenges

Everything will become connected. Known as the Internet of Things (IoT), this revolution will yet raise the issue of the energy autonomy of IoT wireless nodes not connected to the grid. A solution, called Energy Harvesting, consists in extracting energy from the environment (light, thermal gradients, vibrations) and to convert it into electricity to power electronic components and functions. Among small-scale ambient energy sources (light, thermal gradients, vibrations, strains and shocks…), airflow energy harvesting exhibits a great innovation potential and particularly at small-scale. Moreover, airflows are omnipresent around us; they can be felt outside as we are walking, cycling, taking a motorized vehicle; but also inside buildings equipped with ventilation (HVAC); then, they could be a good solution to supply the IoT nodes of the future.

Winds, and more generally airflows, are a source of kinetic energy potentially convertible in electrical energy. Unfortunately, this energy conversion is subject to various losses, especially at small scale, and therefore leads to a small overall efficiency. The first limit is called Betz's law and limits the maximum power extractable at 60% of the kinetic power. The second limitation is related to viscous losses, which are predominant at low Reynolds numbers. As we want to develop a small device for low speed, the negative effects of viscous losses will be high. Finally, a third limitation is linked to mechanical friction losses (bearing losses for example), also accentuated at small scale. In the state of the art, the record of 9.5% has been performed by the University of Sherbrook in 2007, with a windmill of 4.2 cm in diameter and a wind speed of 11.8 m/s.

Main Results

The prototypes shown in Figure 1 are built on an axial turbine architecture and exploit an electret-based electrostatic converter. When the airflow velocity is high enough, the windmill starts rotating and creates a periodic relative motion between a stator and a rotor which induces variations of capacitance. These ones are directly converted into electricity thanks to the use of Teflon electrets charged at −1400 V which polarize the variable capacitors. We have focused our study on axial turbines with a diameter of 40 mm, a depth of 10 mm, for a total volume of 12.6 cm^3. These windmills have been tested at different speeds and output powers up to 90 µW at 1.5 m.s−1 (7.5 $\mu W.cm^{-3}$) and 1.8 mW at 10 m.s−1 (111 $\mu W.cm^{-3}$) have been obtained so far. The coefficient of power reaches 5.8% and among the small-scale airflow energy harvesters previously reported, this one has the lowest cut-in speed (1.5$m.s^{-1}$).

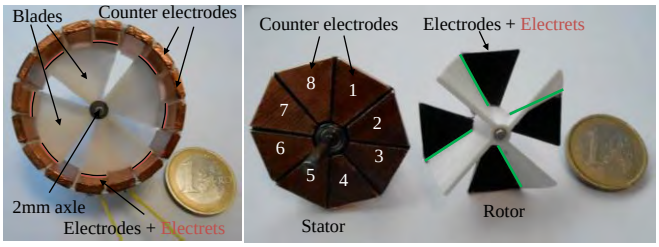

Figure 1. Electret-based electrostatic wind turbines [1].

The second option consists in exploiting fluttering effects coupled to an electret-based conversion to turn the flow-induced movements of a membrane into electricity. The device presented in Figure 2 is made of a polymer membrane placed between two parallel flat electrodes coated with 25-µm thick Teflon PTFE electret layers; a bluff body is placed at the inlet of the device to induce vortex shedding. When the wind or airstream of any kind flows through the harvester, the membrane enters in oscillation due to fluttering and successively comes into contact with the two Teflon-coated fixed electrodes. This periodic motion is directly converted into electricity thanks to the electret-based conversion process. Various geometries have been tested and have led to a 2.7c m^3 device, with an output power of 481 µW (178 $\mu W.cm^{-3}$) at 15 $m.s^{-1}$ and 2.1 mW (782 $\mu W.cm^{-3}$) at 30 m.s−1 with an electret charged at −650 V. The power coefficient of the device reaches 0.54% at 15 m.s−1 which is low, but compares favorably with the other small-scale airflow energy harvesters exploiting fluttering.

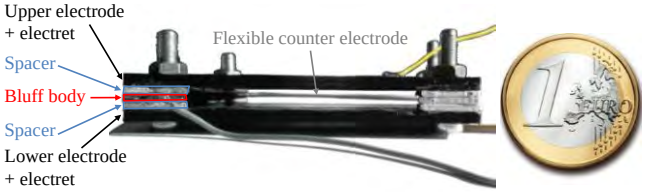

Figure 2. Electret-based electrostatic flutter energy harvester [2, 3].

Perspectives

Future works will be focused on the polarization of the capacitive structure (with or without electret), to obtain stable performances in the long-term (electrets are stable in labs for years, but their stability must be validated in real environment conditions), and on the miniaturization of the transducer to achieve a higher power density for high speed applications.

Related Publications:
[1] M. Perez, S. Boisseau, J.L. Reboud, "Design and performance of a small-scale wind turbine exploiting an electret-based electrostatic conversion", Electrostatics 2015, April 12-16, 2015, Southampton, UK.
[2] M. Perez, S. Boisseau, P. Gasnier, J. Willemin, J.L. Reboud, "An electret-based aeroelastic flutter energy harvester", Smart Mater. Struct. 1–12, 2015.
[3] M. Perez, S. Boisseau, P. Gasnier, J. Willemin, N. Pourchier, M. Geisler, J.L. Reboud, "Electret-based aeroelastic harvester and its self-starting battery-free power management circuit", 13th IEEE Int. NEW Circuits and Systems (NEWCAS) Conf., June 7-10, 2015, Grenoble, France.

Passive and Active Tracking of Electrochemical Impedance of a Drone Battery

Research topic: battery monitoring systems

Authors: H. Piret, N.Sockeel, V. Heiries, PH. Michel, M. Ranieri, V. Cattin, N. Guillet, P. Granjon

Abstract: advanced Battery-Monitoring Systems (BMS) including electrochemical impedance measurements are studied for the management of Lithium-ion battery. The proposed methods estimate the impedance over a predetermined frequency range thanks to an algorithm which can be easily implemented in an embedded system but is also able to track the time variations of the impedance. Methods of estimation in time and frequency domains are developed and compared, in both active and passive identification cases. The evolutionary impedance estimation is then applied to the battery of a drone to evaluate its state of charge and other critical indicators like the remaining flight time thanks to an extended Kalman filter.

Context and Challenges

The estimation of the electrochemical impedance is a substantial way to obtain important informations representative of the dynamic behavior of a battery and extend its monitoring. Unlike most of impedance estimations, the developed methods move away from the assumptions of linearity and time invariance, and allow tracking its time variations [1].

Main Results

Different methods to estimate the impedance both in time and frequency domains are compared. The frequency domain method [2] is based on a discrete Fourier transform as well as an exponential averaging whereas the time domain methods [3] rely on a recursive least-square (RLS) algorithm associated with an infinite or finite impulse-response (IIR or FIR) filter. If each method allows an accurate impedance estimation, the frequency domain method is characterized by a low number of operations and includes a critical notion of coherence, which can ensure the quality of impedance estimation.

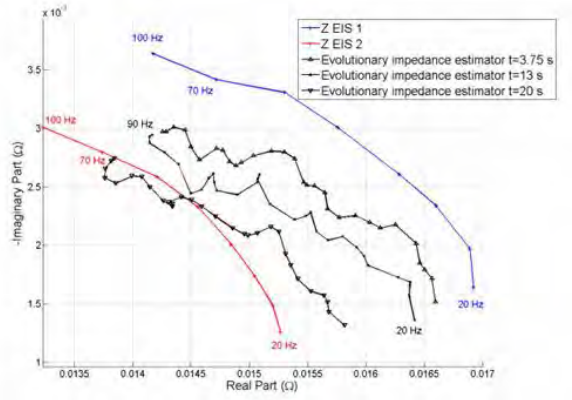

Figure 1. Nyquist diagram of the impedance estimation evolution.

Then, the evolutionary impedance estimation is used to follow the battery impedance variations during the flight both in passive and active contexts. These two approaches are not opposite but complementary. The active methods need to generate an additional signal, but in this case the frequency bandwidth can be chosen by the user. Figure 1 presents the impedance variation during a flight over the 20-100 Hz band. During the discharge, the estimated impedance moves from the first reference measurement (EIS in blue) to the second one (EIS in red).

The passive case does not need any signal generation, only the natural profile is used but limits the frequency band considered. This passive method is preferred if the natural profile is frequency-rich and if the weight and cost are critical constraint as in the case of a drone.

The electrochemical impedance is subsequently used to calculate specific drone indicators (remaining flight time and distance) through the state of charge of the battery (SoC). An extended Kalman filter (EKF) is used to estimate the state of a dynamic nonlinear system (the battery) from noisy measurements (current and voltage) collected from a natural drone profile (passive case). Figure 2 shows the estimates of the remaining flight time and distance. After nearly 4.5 minutes of flight, the remaining flight time is around 2 min left. At this time, the drone could only cover approximatively 1 km. The total duration of the flight was around 6.5 min. The take off and the landing are clearly distinguishable. Before the take-off and after the landing, the drone uses less power, which appears on the figure by steps at the beginning and at the end.

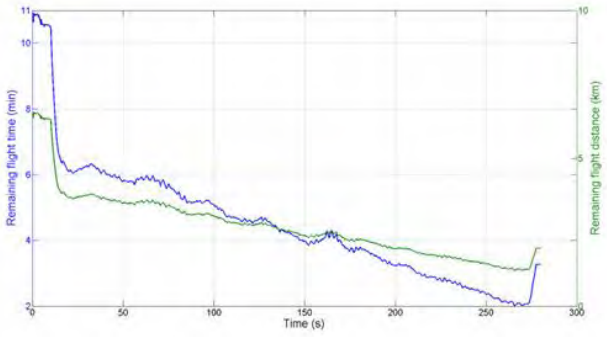

Figure 2. Estimation of remaining flight time and distance over time.

Perspectives

The electrochemical impedance will be further used to evaluate the state of health and the internal temperature of a battery. This method will be embedded into an advanced BMS to estimate battery parameters in real time.

Related Publications:
[1] H. Piret, N. Sockeel, V. Heiries, P-H. Michel, M. Ranieri, V. Cattin, N. Guillet, P. Granjon, “Passive and active tracking of electrochemical impedance of a drone battery”, European Battery, Hybrid and Fuel Cell Electric Vehicle Congress, Dec. 1-4, 2015, Brussels, Belgium.
[2] H. Piret, P. Granjon, V. Cattin, N. Guillet, “Online estimation of electrical impedance”, 7th Int. Workshop on Impedance Spectroscopy (IWIS), Sept. 24-26, 2014, Chemnitz, Germany.
[3] P-H. Michel, V. Heiries, “An Adaptive Sigma Point Kalman Filter Hybridized by Support Vector Machine Algorithm for Battery SoC and SoH Estimation”, 2015 IEEE 81st Vehicular Technology Conf. (VTC-Spring), May 11-14, 2015, Glasgow, UK.

Key Parameters Design for Online Battery Electrochemical Impedance Tracker

Research topic: battery monitoring systems

Authors: H. Piret, B. Portier, S. Bacquet, M. Palmieri, P. Granjon, N. Guillet, V. Cattin

Abstract: advanced Battery-Monitoring Systems (BMS) including electrochemical impedance measurement are studied for the management of Lithium-ion batteries using the existing current-control electronics to minimize cost and complexity. The proposed recursive method relies on a wideband approach and provides both an accurate estimate of the impedance frequency response and a tracking of its time variations. We evaluate the effect of the electronics design on the performance of this frequency evolutionary estimation of the electrochemical impedance and the proposed methodology confirms that a conventional BMS can host this tracking algorithm.

Context and Challenges

To improve the management of the internal temperature and the state of health of a Lithium-ion battery, the knowledge of its electrochemical impedance is a major issue. Taking into account the constraints of cost and simplicity of the intended applications, we use the existing electronics for current control and we study the conditions for the integration of a frequency evolutionary estimation of the electrochemical impedance inside an efficient battery management system (BMS) [1].

Main Results

The recursive method proposed to identify the electrochemical impedance relies on a wideband approach and provides an accurate estimate of this quantity in the frequency area and a tracking of its temporal variations, both in active or passive cases. The methodology for the design of the BMS components consists in the selection of the main algorithm and electronics parameters in function of the requirement for the estimation of the impedance (i.e. frequency band of interest, frequency resolution of the complex impedance, accuracy of the estimate, output refresh rate, time response or convergence delay, calculation of the complex impedance value at a specific frequency or on a particular point in the Nyquist plot, power consumption of the process). For instance, several strategies of averaging are considered to provide a fine tracking of the impedance time variations. A sliding window filtering is interesting as the convergence time is low and can thus be effective to provide a fast response if the application requires only an estimate on request. Exponential averaging limits drastically the amount of data required for the estimation and is therefore preferred for the integration (low memory size), especially if the frequency band of interest is large. A forgetting factor adjusts the noise filtering level on the estimation (figure 1).

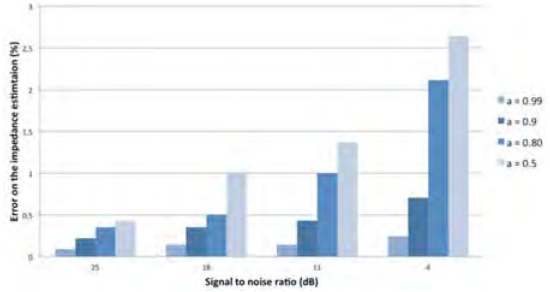

Figure 1. Effect of the forgetting factor on error on the estimated impedance.

The main steps of the algorithm are the centering of the measured data blocks and the computing of discrete Fourier transforms. This requires a small number of operations that can be fully carried out by a target such as a microcontroller, if the frequency band and the tracking rate are not too high. Figure 2 presents the effect of the number of bits used for the signal digitization on the estimated impedance in the Nyquist chart. Assuming no aliasing and that the input dynamic range of the digitizer is matched to the voltage variation to acquire, at least 10 bits (resp. 12 bits) of quantization could provide an error lower than 1% (resp. 0.1%) on the impedance.

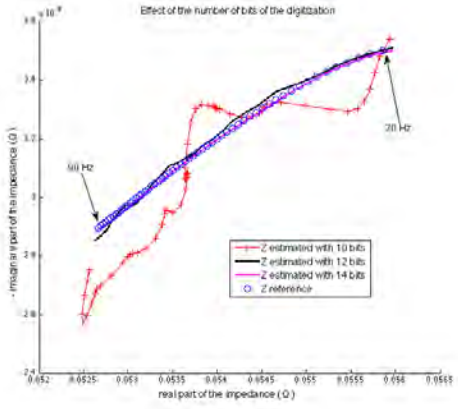

Figure 2. Effect of the number of bits of the digitization.

These design considerations have been applied to define a prototyping environment based on a microcontroller unit from the 32 bits ARM family. Our design tools allowed us to ascertain that the key parameters settings are suited to both provide a correct tracking of the impedance measurement (error near 0.3% for a band of interest covering 20 to 90 Hz, with a tracking rate of 250 ms) and fulfill the timing constraints (with parallel execution through real-time operating system). We have developed a methodology to design the key parameters of electronics dedicated to the impedance tracking of a battery. The electronics of a conventional BMS can host this tracking algorithm and is powerful enough to perform the required calculations.

Perspectives

This methodology will be applied for electronics design in the European collaborative project 3Ccar funded by the ECSEL Joint Undertaking.

Related Publications:
[1] H. Piret, B. Portier, S. Bacquet, M. Palmieri, P. Granjon, N. Guillet, V. Cattin, “Key parameters design for online battery electrochemical impedance tracker”, European Battery, Hybrid and Fuel Cell Electric Vehicle Congress, Dec. 1-4, 2015, Brussels, Belgium.

06

PHD DEGREES AWARDED IN 2015

- Lama Ghattas
- Luca Di Palma
- Mathieu Bouvier des Noes
- Iulia Tunaru
- Baher Mawlawi
- Matthieu De Mari
- Mathieu Baicry
- Marie-Constance Corsi
- Anne-Cécile Pitton

Lama GHATTAS

Centrale-Supélec, France

AUTO-DIAGNOSTIC OF RADIATION PERTURBATIONS OF ANTENNA ARRAYS.

This thesis focuses on the design of an in-situ measurement system to detect variable disturbances in the near field of antenna arrays. The first part investigates the benefit of the monitoring system for direction finding antennas (DFA). A quantitative study of the performances degradation of DFA installed on a carrier in presence of variable obstacles was done. The second part concerns the technology choices for the diagnostic system design. The Optically-Modulated Scatterer Technique (OMS) is selected. A model predicting the OMS backscattered power is developed to select the optimal dimensions of the probe. Following the theoretical studies, a 12-cm OMS probe coupled to the nonlinear device (PDCS30T) was designed. Measurements in anechoic chamber were performed to validate the link budget model and measure the sensitivity of the probe to nearby objects. Finally, an investigation was performed on the sensitivity requirements of diagnostic probes for the detection of obstacles. A dimensioning of the overall system is presented.

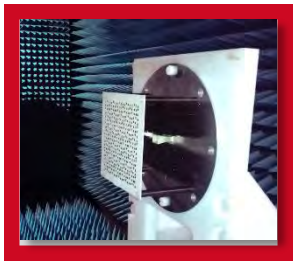

Luca DI PALMA

University of Rennes 1, France

RECONFIGURABLE TRANSMITARRAY ANTENNAS AT MILLIMETER-WAVE FREQUENCIES.

Several civil and military applications (hertzian beams, satellite communications, automotive radars, high resolution imaging systems) require antennas with reconfigurable beam capabilities (beam-scanning, beam-shaping, multiple beam generation). Transmitarray antennas are good candidates and represent an alternative to classical phased arrays or reflect-arrays for these applications. The main objective of this thesis is to demonstrate the feasibility of reconfigurable transmitarrays fabricated with standard technologies in Ka-band (20-30 GHz).
Different unit-cell designs based on p-i-n diodes have been developed to work in linear and circular polarization. Their optimization and experimental characterization have been performed. Waveguide measurements show insertion losses of 1.09 dB at 29.0 GHz with a 3-dB bandwidth of 14.7%. A hybrid simulation technique has been developed in order to analyze efficiently large transmitarrays in which the sequential rotation technique has been applied to optimize the polarization quality and the radiation patterns. A 400-elements transmitarray operating in circular polarization has been realized and tested in anechoic chamber. A beam-scanning angular coverage of ±60° and circular polarization selection (left/right) have been demonstrated.

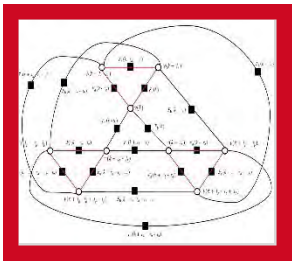

Mathieu BOUVIER DES NOES

University of Grenoble, France

ITERATIVE DETECTION OF PSEUDO-RANDOM SEQUENCES.

Pseudo-random binary sequences are very common in wireless transmission systems and ciphering mechanisms. More specifically, they are used in direct sequence spread spectrum transmission systems like UMTS or GPS or to construct preamble sequences for synchronization and channel estimation purpose like in LTE. It is always required to synchronize with the transmitted sequence. The usual way consists in correlating the received signal with a replica of the sequence. If the correlation exceeds a predefined threshold, the synchronization is declared valid.
This thesis addresses a different approach: the binary sequence is detected with an iterative message-passing decoding algorithm. A redundant graphical model is used to construct the parity check matrix. It is derived from reference parity check polynomials of a given weight t. The number and the degree of such polynomials have been studied for m-sequence and Gold sequence. More specifically, for Gold sequence, we have computed the number of parity check polynomials of weight t = 5 when the degree of the characteristic polynomial is odd. Knowing this number is important because there is no parity check equation of weight t = 3 or 5 in this case. Then, we have analyzed the impact of the selection of K reference parity check polynomials for a decoder using a redundant parity check matrix. We show that the existence of absorbing sets prevent false alarms to occur. When the decoder is only fed with noise, it does not converge to a valid sequence if it is trapped by an absorbing set. We proposed then a method for identifying these absorbing sets for t = 3. We also show that some ‘transverse’ cycles may destroy these absorbing sets and hence favors the occurrence of false alarms or wrong detections. As a result, an algorithm for selecting the parity check polynomials minimizing the probability of false alarm have been proposed. It is based on the minimization of the number of cycles of length 6 and 8, which also minimizes the number of transverse cycles. Simulations results support our theory. Then, the usefulness of detecting m-sequence or Gold sequence with a decoding technique is emphasized. Exploiting the properties of m-sequence, it is detailed how the scrambling code of WCDMA and CDMA2000 systems may be estimated blindly. This could be applied for instance for the detection of a strong interferer in a femtocell system.

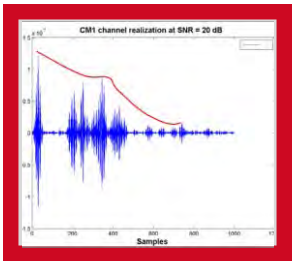

Iulia TUNARU

University of Rennes 1, France

PHYSICAL LAYER SECRET KEY GENERATION FOR DECENTRALIZED WIRELESS NETWORKS.

Emerging decentralized wireless systems, such as sensor or ad-hoc networks, will demand an adequate level of security in order to protect the private and often sensitive information that they carry. Popular security mechanisms enabling confidentiality in such networks are still based on symmetric cryptography, which requires the sharing of a symmetric key between two legitimate parties. In this context, according to the principles of physical layer security, wireless devices within the communication range can exploit the wireless channel in order to generate common secrets and protect their communications accordingly. More specifically, due to the theoretical reciprocity of wireless channels, the spatial decorrelation property (e.g., in rich scattering environments), as well as the fine temporal resolution of the Impulse Radio - Ultra Wideband (IR-UWB) technology, directly sampled received signals or estimated channel impulse responses can thus be used for symmetric secret key extraction under the information-theoretic source model. Firstly, we are interested in the impact of quantization and channel estimation on the reciprocity and random aspect of generated keys. Secondly, we investigate alternative ways of limiting public exchanges needed for the reconciliation phase. Finally, we develop a new signal-based method that extends the point-to-point source model to cooperative contexts, with several nodes intending to establish a common group key.

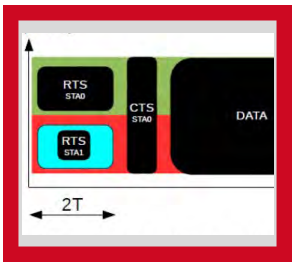

Baher MAWLAWI

Lyon National Institute of Applied Science, France

RANDOM ACCESS FOR DENSE NETWORKS: DESIGN AND ANALYSIS OF MULTIBAND CSMA/CA

Random protocols are promising candidates for future wireless systems dedicated to machine to machine (M2M) communications. Such protocols are usually based on a random access with simple techniques of medium sensing and deferring to reduce collisions while avoiding the use of complex schedulers. Among different protocols, Carrier sense multiple access/collision avoidance with a Request-To-Send/Clear-To-Send (CSMA/CA-RTS/CTS) is an opportunistic protocol which could be adopted for M2M scenarios. Such an approach is efficient to avoid collisions between data packets but in a very dense network, the random access used to send the RTS suffers itself from a high probability of collision which degrades the performance. In order to mitigate this effect, RTS collisions should be reduced. This thesis addresses this issue by splitting the common channel in sub-channels for transmitting the RTS messages. While the common channel is used as a whole for data transmission. Multiple nodes can then contend in time and frequency for these RTS sub-channels, thereby reducing RTS collisions and increasing overall efficiency. In this work, we thus derive a complete protocol solution relying on CSMA/CA - RTS/CTS multiplexing a multi-channel configuration for RTS messages and a unique channel for data transmission. An enhanced version based on users scheduling is integrated as well. The proposed protocol is investigated from a joint PHY-MAC point of view. This strategy is shown to provide better system performance particularly for loaded networks. An accurate analytical model derived as a straightforward extension of the Bianchi model is analyzed and validated by simulations. Performance in terms of saturation throughput, transmission delay and packet drop

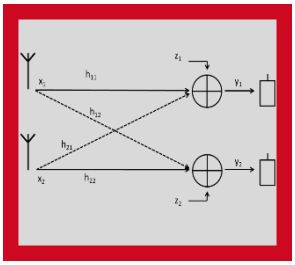

Matthieu DE MARI

Centrale-Supélec, France

RADIO RESOURCE MANAGEMENT FOR GREEN WIRELESS NETWORKS.

In this thesis, we investigate two techniques for energy or spectral efficiency enhancement of the network. In the first part of the thesis, we propose to combine the network future context prediction capabilities with the well-known latency vs. energy efficiency tradeoff. In that sense, we consider a proactive delay-tolerant scheduling problem. In this problem, the objective consists of defining the optimal power strategies of a set of competing users, which minimizes the individual power consumption, while ensuring a complete requested transmission before a given deadline. We first investigate the single user version of the problem, which serves as a preliminary to the concepts of delay tolerance, proactive scheduling, power control and optimization, used through the first half of this thesis. We then investigate the extension of the problem to a multiuser context. The conducted analysis of the multiuser optimization problem leads to a non-cooperative dynamic game, which has an inherent mathematical complexity. In order to address this complexity issue, we propose to exploit the recent theoretical results from the Mean Field Game theory, in order to transition to a more tractable game with lower complexity. The numerical simulations provided demonstrate that the power strategies returned by the Mean Field Game closely approach the optimal power strategies when it can be computed (e.g. in constant channels scenarios), and outperform the reference heuristics in more complex scenarios where the optimal power strategies cannot be easily computed.

In the second half of the thesis, we investigate a dual problem to the previous one; namely, we seek to optimize the total spectral efficiency of the system, in a constant short-term power configuration. To do so, we propose to exploit the recent advances in interference classification. The analysis reveals that the system benefits from adapting the interference processing techniques and spectral efficiencies used by each pair of Access Point (AP) and User Equipment (UE). The performance gains offered by interference classification can also be enhanced by considering two improvements. First, we propose to define the optimal groups of interferers: the interferers in a same group transmit over the same spectral resources and thus interfere, but can process interference according to interference classification. Second, we define the concept of 'Virtual Handover': when interference classification is considered, the optimal Access Point for a user is not necessarily the one providing the maximal SNR. For this reason, defining the AP-UE assignments makes sense when interference classification is considered. The optimization process is then threefold: we must define the optimal i) interference processing technique and spectral efficiencies used by each AP-UE pair in the system; ii) the matching of interferers transmitting over the same spectral resources; and iii) define the optimal AP-UE assignments. Matching and interference classification algorithms are extensively detailed in this thesis and numerical simulations are also provided, demonstrating the performance gain offered by the threefold optimization procedure compared to reference scenarios where interference is either avoided with orthogonalization or treated as noise exclusively.

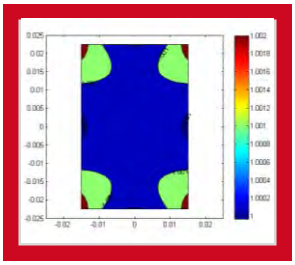

Mathieu BAICRY

University of Grenoble, France

INVESTIGATION OF A MARINE MAGNETO-ELECTROMETER: DESIGN, OPTIMIZATION AND PROOF OF CONCEPT.

The measurement of electric and magnetic fields at sea is of great interest for many applications (geophysics, oil prospection, vessels detection...). Most marine electrometers measure the potential difference between two separated electrodes. Due to the amplification electronics, their noise level decreases with frequency and therefore is very high at low frequencies. Another type of electrometer is based on low-impedance current measurements. We designed a current-based electrometer that simultaneously measures the electric and magnetic fields, thereby solving the issues of former devices. First, we describe the medium in which the sensor will be used, the targeted applications, and the state of the art of existing sensors and their limitations. Then, we describe in detail the properties of the sensor. In particular, we determine by simulation and experimentally the multiple transfer functions of the sensor, taking into account its geometrical characteristics and its environment. After presenting several potential architectures meeting the targets, we scale an electrometer, whose equivalent conductivity is not necessarily equal to that of seawater. This additional degree of freedom in comparison with the design constraints of the former current measurement electrometers allows us to improve the performance of the sensor. Next, we propose two calibration methods of the electrometer, without prior knowledge of its environment. Finally, we characterize the various parts of a laboratory prototype, and we present the experimental results of the complete prototype.

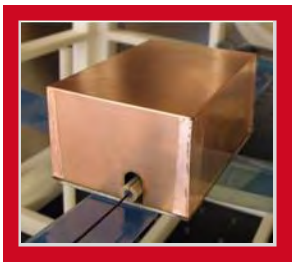

Marie-Constance CORSI

University of Grenoble, France

HELIUM-4 OPTICALLY-PUMPED MAGNETOMETERS : DEVELOPMENT AND PROOF OF CONCEPT IN MAGNETOCARDIOGRAPHY AND MAGNETOENCEPHALOGRAPHY

MagnetoCardioGraphy MagnetoEncephaloGraphy (MCG, MEG) are two non-invasive techniques measuring respectively cardiac and brain magnetic fields, based on SQUIDs recordings. Motivation to develop alternative sensors comes from the high costs of the current technology that requires a cryogenic cooling system and has significant technical constraints. Viable alternative to SQUIDs based on cryogenic-free OPM (Optically-Pumped Magnetometers) have emerged recently.

This work focus on the development of room temperature ^{4}He OPM - a promising sensor for MCG/MEG measurements based on the parametric resonance of ^{4}He in a near zero magnetic field in a gradiometer mode. In the first instance, a former existing prototype has been miniaturized taking into account biomedical and electromagnetic compatibility constraints (achieved sensitivity around 350 fT/√Hz). A noise analysis revealed that the laser and the HF discharge were the main sources of disturbance. The demonstrator has been successfully tested in MCG with the detection of QRS complex and T-waves: simulation studies on phantom were cross-validated by measurements on two healthy subjects demonstrating the operability of the OPM within a clinical environment. Further optimization of the optical part has improved the sensitivity up to 210 fT/√Hz between 2 and 300 Hz, suitable for the MEG application. MEG experiments such as auditory evoked field were successfully performed on a healthy subject.

These results form a clinical proof-of-concept confirming the possibility to record MCG/MEG signal with a room-temperature ^{4}He magnetometer.

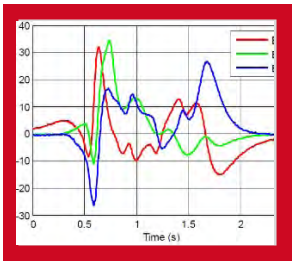

Anne-Cécile PITTON

University of Grenoble, France

CONTRIBUTIONS TO VEHICLES RE-IDENTIFICATION BY AN ANALYSIS OF MAGNETIC SIGNATURES MEASURED WITH A MATRIX OF THREE-AXIS MAGNETIC SENSORS.

Vehicle re-identification gives access to two essential data for dynamic traffic management: travel times and origin-destination matrices. In this thesis, we chose to re-identify vehicles by analyzing their magnetic signatures measured with several 3-axis magnetic sensors located on the road. A magnetic signature is created by the vehicle magnetization. Therefore, the vehicle orientation to the Earth's magnetic field (which determines the induced magnetization) and the variation of the lateral position of the vehicle relative to the sensors might both have an impact on the magnetic signature. We gathered our experiments' results into a database of magnetic signatures that we used to evaluate the performances of the two vehicle re-identification methods we developed.

The first method is a direct comparison of pairs of magnetic signatures measured by the sensors. Distances between pairs of signatures are computed using classic algorithms such as the Euclidean distance. This method's results are very positive and the vehicle change of orientation has only a slight impact on them. However, the distortion of signals due to a lateral offset in the vehicle position has a strong impact on the results. As a consequence, sensors have to be placed every 0.20m over the road's entire width.

The second proposed method compares pairs of vehicles' magnetic models. Those models are composed of several magnetic dipoles and are determined from the measured signatures. Magnetic modelling aims to suppress the influence of the vehicle lateral position on the results by assessing the relative position of the vehicle above the sensors. Although the vehicle orientation has slightly more impact on the performances than with the first method, the overall results are more promising. This method also allows us to divide by two the number of sensors used.

SYSTEMS AND SOLUTIONS INTEGRATION

Contacts

Sébastien Dauvé
Head of Systems Division
sebastien.dauve@cea.fr

François Vacherand
Deputy Head of Systems Division
françois.vacherand@cea.fr

Laurent Dussopt
Scientific Manager
laurent.dussopt@cea.fr

Jean-Michel Léger
Program Manager
jean-michel.leger@cea.fr

Marc Donikian
Commercial Manager
marc.donikian@cea.fr

Dominique Noguet
Head of Telecom Lab.
dominique.noguet@cea.fr

Stéphanie Riché
Head of Sensors and Systems Lab.
stephanie.riche@cea.fr

Bruno Charrat
Head of Security Lab.
bruno.charrat@cea.fr

Sylvie Mayrargue
International Telecom Expert
sylvie.mayrargue@cea.fr

Leti, technology research institute
Commissariat à l'énergie atomique et aux énergies alternatives
Minatec Campus | 17 rue des Martyrs | 38054 Grenoble Cedex 9 | France
www.leti.fr